

**SYNTHESIS, CHARACTERIZATION AND  
THEORETICAL STUDY OF AMINO ACID-BASED  
MAGNETIC MOLECULARLY IMPRINTED  
POLYMER FOR RECOGNITION OF  
SULFONAMIDE DRUGS**

**CHEN LEI**

**FACULTY OF SCIENCE  
UNIVERSITY OF MALAYA  
KUALA LUMPUR**

**2015**

**SYNTHESIS, CHARACTERIZATION AND  
THEORETICAL STUDY OF AMINO ACID-BASED  
MAGNETIC MOLECULARLY IMPRINTED POLYMER  
FOR RECOGNITION OF SULFONAMIDE DRUGS**

**CHEN LEI**

**DISSERTATION SUBMITTED IN FULFILMENT OF THE  
REQUIREMENTS FOR THE DEGREE OF MASTER OF  
SCIENCE**

**DEPARTMENT OF CHEMISTRY  
FACULTY OF SCIENCE  
UNIVERSITY OF MALAYA  
KUALA LUMPUR**

**2015**

**UNIVERSITI MALAYA**

**ORIGINAL LITERARY WORK DECLARATION**

Name of Candidate: Chen Lei (I.C/Passport No: G51579860)  
Registration/Matric No: SGR120028  
Name of Degree: Master of Science  
Title of Project Paper/Research Report/Dissertation/Thesis ("this Work"):

**SYNTHESIS, CHARACTERIZATION AND THEORETICAL STUDY OF AMINO  
ACID-BASED MAGNETIC MOLECULARLY IMPRINTED POLYMER FOR  
RECOGNITION OF SULFONAMIDE DRUGS**

Field of Study: Analytical Chemistry  
I do solemnly and sincerely declare that:

- (1) I am the sole author/writer of this Work;
- (2) This Work is original;
- (3) Any use of any work in which copyright exists was done by way of fair dealing and for permitted purposes and any excerpt or extract from, or reference to or reproduction of any copyright work has been disclosed expressly and sufficiently and the title of the Work and its authorship have been acknowledged in this Work;
- (4) I do not have any actual knowledge nor do I ought reasonably to know that the making of this work constitutes an infringement of any copyright work;
- (5) I hereby assign all and every rights in the copyright to this Work to the University of Malaya ("UM"), who henceforth shall be owner of the copyright in this Work and that any reproduction or use in any form or by any means whatsoever is prohibited without the written consent of UM having been first had and obtained;
- (6) I am fully aware that if in the course of making this Work I have infringed any copyright whether intentionally or otherwise, I may be subject to legal action or any other action as may be determined by UM.

Candidate's Signature

Date

Subscribed and solemnly declared before,

Witness's Signature

Date

Name: DR. TAY KHENG SOO

Designation

Witness's Signature

Date

Name: PROF. DR. NOORSAADAH BINTI ABD RAHMAN

Designation

## ABSTRACT

Sulfonamides antibiotics (SAs) are the oldest and among the most widely used antibacterial agent in the world. Due to its low cost and their relative efficacy in controlling some common bacterial related diseases, SAs have been widely used in various sectors. Since huge amount of SAs have been consumed every year, SAs have been released into the environment through various human activities. Among various classes of pharmaceutical, the presence of antibiotics in the environments has been one of the major concerns due to its ability to develop antibiotic-resistant bacteria. Thus, it is essential to develop an efficient method for the determination of SAs in the environment.

The main objective of this study was to develop a multi-functional magnetic MIP for the extraction of SAs. The experiment was started from the computational study to design a suitable monomer for the multi-functional MIP. Based on the crystal structure of sulfamethoxazole (SMO) and dihydropteroate synthase, a serine-based monomer (Monomer-2) was designed and synthesized for this study. The performance of magnetic serine-based MIP (SMIP) was then compared with magnetic acrylamide-based MIP (AMIP). In this case, serine is an amino acid whereas acrylamide is a common commercially available monomer. The experimental study was started from the preparation of AMIP and followed by the evaluation of the performance of AMIP. The acrylamide-based MIP was imprinted directly onto the surface of MPS-modified MION. The result showed that the obtained AMIP possessed adsorption kinetics with 400 s to reach equilibrium. The results also indicated that the maximum adsorption capacity of  $775 \mu\text{g g}^{-1}$  was achieved. Langmuir adsorption isotherm model was found to describe well the equilibrium adsorption data. The results from the

competitive binding experiment showed that AMIP was not only selective towards sulfadiazine as the adsorption of sulfamerazine was dramatically high. Sulfadiazine and sulfamerazine have almost similar sub-structure where these two compounds were only differentiated by one methyl group. In order to explain this result, computational study was carried out. From different level of calculation with PM3, HF, and DFT calculation, both sulfadiazine and sulfamerazine showed similar interaction energy and mechanism with acrylamide monomer. This result indicated that, both sulfadiazine and sulfamerazine could have the same binding property in the AMIP.

By using the similar approach as AMIP, SMIP was synthesized. As compared to the AMIP, SMIP showed a faster adsorption rate on sulfadiazine with only 200 s to reach equilibrium level. The maximum adsorption capacity of SMIP was around 1547  $\mu\text{g g}^{-1}$ . This result is in agreement with the computational study. The computational study indicated that Monomer-2 (serine-based monomer) showed more favorable interaction with template as compared with acrylamide. Importantly, in the selectivity experiment, SMIP showed overwhelming advantage in the recognition of different SAs with the presence of 2 structural unrelated compounds.

Therefore, it can be concluded that the multifunctional magnetic MIP can be designed by using computer modelling method. Amino acid based monomer can be used for the preparation of MIP and this MIP showed the characteristic that mimic to the ligand-enzyme interaction.

## ABSTRAK

Antibiotik sulfonamida (SAs) merupakan agen antibakteria yang paling lama dan paling banyak digunakan. SAs mempunyai penggunaan yang luas di pelbagai sektor disebabkan oleh kosnya yang rendah dan keberkesannya dalam pengawalan penyakit berkaitan bakteria. Disebabkan penggunaannya yang meluas, SAs telah dilepaskan ke alam sekitar melalui pelbagai aktiviti manusia. Di antara pelbagai kelas farmaseutikal, kehadiran antibiotik dalam alam sekitar telah menjadi kebimbangan utama kerana kemampuannya untuk menghasilkan bakteria tahan antibiotik. Oleh itu, adalah penting untuk membangunkan kaedah yang cekap untuk penentuan SAs dalam pelbagai sample dari alam sekitar.

Objektif utama kajian ini adalah untuk menyediakan satu MIP bermagnet yang boleh digunakan untuk mengesktrak pelbagai jenis SAs. Eksperimen ini bermula dengan mereka bentuk monomer yang sesuai untuk menyediakan MIP yang boleh digunakan untuk mengesktrak pelbagai jenis SAs. Berdasarkan struktur hablur sulfamethoxazole (SMO) dan dihydropteroate sintase, monomer berasaskan serina (Monomer-2) telah dipilih untuk kajian ini. Seterusnya, prestasi bagi MIP bermagnet yang berasaskan serina (SMIP) dibandingkan dengan MIP bermagnet yang berasaskan acrylamida (AMIP). Dalam kes ini, Serina adalah asid amino manakala acrylamida adalah monomer yang boleh didapati secara komersial.

Kajian secara eksperimen dimulakan dengan penyediaan AMIP dan diikuti oleh penilaian prestasinya. Dari segi kinetik penjerapan, AMIP yang diperolehi mencapai keseimbangan dalam 400 s. Keputusan juga menunjukkan bahawa kapasiti penjerapan maksimum bagi AMIP adalah  $775 \mu\text{g g}^{-1}$ . Isoterma model langmuir dapat digunakan

untuk menggambarkan mekanisme penjerapan sulfadiazine (sebatian templat) oleh AMIP. Hasil daripada eksperimen pengikatan kompetitif menunjukkan AMIP bukan sahaja selektif terhadap sulfadiazine tetapi juga sulfamerazine. Sulfadiazine dan sulfamerazine mempunyai struktur yang hampir sama di mana kedua sebatian ini hanya dibezakan oleh satu kumpulan metil. Dalam usaha untuk menjelaskan keputusan ini, kajian pengiraan secara pengkomputan dilakukan. Dari tahap pengiraan yang berbeza (PM3, HF, dan DFT), kedua-dua sulfadiazine dan sulfamerazine menunjukkan interaksi yang sama dengan acrylamida monomer dari segi tenaga dan mekanisme. Oleh itu, kedua-dua sulfadiazine dan sulfamerazine menunjukkan interaksi ikatan yang sama dalam AMIP.

Dengan menggunakan kaedah yang sama seperti AMIP, SMIP disediakan. Berbanding dengan AMIP, SMIP menunjukkan kadar penjerapan yang lebih cepat pada sebatian templat (sulfadiazine) dengan hanya 200 s untuk mencapai keseimbangan. Kapasiti penjerapan maksimum SMIP adalah sekitar  $1547 \text{ ug g}^{-1}$ . Keputusan ini adalah setuju dengan keputusan dari kajian pengiraan pengkomputan. Kajian pengkomputan telah menunjukkan bahawa Monomer-2 menunjukkan interaksi yang lebih baik dengan sulfadiazine berbanding dengan acrylamida. Yang penting, dalam eksperimen pemilihan, SMIP menunjukkan kelebihan yang amat menggalakkan dalam penjerapan SAs yang berlainan.

Kesimpulannya, penyelidikan ini menunjukkan MIPs pelbagai fungsi boleh direka bentuk dengan menggunakan kaedah pengiraan pengkomputan. MIP yang disintesis dengan menggunakan asid amino sebagai monomer juga menunjukkan sifat interaksi yang sama seperti interaksi antara ligan dan enzim.

## ACKNOWLEDGMENT

My sincere thanks first and foremost go to my supervisors Dr. Tay Kheng Soo and Prof. Dr. Noorsaadah Abd Rahman, who gave me this great opportunity to do my research at the Department of Chemistry, Faculty of Science, University of Malaya. Dr. Tay and Prof Noorsaadah have been a great scientific advisor and mentor. Their guidance, inspiration and generous support help throughout my research and thesis writing process.

In addition, I wish to express my heartfelt thanks to all my friends and colleagues in the research group, Dr Lee Yean Kee, Dr. Chee Chin Fei, Dr. Mona Yaeghoobi, Mr. Iskandar Abdullah, Ms. Tee Jia Ti, Mr. Thy Chun Kheng, Mr. Shah Bakhtiar and other staff members of the Department of Chemistry. I would like to thank the Department of Chemistry for providing the laboratory space for my experiment throughout my study. Last but not least, I would like to dedicate this thesis to my parents, who have been standing by me all the time. Without their love, concern and understanding, I would not have completed my Master's study.



## TABLE OF CONTENTS

	Page
<b>ORIGINAL LITERARY WORK DECLARATION</b>	<b>ii</b>
<b>ABSTRACT</b>	<b>iii</b>
<b>ABSTRAK</b>	<b>v</b>
<b>ACKNOWLEDGMENT</b>	<b>vii</b>
<b>TABLE OF CONTENTS</b>	<b>viii</b>
<b>LIST OF FIGURES</b>	<b>xi</b>
<b>LIST OF TABLES</b>	<b>viii</b>
<b>LIST OF SYMBOLS AND ABBREVIATIONS</b>	<b>xiv</b>
<b>CHAPTER 1 INTRODUCTION</b>	<b>1</b>
1.1 Overview of Sulfonamide (SA) antibiotics	1
1.1.1 Occurrence and environmental behavior of SAs	4
1.1.1.1 Residues of SAs in the environment	4
1.1.1.2 Negative impact of SA residues to the environment	5
1.1.2 Monitoring and management of SAs residues	6
1.1.3 Analysis of SAs in the environment	8
1.2 Molecular Imprinting Technology	10
1.2.1 The history of MIP	10
1.2.2 General principle of molecular imprinting technique	11
1.2.3 Molecular imprinting approaches	12
1.2.4 Optimizing the performance of MIP	14
1.2.5 Methods of polymerization	21
1.3 Magnetic molecularly imprinted polymer (MMIP)	24
1.3.1 History of MMIP	24
1.3.2 Application of MMIP	27
	viii

1.4 Objectives of study	30
<b>CHAPTER 2 MATERIALS AND METHOD</b>	<b>31</b>
2.1 Docking methods	31
2.1.1 Software and Hardware	31
2.1.2 Molecular file preparations	31
2.1.2.1 Molecular 3D structure information	31
2.1.2.2 AutoDock input file preparation and docking experiment	32
2.1.3 Computational study of MIP and template interaction	33
2.2 Synthesis of amino acid based monomer	33
2.2.1 Materials	33
2.2.2 Procedure of monomer-2 synthesis	34
2.3 Preparation of MMIP	35
2.3.1 Synthesis of MION	36
2.3.2 Synthesis of MION@MPS	37
2.3.3 Preparation of MMIP and MNIP	37
2.3.3.1 Preparation of AMIP and ANIP	37
2.3.3.2 Preparation of SMIP and SNIP	38
2.4 Binding experiments	38
2.4.1 Binding experiment of AMIP and ANIP	38
2.4.2 Binding experiment of SMIP and SNIP	39
2.4.3 Specific recognition of AMIP and ANIP	39
2.4.4 Specific recognition of SMIP and SNIP	40
2.5 Instrumental analysis	40
<b>CHAPTER 3 RESULTS AND DISCUSSION</b>	<b>42</b>
3.1 Design of monomer through the molecular docking	42
3.2 Synthesis of Monomer-2	49

3.3 Characterization of synthesized MMIP	50
3.3.1 AMIP	51
3.3.2 SMIP	54
3.4 Binding properties of MMIP	57
3.4.1 Adsorption kinetic studies	57
3.4.2 Binding isotherm	59
3.5 Binding specificity of AMIP, ANIP, SMIP and SNIP	64
<b>CHAPTER 4. CONCLUSION</b>	<b>72</b>
4.1 Conclusions	72
4.2 Future studies	74
<b>Reference</b>	<b>75</b>
<b>Appendix 1 <math>^1\text{H}</math> and <math>^{13}\text{C}</math> NMR SPECTRUM OF SYNTHESIZED MONOMER-2</b>	<b>90</b>
<b>Appendix 2 DATA FROM ISOTHERM STUDIE</b>	<b>93</b>
<b>Appendix 3 PUBLICATION</b>	<b>96</b>

## LIST OF FIGURES

	<b>Page</b>
Figure 1.1 Comparison of structures between SAs and PABA.	3
Figure 1.2 Occurrence and fate of SAs in the environment.	5
Figure 1.3 Structures of some commonly used functional monomers.	16
Figure 1.4 Chemical structures of common initiator used in molecular imprinting.	21
Figure 2.1 Synthesis pathway of Monomer-2.	35
Figure 2.2 Overview of the synthesis of MMIPs and MNIPs.	36
Figure 3.1 The crystal structure of SMO-dihydropteroate synthase.	43
Figure 3.2 Interaction between SMO and serine in dihydropteroate synthase.	43
Figure 3.3 The structure of Monomer-1.	44
Figure 3.4 Interaction between SMO and Monomer-1. (Green line representing the hydrogen bonding).	45
Figure 3.5 Structure of serine with different protecting groups.	47
Figure 3.6 The structure of Monomer-2.	48
Figure 3.7 The interaction between Monomer-2 and SDZ.	49
Figure 3.8 Mechanism for the formation of Monomer-2.	50
Figure 3.9 FTIR spectra recorded between 4000 and 400 $\text{cm}^{-1}$ of MION, MION@MPS	52
Figure 3.10 TGA curves of MION, MION@MPS and AMIP.	52
Figure 3.11 SEM images of (a) MION, (b) MION@MPS and (c) AMIP.	53
Figure 3.12 FTIR spectra recorded between 4000 and 400 $\text{cm}^{-1}$ of MION@MPS and SMIP.	54
Figure 3.13 TGA curves of MION@MPS and SMIP.	55

Figure 3.14	SEM images of SMIP.	56
Figure 3.15	EDX pattern for SMIP and the result of elemental analysis.	56
Figure 3.16	Adsorption kinetics of (a) AMIP and ANIP, and (b) SMIP and SNIP.	58
Figure 3.17	(a) Adsorption isotherm of SDZ onto AMIP and ANIP; (b) Langmuir plot to estimate the binding mechanism of AMIP towards SDZ.	60
Figure 3.18	(a) Adsorption isotherm of SDZ onto SMIP and SNIP; (b) Langmuir plot to estimate the binding mechanism of SMIP towards SDZ.	61
Figure 3.19	Freundlich plot for the adsorption of SDZ by AMIP and SMIP.	63
Figure 3.20	Adsorption capacity of MION-MIP and MION-NIP towards SDZ, SMR, SAA, SMZ and SMO.	64
Figure 3.21	The interaction between the template and the monomer in comparison of the crystal structure of SA drug (SMO) from the protein database (PDB ID: 3TZF). The dashed line shows the hydrogen bonding interaction.	66
Figure 3.22	Interaction energy plotted against the O–H-distance for (a) SDZ and AA1; (b) SDZ and AA2; (c) SMR and AA1; (d) SMR and AA2.	70
Figure 3.23	Structure of DEET and benzylparaben.	71
Figure 3.24	Adsorption capacity of SMIP and SNIP towards sulphonamides, DEET and benzylparaben.	71

## LIST OF TABLES

		Page
Table 1.1	Common structure of SAs.	2
Table 1.2	Concentration of SAs in various sample obtained from several countries.	7
Table 1.3	Sample extraction techniques that are employed in the adsorption of SAs with aid of MIP technology.	10
Table 1.4	Molecular structures of some cross-linking agents that have been used in the preparation of MIPs.	18
Table 3.1	Binding energies of SMO with Monomer-1 and commercially available monomers estimated using the Autodock Tools 1.5.6.	44
Table 3.2	Binding energy between selected monomers and new template molecule (SDZ) estimated using the AutoDock Tools 1.5.6.	48
Table 3.3	The interaction energy between the templates and monomers with three different basis sets calculations.	67
Table 3.4	The partition coefficients, imprinting factors and selectivity coefficients of SDZ and its analogues STZ, SPY, SMR, DEET and Benzylparaben for SMIPs and SNIPs.	70

## LIST OF SYMBOLS AND ABBREVIATIONS

4-VP	4-Vinylpyridine
$\beta$ -CD	$\beta$ -Cyclodextrin
AA	acrylamide
AA1	Acrylamide1
AA2	Acrylamide2
ACN	Acetonitrile
ASE	accelerated solvent extraction
B3LYP	Becke's three-parameter Lee-Yang-Parr
BPO	Benzoyl peroxide
EA	Ethyl acetate
EDCI HCl	1-Ethyl-3-(3-dimethylaminopropyl)carbodiimide hydrochloride
EGDMA	Ethyleneglycol dimethacrylate
EGMP	Ethylene glycol methacrylate phosphate
DCM	dichloromethane
DEET	Diethyltoluamide
DFT	Density Functional Theory
DIEA	N,N-Diisopropylethylamine
DMF	Dimethylformamide
DVB	divinylbenzene
EDX	Energy-dispersive X-ray spectroscopy
FeCl <sub>2</sub> 4H <sub>2</sub> O	Iron(II) chloride tetrahydrate
FeCl <sub>3</sub>	Iron(III) chloride
HAc	Acetic acid
HF	Hartree-Fock

HOBT	Hydroxybenzotriazole
HPLC	high performance liquid chromatography
IAA	3-indole acetic acid
IF	imprinting factor
IR	Infrared
LME	liquid membrane extraction
LPME	liquid phase micro extraction
LOD	limit of detection
MAA	methacrylic acid
MAE	microwave assisted extraction
MION	magnetic iron oxide nanoparticles
MIP	molecularly imprinted polymer
MMIP	Magnetic molecularly imprinted polymer
MRL	maximum residue level
PABA	aminobenzoic acid
PDB	Protein Data Bank
PM3	Semiempirical
SA	sulfonamide
SAA	Sulfacetamide
SC	selectivity coefficient
SDM	Sulfadimethoxine
SDZ	Sulfadiazine
SER	serine
SEM	Scanning electron microscope
SFE	supercritical fluid extraction
SIZ	Sulfisoxazole



SMD	Sulfamethoxydiazine
SMR	Sulfamerazine
SMM	Sulfamonomethoxine
SMO	Sulfamethoxazole
SMZ	Sulfamethazine
SPE	solid phase extraction
SPY	Sulfapyridine
SQX	Sulfaquinoxaline
STZ	Sulfathiazole
TGA	Thermogravimetric analysis
THR	Threonine
TRIM	trimethylolpropane trimethacrylate
UAE	ultrasonic assisted extraction

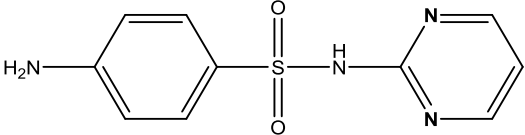
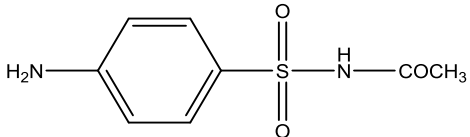
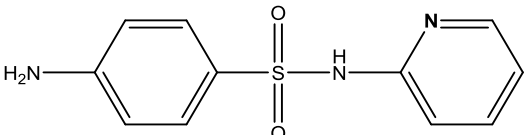
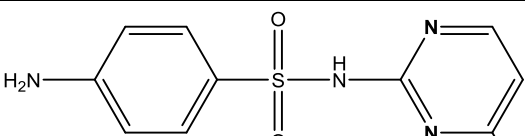
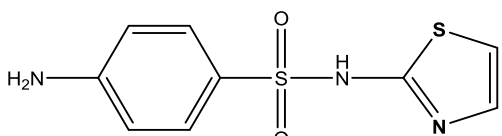
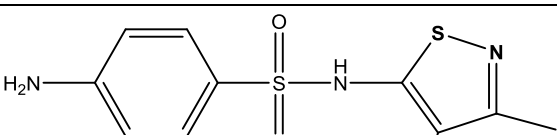
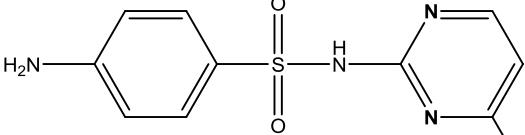
## CHAPTER 1 INTRODUCTION

### 1.1 Overview of Sulfonamide (SA) antibiotics

Antibiotics are common pharmaceuticals that have been used to kill or hinder the growth of microorganisms such as bacteria and fungi. Among various types of antibiotic, SAs containing the common structure of para-aminobenzenesulfonamide (Table 1.1) (Burkhart and Burkhart, 2009), are among the most widely used pharmaceutical to prevent bacterial infectious diseases for human being (García-Galán et al. 2008) and livestock (Kong et al., 2012). Generally, SAs are odourless, tasteless, and slightly soluble in water (Hanaee et al., 2005). SAs are efficient in inhibiting various kinds of bacteria such as *Pneumococci*, *Streptococci*, *Meningococci*, *Staphylococci*, *coliform bacteria*, and *Shigellae* (Singh et al., 2013). It has been used to inhibit Chlamydia that contributes to sexual transmitted diseases and protozoa (Kuo et al., 1977).

SAs inhibit the growth and reproduction of bacteria by interfering the folic acid-metabolism of the bacteria. Folic acid is essential for the synthesis of precursors for DNA and RNA in bacteria. Unlike animal cells, bacteria are not able to utilize the available folic acid at its surrounding directly. It can only utilize the aminobenzoic acid (PABA) and dihydropteridine to synthesis the dihydrofolic acid and this process is catalytically biosynthesized by dihydrofolate synthase. Owing to the structure similarity between PABA and SAs (Figure 1.1), SAs can compete with PABA for dihydrofolate synthase and interferes the formation of dihydrofolic acid that required by the bacteria (Doungsoongnuen et al., 2011). As a result, the reproduction of bacteria is inhibited.

**Table 1.1** Common structure of SAs.

SA	Abbreviation	Structure
Sulfadiazine	SDZ	
Sulfacetamide	SAA	
Sulfapyridine	SPY	
Sulfamerazine	SMR	
Sulfathiazole	STZ	
Sulfisoxazole	SIZ	
Sulfamethazine	SMZ	

Sulfadimethoxine	SDM	
Sulfamethoxydiazine	SMD	
Sulfamonomethoxine	SMM	
Sulfamethoxazole	SMO	
Sulfaquinoxaline	SQX	
Sulfachloropyrazine	SCP	

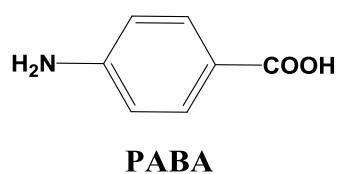
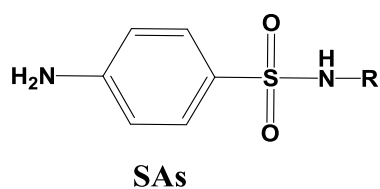


**Figure 1.1** Comparison of structures between SAs and PABA.

### **1.1.1 Occurrence and environmental behavior of SAs**

#### **1.1.1.1 Residues of SAs in the environment**

In recent years, the occurrence and fate of SAs in the aquatic environment has been regarded as one of the rising issues in environmental chemistry (Heberer, 2002). Owing to their antimicrobial activity, effectiveness and relatively inexpensive, huge amount of SAs have been consumed every year (Becheker et al., 2014). In the meanwhile, plenty of SAs have been released into the environment through various human activities. So far, SAs have been detected in various aquatic environment which include groundwaters (Peng et al., 2006), surface waters (Batt et al., 2006); and terrestrial environments such as soils (Kemper, 2008) and sludges (Göbel, et al., 2005). Many of the pharmaceuticals applied in human medical care are not completely metabolized in the human body. Usually, pharmaceuticals are excreted with slight transformation or even unchanged (Jones et al., 2005). Pharmaceuticals such as SAs will then be released into the aquatic environment by effluents from municipal sewage treatment plants (Huber et al., 2005). Several investigations have shown that pharmaceuticals are often not eliminated during waste water treatment and also not biodegraded in the environment (Zwiener and Frimmel, 2000). On the other hand, the presence of SAs residues in the environment also caused by veterinary drugs and feed additives in livestock breeding as agriculture employing huge amount of SAs (Halling-Sørensen et al., 1998). The use of antibiotics in livestock production could be a potential source of antibiotic contamination, which may increase the presence of antibiotic resistant bacteria in the environment. Antibiotic resistance genes can be spread via the food web and through hydrologic processes to

human pathogens (Hoa et al., 2010). Figure 1.2 illustrated the fate and transformation of SAs in the environment.

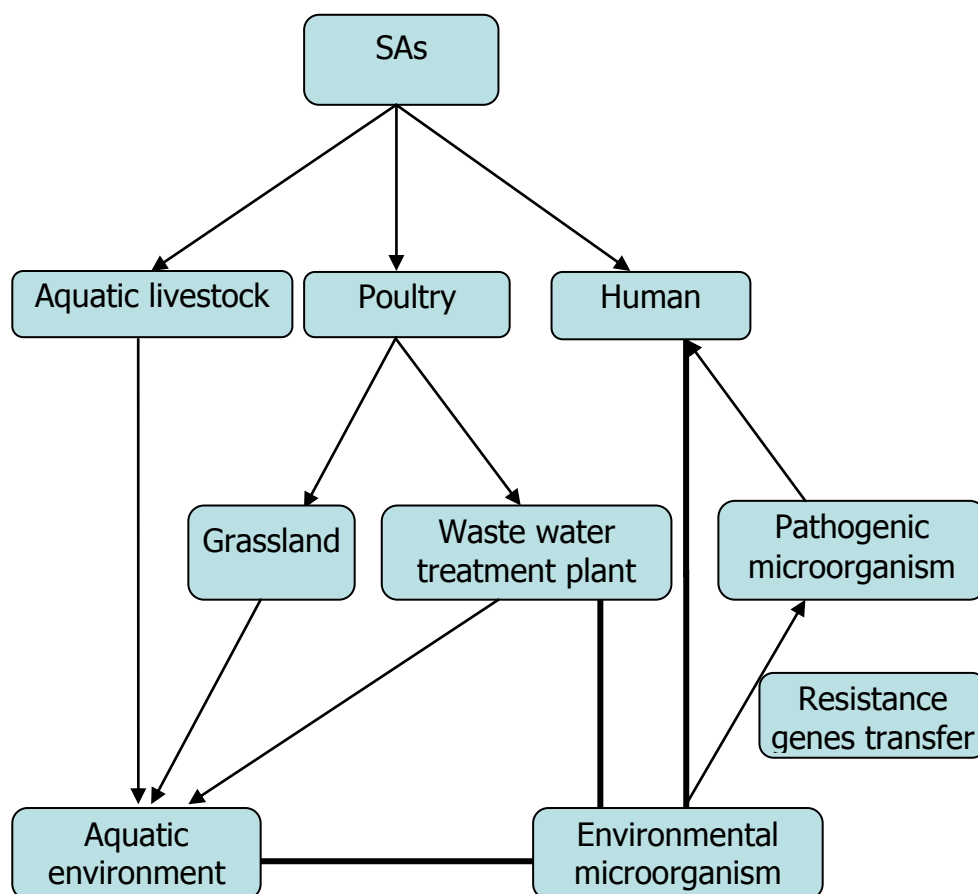


**Figure 1.2** Occurrence and fate of SAs in the environment.

#### 1.1.1.2 Negative impact of SA residues to the environment

SAs have been widely used in veterinary drugs, feed additives, and aquaculture (Gao et al., 2012; Galarini et al., 2014). Once these drugs are released into the environment, it would be absorbed by soil and also transported into groundwater or surface water (Table 1.2). Consequently, microorganisms in the environment are exposed to the SA residues and resulting in the changed of microbial community, development of antimicrobial resistance microorganisms, and even causing the transgenation of

bacterium (Nikaido et al., 2009). Because of continual widespread of SAs in the environment, sources of food stuffs such as plants have been found to be contaminated by SA residues as well (Hruska and Franek, 2012). As a result, SAs have been detected in food stuffs that derived from the SAs contaminated areas (Cheong et al., 2010). Long-term exposure of these residuary drugs through contaminated food stuffs was found to develop potential toxic effects such as allergy, tumors, carcinogenesis and the development of antibiotic resistance bacteria in human body (Lopes et al. 2012). So far, the presence of these chemicals in milks that causing allergic or toxic reactions that risk the human health have been reported (Sicherer and Leung, 2012). Also, SAs can cause serious damage to the liver due to its poor solubility. SAs have been found to precipitate inside the renal tubules and causing hematuria, dysuria and other symptoms (Lipmann, 1945). SAs also led to allergic and rash where drug fever is the most common symptom (Stohs and Miller, 2014). Research on livestock also found that low laying rate and weak eggshell hardness of livestock are related to SA residues (Kan and Petz, 2000).

### **1.1.2 Monitoring and management of SAs residues**

In order to improve human living standards, issues regarding the food safety are getting increasingly attraction. To protect consumers from the risk of SAs exposure, the allowed maximum residue level (MRL) of SAs has been established in many countries. Codex Alimentarius Commission (CAC) regulated that the total amount of residual SAs in food and animal feed shall not exceed  $100 \mu\text{g kg}^{-1}$ . MRL of SAs in food was also established in administrative regulations of Canada, European Union, America, China and Japan (Baran et al. 2011). According to the European Union (EU) (EU Commission, 2010), the MRL for the total amount of SAs in edible tissues was  $100 \text{ mg kg}^{-1}$ . Canada

(Health Canada, 2014) and Australia (National Registration Authority, 2000) also have the similar regulations on this issue. All of these regulations together with harmful effects of SAs in the environment underline the importance of sensitive analytical method to monitor and determine the concentration of SAs in various food and environmental samples.

**Table 1.2** Concentration of SAs in various sample obtained from several countries.

Source	Country	SAs	Concentration	Reference
Soil	China	SMR	$16.0 \pm 24.3 \mu\text{g kg}^{-1}$	Li et al., (2011)
		SMZ	$5.5 \pm 15.0 \mu\text{g kg}^{-1}$	
		SDZ	$13.4 \pm 23.0 \mu\text{g kg}^{-1}$	
		SMO	$23.5 \pm 13.0 \mu\text{g L}^{-1}$	
		SDM	$4.9 \pm 10.3 \mu\text{g L}^{-1}$	
Effluent of wastewater treatment plant	Thailand	SMO	$3\text{--}30.5 \text{ ng L}^{-1}$	Tewari et al.,(2013)
		SMZ	$1\text{--}180 \text{ ng L}^{-1}$	
Animal waste water	China	SMO	$63.6 \mu\text{g L}^{-1}$	Wei et al.,(2011)
		SDZ	$17.0 \mu\text{g kg}^{-1}$	
Sewage sludge	Estonia	SDM	$73 \mu\text{g kg}^{-1}$	Haiba et al., (2013)
		SMO	$22 \mu\text{g kg}^{-1}$	
River sample	China	SPY	$16.60 \text{ ng L}^{-1}$	Jiang et al., (2011)
		SDZ	$22.33 \text{ ng L}^{-1}$	
		SMO	$28.34 \text{ ng L}^{-1}$	
		SMZ	$313.44 \text{ ng L}^{-1}$	



### 1.1.3 Analysis of SAs in the environment

A complete sample analysis of organic pollutants containing in different sample matrices can be divided into four steps: sampling, sample preservation, sample preparation and analysis. In nature, most samples are not suitable for direct analysis by using analytical instruments due to the low analyte concentration and complicated interference from sample matrices. Therefore, sample preparation is usually needed to extract, isolate and concentrate the interested analytes to a suitable level, which can be analyzed by an analytical instrument. Sample preparation might involve several time consuming steps such as homogenization, extraction, preconcentration, and clean-up before instrumental analysis (Mitra, 2004). Therefore, sample pretreatment is vital process in analytical chemistry. As a result, development of sample pretreatment methods and technologies has attracted extensive attention from analytical chemists all over the world.

In terms of SAs analysis, sample extraction techniques can be divided into different categories according to the type of samples. Solid samples such as soil (Chen et al., 2009a), chicken meat (Tadeo et al., 2010), spiked matrix (Combs et al., 1997b) sewage sludge (Göbel et al., 2005), microwave assisted extraction (MAE) (Akhtar et al., 1998), ultrasonic assisted extraction (UAE) (Chen et al., 2015), supercritical fluid extraction (SFE) (Combs et al., 1997a), and accelerated solvent extraction (ASE) (Sun et al., 2012) are commonly used method for the extraction of SAs. As liquid samples such as environmental water (Liu et al., 2010), waste water (Renew and Huang, 2004), honey sample (Bedendo, 2010), liquid - liquid extraction (LLE) (Spielmeyer et al., 2014), solid phase extraction (SPE) (Lindsey et al., 2001), liquid membrane extraction

(LME) (Msagati and Nindi, 2004), liquid phase micro extraction (LPME) have been frequently used in the extraction of SAs (Payán et al., 2011).

Determination of trace amount of analytes in complex matrices often relies on extensive sample extraction and preparation prior to chromatographic analysis. Suitable sample preparation method can reduce analysis time, sources of error, enhance sensitivity, and enable unequivocal identification, confirmation, and quantification (Olariu et al., 2010). However, when it comes to substantial amount of samples, low selectivity and capacity towards the target analytes often become hindrance to the current enrichment techniques (Tan et al., 2011). Moreover, most of the traditional methods are not appropriate in rapid on-site detection due to the several limitations such as high cost and poor reproducibility. Thus, development of more rapid, selective and sensitive analytical detection methods has therefore become an urgent need. In this context, many researchers enthusiastically develop novel approaches of enrichment and separation technology (Pavlović et al., 2007).

Recently, different extraction techniques using high selectivity molecularly imprinted polymer (MIP) as solid phase have been developed in the field of SAs determination (Karimi et al., 2014). Table 1.3 revealed the overall application of various extraction techniques combined with molecularly imprinted technology.

**Table 1.3** Sample extraction techniques that are employed in the adsorption of SAs with aid of MIP technology.

Sample	Method	Template	Monomer	LOD	Reference
Plant	MAE	IAA	4-VP and $\beta$ -CD	0.47 ng g <sup>-1</sup>	Hu et al., 2011
Milk	ASE	SMZ	Methacrylic acid (MAA)	$3.0 \times 10^{-7}$ mol L <sup>-1</sup>	De Prada et al., 2005
Honey	LLE	SMD	MAA	1.5-4.3 ng g <sup>-1</sup>	Chen et al., 2009b
Aquaculture product	SPE	SDM	MAA	8.4–10.9 g kg <sup>-1</sup>	Shi et al., 2011
Milk powder	SPME	Estrogen	Acrylamide (AA)	1.5–5.5 ng g <sup>-1</sup>	Lan et al., 2014
Environmental water	LME	SDM	MAA	0.2–3 $\mu$ g L <sup>-1</sup>	D áz-Álvarez et al., 2014

## 1.2 Molecular Imprinting Technology

### 1.2.1 The history of MIP

Molecular imprinting technology is a development of functional materials for sample preparation technique which was rising up in the 1990s. In general, MIP show specific recognition which is similar to the antigen and antibody interaction. When it comes to the preparation of MIP, a target molecule is employed as a template, which is pre-polymerized with functional monomer through covalent or non-covalent approach. The crosslinking agent and initiator help to complete the polymerization process. After

polymerization, template molecule is removed and yielding a three-dimensional polymer network where target molecules can be absorbed (Cheong et al., 2013).

In the early 1940s, Pauling (1940) proposed the possibility of using antigen as a template in the synthesis of antibody, which becomes the first description of molecular imprinting technique. Owing to the advent of molecular imprinting in organic polymers by Wulff and Sarhan (1972), a new era of molecular imprinting was ushered. Later, Arshady and Mosbach (1981) successfully developed the artificial antibody by using theophylline as template and applied it in drug analysis. After that, molecular imprinting techniques have become a popular research area over the world (Vlatakis et al., 1993).

### **1.2.2 General principle of molecular imprinting technique**

The technique of molecular imprinting aims at fabricating functional polymers with specific binding sites aimed at a target molecule (Puoci et al., 2010). The concept of molecular imprinting involves three major steps:

- (1) First, polymerizable monomers bearing with a functional group is arranged around the target molecule through either covalent (Wulff et al., 1973) or non-covalent interaction (Andersson and Mosbach, 1990).
- (2) Then, polymerization is initiated by initiator with the participation of cross-linker. This step is held in order to form the polymer network where template and monomer are optimally set for binding (Hu et al., 2008).

(3) The last step would be the removal of template molecules from the polymer matrices after polymerization (Lorenzo et al., 2011). This step releases the template from the polymer matrix and leaving the cavities that are complementary to the targeted analyte (Andersson et al., 2000).

Therefore, the tailor-made MIP possess a permanent cavity, enabling the resultant polymer selectively rebind in preference to the template which is also the target compounds (Rahiminezhad et al., 2010).

### **1.2.3 Molecular imprinting approaches**

Molecular imprinting technique is based on the formation of a complex between an analyte (template) and a functional monomer. In the presence of a large excess of a cross-linking agent, a three-dimensional polymer network is formed (Vasapollo et al., 2011). The interaction between template and monomer is essential in the formation of the template-monomer complex and is therefore responsible for the specific recognition of the binding site in the resultant polymer. Currently, there are plenty of processes which allow the functional monomer to interact with the template molecule according to the chemical bonding between template and molecular. The most popular molecular imprinting strategies are covalent and non-covalent approaches (Caro et al., 2002).

Covalent imprinting, also called pre-organized approach, was established by Wulff and co-workers in 1970s (Wulff et al., 1977). In the covalent system, template is coupled to monomer, which is usually low molecular weight compound, through reversible covalent binding. The main advantage of this approach is the covalent

imprinted polymers can form more specific binding sites where the nonspecific binding sites can be reduced. So far, the most common compounds used in covalent bonding are such as boronic acid (Liu et al., 2013), Schiff bases (Huang et al., 2009), acetal (Bergmann and Peppas, 2008), etc. A typical example was boronic acid esters, which is known to bind effectively with carbohydrates that containing diol moiety through reversible ester formation (Shen and Ren, 2014). The major drawback of this method is that the process is much more complicated as the template–monomer complex need to be fabricated before the polymerization and this process is tedious and time-consuming. Due to high stability of covalent bond, sometime, it is difficult to cleave the bond between template–monomer complex during the process of removing template from the polymer matrix.

Non-covalent, namely self-assembling, is so far the most frequently used method in MIPs synthesis because of its experimental simplicity and flexibility (Andersson, 2000). This approach, similar to biological recognition, employs non-covalent forces. In this method, interaction between template–monomer involved hydrogen-bonding, electrostatic forces, Van der Waals forces, hydrophobic interaction,  $\pi$ - $\pi$  interaction and metal-coordination. Functional monomers are usually mixed with template in a suitable porogen to form complex, followed by polymerization with the presence of cross-linker and radical initiator. Since the interaction between template and monomer is not so strong as compared with covalent bond, the template can be easily extracted from the MIPs under mild conditions. However, non-covalent bonding was found to be not strong enough to prevent the leaking of monomers to the reaction mixture from template–monomer complex and resulting in heterogeneous property of the binding sites. Another limitation of this method is that non-covalent bonding

interaction is hardly survived in the polar environment as their complex are stabilized under hydrophobic conditions (Yan and Row, 2006).

#### **1.2.4 Optimizing the performance of MIP**

In the process of MIP synthesis, many factors such as selection of monomer (Trehan et al., 2013), template (Andersson et al., 1999), cross-linker (Cai and Gupta, 2004), and solvent (Masque et al., 2001) have to be taken into consideration since they can affect the morphology, properties and the performance of MIP. Thus, it is vital to investigate the every potential composition of the polymer during synthesis. In general, template is a target substance which needs to be separated or recognized from various samples. Since the MIP has the ability to recognize the template, ideally, any molecule can be applied as template. The potential templates could be carbohydrate, organic amine, carboxylic acid, sterol, nucleotide, polypeptide, protein, metal ions, amino acid and their derivatives (Spivak and Shea, 1998; Hirayama et al, 2001). There are several requirements that an ideal template molecule should possess. Firstly, template should have good solubility in the chosen solvent (porogen) (Yan and Row, 2006). Secondly, the template has to be stable enough during the polymerization reaction (Andersson et al., 1997). Thirdly, functional groups assemble with corresponding monomer are absolute necessary (Haupt and Mosbach, 2000).

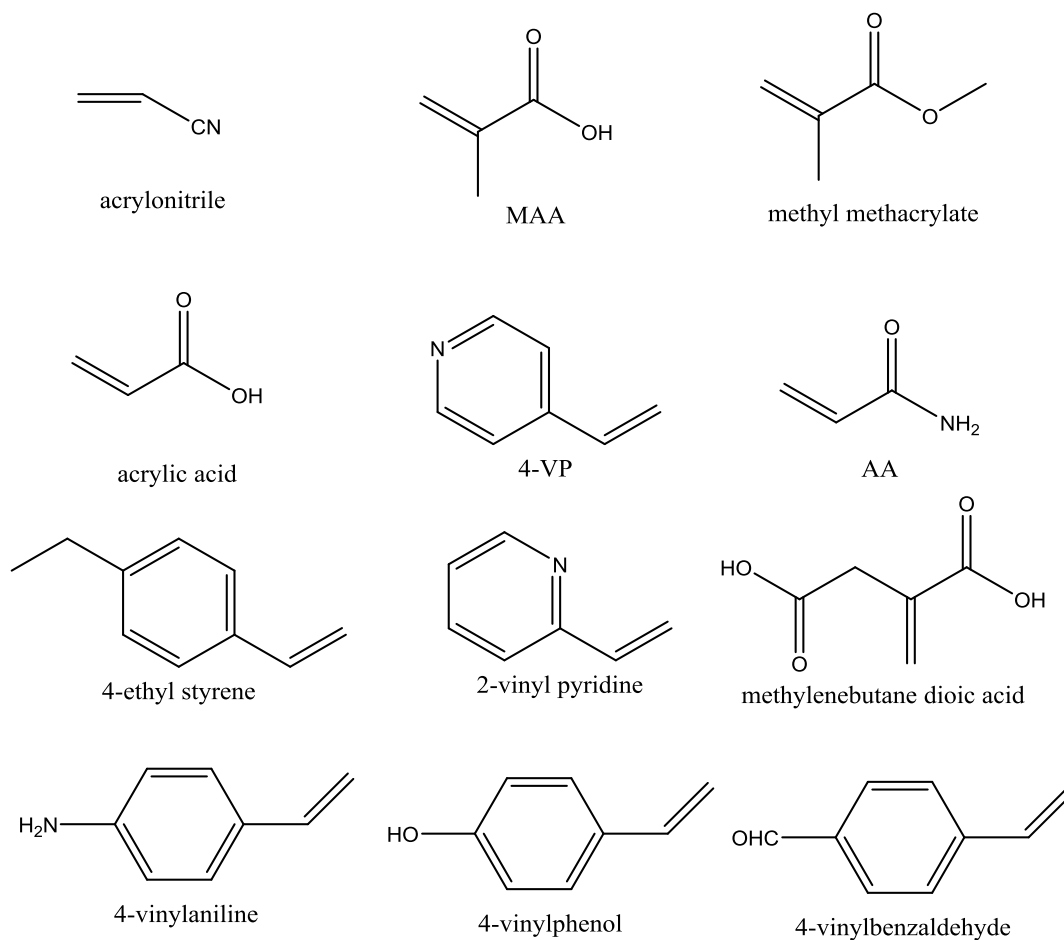
The selection of monomer is of vital importance in creating highly recognition sites of MIP towards target molecule. The key to synthesis MIP successfully is also depending on the monomer selection (Yan and Row, 2006). Generally, the main criteria for the selection of monomer are based on the molecular structure and functional group

of the template. There are two principles that need to abide strictly when choosing functional monomer. First, the monomer should be capable of matching the template in a complementary fashion in order to promote the formation of complex. Another requirement is that the monomer must be able to copolymerize with the crosslinking agent (Karim et al., 2005). Figure 1.3 illustrated the frequently applied commercially available monomers in the MIP preparation. The most commonly used monomer in MIP syntheses is MAA, due to its capabilities such as forming hydrogen bond, can act as proton donor as well as hydrogen bond acceptor. It has been employed extensively all the time (Sanagi et al., 2011). Moreover, amide and pyridine based monomer (such as AA, 2-vinylpyridine that containing) are also excellent functional monomers (Kartasasmita et al., 2013). These compounds can copolymerize with crosslinking agent while leaving nitrogen atoms suspending on the polymer chain. Thus, the template with  $-\text{COOH}$  or  $-\text{OH}$  groups can be bind to the nitrogen atoms through hydrogen bond. Recently, application of AA as functional monomer for MIP has been reported (Zhang et al., 2009; Jiang et al., 2012; Ji et al., 2013). All of these AA based MIPs showed strong hydrogen bonds even in polar solvent (Zakaria et al., 2009).

Optimization of functional monomer is of vital importance in the preparation of MIP with specific recognition. Traditional selection of monomer is based on the extensive and repetitive experimental trials (He et al., 2007). Owing to the rapid development in the computational science, computer simulation has been applied to study the selection of monomer in molecular imprinting technology (Piletsky et al., 2001). An increasing number of publication on theoretical studies towards MIP with the aid of computer simulation proved that this method could be useful in the rational



design, evaluation and prediction of adsorption behavior of MIPs (Chianella et al., 2002).

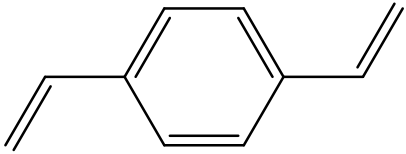
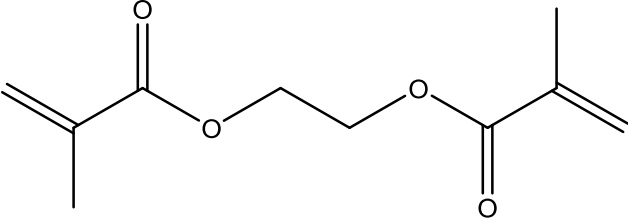
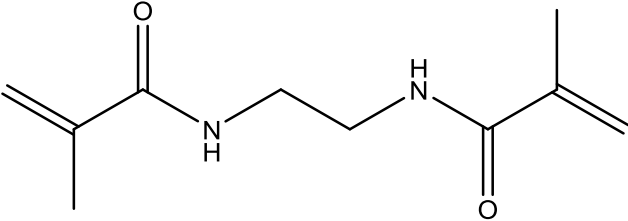
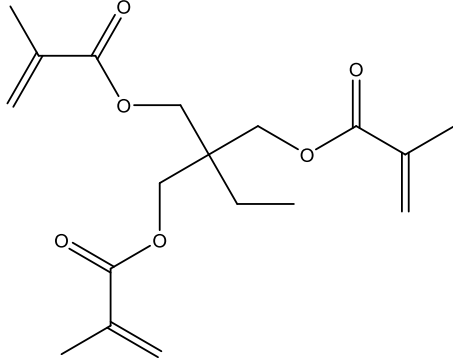
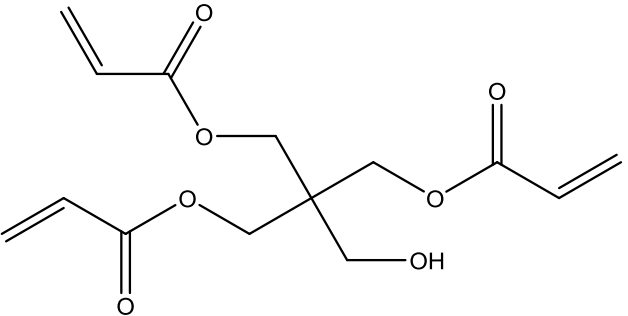


**Figure 1.3** Structures of some commonly used functional monomers.

The selection of cross-linker is another important factor in the synthesis of MIP. It is because cross-linker controls the polymer morphology, retains the binding site and enhances mechanical stability of the polymer matrix (Cormack and Elorza, 2004). Molecular imprinting technique requires high degree of crosslinking (above 80%), thus it accounts a high ratio in the reaction mixture. The amount of cross-linker also influences the performance of the polymer. It was shown that when the covalent approach was employed, decreasing the apparent degree of cross-linking resulted in a decrease in recognition sites and weak rigidity of the polymer (Yu and Mosbach, 2000).

High cross-link ratios are generally preferred in order to access porous materials and to generate materials with adequate mechanical stability (Vasapollo et al., 2011). Therefore, the appropriate MIP should have a certain rigidity to maintain the shape of the cavity and also possess good accessibility, thereby enhance binding capacity of the polymer (Arnold et al., 1999). Table 1.4 shows the most frequently used cross-linkers in the preparation of MIPs (Vasapollo et al., 2011). Among these cross-linkers, divinylbenzene (DVB) was the first crosslinker employed with the purpose of modern MIP preparation (Wulff and Sarhan, 1972). A later study by Wulff et al. (1987) compared the DVB with three other candidates namely, EGDMA, trimethylolpropane trimethacrylate (TRIM) and methylenebis-acrylamide. Their results suggested that the EGDMA was the best cross-linker and polymer fabricated using 70-95% proportion of EGDMA produced the MIP with the best performance for racemic resolution (Wulff et al., 1987). Nowadays, EGDMA has become the most widely used cross-linker.

**Table 1.4** Molecular structures of some cross-linking agents that have been used in the preparation of MIPs

DVB	
EGDMA	
N,N-Ethylenebis(methacrylamide) (EBMAA)	
Trimethylolpropane trimethacrylate (TRIM)	
Pentaerythritol triacrylate (PETRA)	

The solvent (porogen) or the medium of polymerization has a great influence on the imprinting process. This is because the assembly between the template and the monomer is related to the physical and chemical characteristics of the solvent (Pichon, 2007). The porogen serves to mix and solubilize all the reagents into homogeneous phase and also produces the pore in macroporous polymer that allows the target molecule to penetrate into the internal binding cavities (Spivak, 2005). The selection of solvent is according to the imprinting method. In the covalent imprinting, different solvents can be used, as long as all the components can be dissolved in the selected solvent. However, the solvent used for non-covalent imprinting polymerization required not only solubility to all reactants but also able to promote the non-covalent interaction between functional monomer and template molecule. The presence of solvent should not interfere the hydrogen bond, Van der Waals, and electrostatic forces between monomer and template (Zhou et al., 2010). MIPs are generally prepared using moderately polar or aprotic solvent, such as toluene, dichloromethane (DCM), chloroform and acetonitrile (ACN) as porogen. Therefore, polar interactions such as hydrogen bonds and electrostatic interactions can strongly take place in these organic media. Since the major interaction between template and monomer is hydrogen bonding, polar solvent can impact or even dissociate the non-covalent interaction in the prepolymerization complex. Thus, polar or protic solvents are not recommended in the preparation of MIPs (Pichon, 2007). On the contrary, less polar solvent, such as chloroform and toluene, provide better environment for the formation of monomer-template complex, and it leads to improve the performance of MIP (Spivak, 2005). Moreover, it was observed that, after the polymerization, the rebinding performance is optimized when carried out in the same solvent used for the imprinting (Fitzhenry et al., 2011).

Generally, free radical reaction is the most widely used approach to prepare MIPs because of its simplicity and time effectiveness (Boonpangrak et al., 2006). The polymerization process has three major steps: activation of monomer by initiator, propagation of the polymer chain by adding more and more monomers onto the reactive sites and termination that leads to the final product (Cormack and Elorza, 2004). The strict inert reactor is very essential in free radical polymerization as the oxygen from the environment can deactivate the radical species and stop the polymerization process. There are several common approaches to generate radical from radical initiator to initiate the polymerization reaction (Andersson, 2000). These approaches are thermal initiation, photo initiation and radiation-induced polymerization (Fitzhenry, 2011). Among these approaches, the thermal initiation is the most popular and simple method employed in MIPs preparation (Wei and Husson, 2007). Figure 1.4 showed the chemical structures of common radical initiator used in the preparation of MIPs. As in thermal initiation, in order to stabilize the template-monomer complex, the temperature of the reaction are often set at around 60 - 80 °C depending on the type of radical initiator. On the other hand, photo initiation has some advantages by allowing lower temperature for MIPs preparation but this method required additional instrumentation (Lu et al., 2004). Most photopolymerization reactions are chain-growth polymerizations which are initiated by the absorption of visible or ultraviolet light. The light may be absorbed either directly by the reactant monomer (direct photopolymerization), or else by a photosensitizer which absorbs the light and then transfers energy to the monomer. In general only the initiation step differs from that of the ordinary thermal polymerization of the same monomer; subsequent propagation, termination and chain transfer steps are unchanged (Zheng et al., 2013).

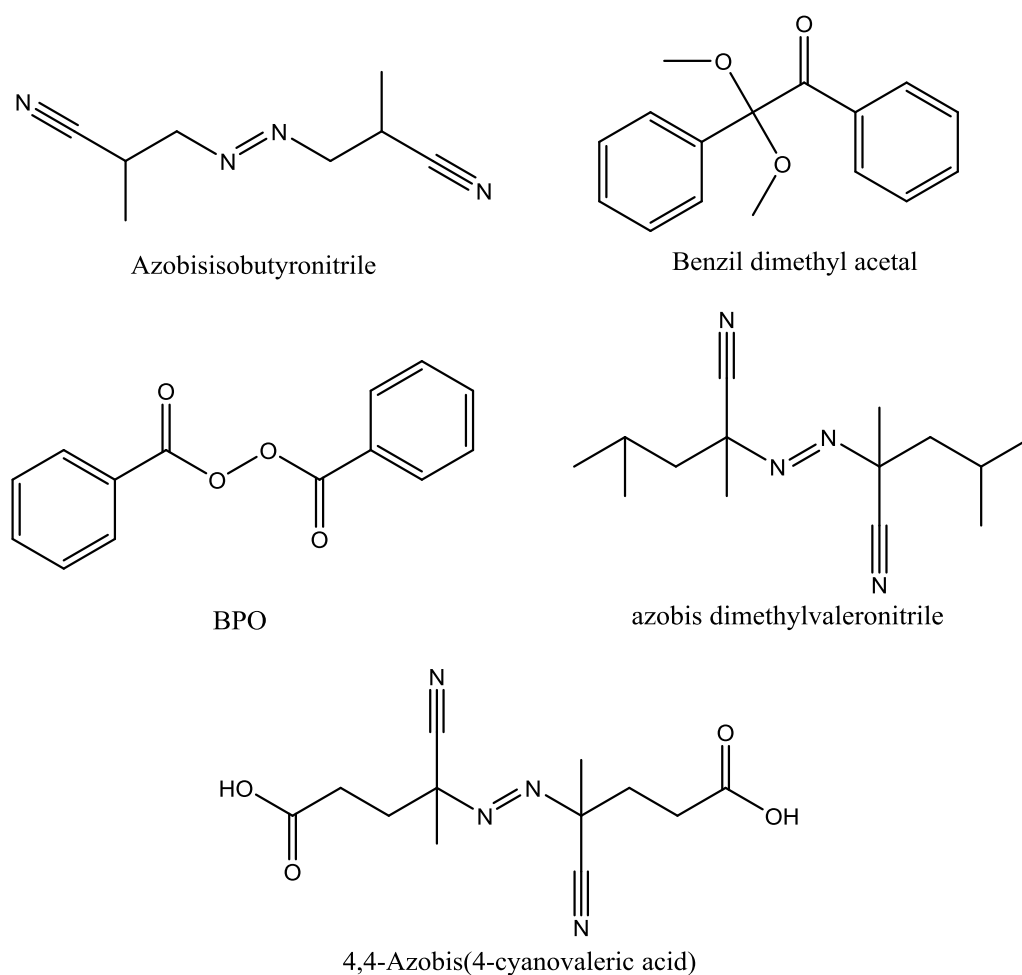


**Figure 1.4** Chemical structures of common initiator used in molecular imprinting.

### 1.2.5 Methods of polymerization

Recently, various polymerization approaches have been adopted in the preparation of MIPs. The most commonly used methods include bulk polymerization, suspension polymerization, precipitation polymerization, emulsion polymerization and multi-step swelling polymerization (Pérez-Moral and Mayes, 2004).

Bulk polymerization is the most widely used method to prepare the monolithic MIPs (Vasapollo et al., 2011). This method is achieved by mixing template, monomer, crosslinker and radical initiator in accordance with a certain proportion, in a solvent

(porogen). The polymerization reaction is triggered by thermal or photo initiation, of which generate a polymeric block after a few hours, grinding and sieving are required to obtain polymer particles with appropriate particle size. Soxhlet extraction and other extraction methods are often applied to remove the template molecule (Schumacher et al. 2011). This approach has been widely used due to its simplicity and applicability; however, it also has some disadvantages such as required grinding process that has the potential to damage the binding sites and low percentage of polymer yield (Diaz-Diaz et al. 2011).

Aqueous suspension polymerization (Lai et al. 2001) is performed by dispersing the mixture of template, monomer, crosslinker and radical initiator that pre-dissolved in organic phase, in water. Polymerization is occurred in water by forming MIPs in spherical shape. The size of MIP particles obtained through this method can reach the level of micro-meter and the grain size can be controlled by adjusting the volume of the organic phase as well as the stirring speed. Compared to other methods, suspension polymerization showed relatively simple operation and it produced MIPs with uniform particle size. Crushing and grinding is not required in this method. By using this method, Lee et al. (2008) successfully synthesized MIPs with micron-sized for the extraction of cholesterol. The column packed with this MIPs was found to be effective in the chromatographic separation of cholesterol from other steroids. On the other hand, in most syntheses, water or highly polar organic solvents (e.g., alcohol) are used as the medium for polymerization (Mayes and Mosbach, 1996). However, these solvents are incompatible with most covalent and noncovalent imprinting mixtures due to the competition between solvent and functional monomers for specific interaction with the target molecule. Since the dispersing solvent is present in excess, it saturates the

monomer and drastically reduces the number and strength of the interactions between functional monomers and target molecule. Later, this disadvantage was overcome by replacing water with tetrafluoride (Ansell et al., 1997). Even though fluorocarbon does not influence the interaction between monomer and template but this method is expensive.

Precipitation polymerization is also known as heterogeneous solution polymerization (Chaitidou et al., 2008). It begins initially as a homogeneous system in the continuous phase, where the monomer and initiator are completely soluble, but the synthesized polymer is insoluble in the selected solvent and thus precipitated (Cai et al., 2013). The polymerization reaction is triggered by light or heat to introduce free radical polymerization. Since this method does not require any additional stabilizer, thus, the surface of the resulting product is smooth and clean. The non-selective adsorption caused by stabilizer or surfactant also can be avoided (Wang et al. 2003).

Emulsion polymerization is implemented through emulsification of the relatively hydrophobic monomer in water with the aid of an emulsifier, followed by the initiation reaction with either a water-soluble or an oil-soluble free radical initiator (Yamak, 2013). The obtained MIP particles showed fine spherical shape with uniform particle size (Chern, 2006). The particle size of the resulting MIPs is reported to range from 50 to 500 nm. Due to its large specific surface area and strong adsorption capability, it has been widely used in the preparation of polymer of metal ion.

Multi-step swelling and polymerization is perhaps the best way to give monodisperse microspheres MIP (Sambe et al., 2007). In this method, the



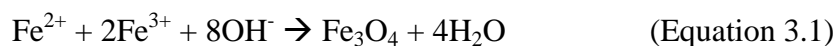
polymerization takes place in the aqueous solution, which resulting in the MIP that can be used in polar environment. At the same time, MIPs can be prepared in the form of spherical beads of controlled diameter. MIP beads synthesized in this way can be rendered magnetic through inclusion of iron oxide particles (Yan and Row, 2006). Previous study (Haginaka et al, 1998) has successfully prepared MIP that can recognize (S)-Naproxen by using this method. Although the particle showed preferably monodispersity with recognition ability, however, fairly complicated procedures and reaction conditions are required, and the aqueous suspensions used in this technique could interfere with the imprinting and thus lead to a decrease in selectivity (Fontanals et al., 2011).

### **1.3 Magnetic molecularly imprinted polymer (MMIP)**

#### **1.3.1 History of MMIP**

Magnetic nanoparticles are unique materials that emerged since 1980s. These magnetic nanomaterials have a unique characteristic where it can interact with magnetic fields and field gradients. At present, the magnetic nanoparticles are commonly consisting of magnetic elements such as iron, manganese, cobalt and their chemical compounds (Tan and Tong, 2007). Various types of magnetic nanoparticles have been synthesized and it includes iron oxides; ferrites of cobalt, manganese, nickel, and magnesium; and FePt,  $\gamma$ -Fe<sub>2</sub>O<sub>3</sub>, cobalt, iron, nickel,  $\alpha$ -Fe, CoPt, and FeCo particles (Beveridge et al., 2011). Among these magnetic nanoparticles, Fe<sub>3</sub>O<sub>4</sub> or magnetic iron oxide nanoparticles (MION) has been the most commonly employed magnetic nanoparticles in various researches since it can be easily synthesized through co-precipitation method.

Co-precipitation method is the most economical pathway in order to obtain MION from aqueous  $\text{Fe}^{2+}/\text{Fe}^{3+}$  salt solutions by the addition of a base at room temperature or at elevated temperature (Karaagac et al., 2010) as shown by the following chemical equation.



So far, only MION is considered biocompatible, thus, it is the only nanoparticle material that have been approved by U.S. Food and Drug Administration (Beveridge et al., 2011). MION has been used in very versatile ways in different researches due to their nano-size, can be easily surface modified and magnetic properties (Bucak et al., 2012). MION can be surface modified by coating it with silane or silica gel to form the core-shell structurally microspheres. The resultant microspheres exhibit not only magnetism but also functionality which feasible the coupling of variety chemicals such as biological molecules, ligands and polymers. Under the external magnetic field, the magnetic microspheres can be easily separated from the substrate. In addition, the magnetic microspheres posses large surface area, from which provide a broad application prospect towards cell separation, protein purification, DNA testing as well as analytical method.

The development of analytical techniques has begun to integrate MION to take advantage of its ability to magnetically induce motion, enhance signals, and switch behaviors. The applications of MION for analytical methodologies are include pre-concentration, separation, sensors, detections and imaging (Beveridge et al., 2011). Recently, MMIP have been frequently used in the separation of various target chemicals from different complex matrices such as environmental samples and biological fluids. Conventional MIPs are often prepared by bulk polymerization or precipitation

polymerization (Cheng et al., 2014). These MIPs showed poor binding capacities and low binding kinetics of the target compounds because of the embedded binding sites (Xie et al., 2014). The application of these conventional MIPs as adsorbent for solid phase extraction (SPE) also involved additional preparation steps such as crushing and grounding of these polymers into the fine powder followed by the SPE cartridge packing (Wulandari et al., 2014; Sun et al., 2014). The major disadvantage of this convention SPE is its extraction efficiency that influences by the uploading rate of sample and the eluent. As a result, various approaches have been developed in imprinting MIP onto the surface of different solid supports (Xie et al., 2014). This method can enhance the binding capacity of MIP through the provided high surface area. MION with small particle size have been considered as an ideal solid support in the preparation of MMIP due to its large surface area for adsorption (Xie et al., 2014). As compared to other solid supports, MION offers an added advantage of being magnetically separable and thereby eliminating the requirement of filtration and SPE cartridge packing (Zheng et al., 2014). The MMIP have been synthesized by using different methods. However, the most commonly used preparation process often involved the following four steps (Chen and Li, 2012);

(1) Preparation of MION (Businova et al., 2011) through co-precipitation method.

(2) Surface modification or functionalization of MION (Hood et al., 2014). So far, two methods are usually applied in the surface modification or functionalization of MION. The first approach is silanization method where MION are coated with SiO<sub>2</sub> shell through Stober method and then modified by silane coupling agent, such as 3-(trimethoxysilyl)propyl methacrylate (Courtois, 2006). Another approach is to coat

MION with surfactants or organic molecule, such as ethylene glycol or oleic acid (Cai et al., 2013).

(3) Surface-imprinted polymerization using functionalized MION as solid support. The polymerization is performed with the presence of the template molecule, functional monomer and cross-linker (Kong et al., 2012).

(4) Removal of template molecules from MMIP (Vasapollo et al., 2011).

### **1.3.2 Application of MMIP**

Magnetic polymer composite particles, agarose–polyacrylamide beads, were first synthesized in the 1970s (Ansell and Mosbach, 1997). Since then, a wide range of MMIP have been developed for various purposes. For example, magnetic polymer particles coated with specific organic ligands have been used in immunoassay, isolation of nucleic acid sequence, isolation of microorganisms from samples in the food industry, chromatographic separation of proteins from fermentation broths and magnetically stabilized fluidised-bed separations (Ansell and Mosbach, 1997; Guesdon and Avrameas, 1981; Albretsen et al., 1990; Safarik et al., 1995; Burns and Graves, 1987). Magnetic particles derivatized with proteins have been used as biosensors, either for the measurement of magnetic forces or using magnetism to trap the recognizing element (Baselt et al., 1997; Miyabashi and Mattiasson, 1988) or compounds such as dibutyl phthalate, 2,4,6-trinitrotoluene, HIV-1 antibody and bisphenol-A (Alizadeh, 2014; Zhou et al., 2014; Zhu et al., 2014; Li et al., 2015). In addition, MMIP also has been used to isolate and separate bioactive compounds such as curcuminoids, gastrodin,

quercetagenin and rhaponticin from plants extracts (Chen et al., 2012; You et al., 2014; Ji et al., 2014; Ma and Shi, 2015).

In analytical chemistry, MMIP are mainly used as solid phase in the determination of various organic pollutants including antibiotics. Like antibiotics, Chen et al (2010) synthesized the MAA-based MMIP with ciprofloxacin as template for the recognition of fluoroquinolone antibiotics in environmental water. This MMIP was found to have the ability to recognize fluoroquinolones antibiotics from SAs. Zhang et al (2010) synthesized the MAA-based MMIP by using penicillin V, a  $\beta$ -lactam antibiotic, as template. This MMIP showed high affinity and selectivity towards penicillin V and other structurally related  $\beta$ -lactam antibiotics. By using erythromycin as template, MAA-based MMIP has been synthesized by Zhou et al (2015) for the recognition of macrolide antibiotics. This MMIP showed favorable selectivity towards multiple macrolide antibiotics as compared with SAs.

Nowadays, only 4 studies were focused on the application of MMIP in the extraction of SAs. The first study reported by Chen et al. (2009b) involved the application of MAA-based MMIP employed in the extraction of SAs from honey. In this study, SMD was selected as template and the result indicated that the synthesized MMIP was selective towards the adsorption of different SAs include sulfadiazine (SDZ), sulfamerazine (SMR), sulfamethoxydiazine (SMD), sulfamonomethoxine (SMM), sulfadimethoxine (SDM), sulfamethoxazole (SMO) and sulfaquinoxaline (SQX) as compared with structural unrelated chloramphenicol. The second study was reported by Kong et al. (2012) where MAA-based MMIP was used to recognize SAs in the poultry feed. In this study, SMZ was used as template and the result indicated that the MMIP

was only selective towards the recognition of template molecule. Chen et al (2013) applied the MAA-based MMIP for the recognition of SAs and their acetylated metabolites from environmental water. In this study, SMD was used as template for MAA-based MMIP and the selectivity study was performed by using SDZ, SMD, SMM, SQX, *N*<sub>4</sub>-acetyl-sulfadiazine, *N*<sub>4</sub>-acetyl-sulfamethoxydiazine, *N*<sub>4</sub>-acetyl-sulfamonomethoxine and *N*<sub>4</sub>-acetyl-sulfaquinoxaline. The result indicated that this MMIP can be used to recognize all selected compounds except sulfadiazine and *N*<sub>4</sub>-acetyl-sulfadiazine. Recently, Zhao et al (2014) reported the application of core-shell nanoring amino-functionalized MMIP for the extraction of 22 SAs in chicken breast muscle. In this study, 22 selected SAs that complexed with tetraethylenepentamine were used as template. By using this approach, the synthesized MMIP have been successfully used to extract 22 selected SAs from chicken breast muscle.

Based on these 4 studies, it can be concluded that the recognition property of MMIP was largely influence by selection of template molecules. The template such as SMD yielded multi-functional MMIP whereas another template such as SMZ yielded very selective MMIP. The study by Zhao et al (2014) indicated that multi-functional MMIP can be synthesized but it involved the usage of all interested SAs as template. In this study, a multi-functional MMIP was synthesized based on the designed amino acid-based monomers according to computational study.

## 1.4 Objectives of study

The main focus of this study was to develop a multi-functional magnetic MIP in the extraction of SA antibiotics namely, SDZ, SMR, SPY and STZ. It has been reported that the adsorption of template molecule by MIPs was mimicked to the natural recognition pathways by natural recognition elements such as enzyme (Kryscio and Peppas, 2012). Therefore, the interaction between the selected SAs and monomers are expected to mimic the interaction of SMO with dihydropteroate synthase found in the protein databank. The x-ray crystal structure of dihydropteroate synthase-SMO complex (PDB (Protein Data Bank) ID: 3TZF) shows the SMO was bound to serine through hydrogen bonding at sulfonyl group of SAs. Presumably, SAs also have relatively similar interactions as the interaction between amino acid with SMO in dihydropteroate synthase-SMO complex. Therefore, the main objectives of this study were:

- (1) determine the most suitable amino acid based monomer so as to prepare multi-functional MMIP by using computational method,
- (2) synthesize and characterize the amino acid-based magnetic MIP (SMIP),
- (3) investigate the adsorption property of to investigate the adsorption property of SMIP towards selected SA antibiotics,
- (4) compare the performance of SMIP with acrylamide-based magnetic MIP (AMIP) in the adsorption of SA antibiotics.

## **CHAPTER 2 MATERIALS AND METHOD**

### **2.1 Docking methods**

#### **2.1.1 Software and Hardware**

Computer modeling was carried out using well known molecular modeling software program AutoDock Tools 1.5.6, Chemdraw Ultra 8.0 and Hyperchem Professional 8.0 software package (Hypercube, Inc.) were used to assist in providing necessary files for further application. Computer workstation with the configuration of Inter Core2 Quad CPU Q9300@2.50 GHz, 4.00 gigabyte RAM, 200 gigabyte hard disk, Windows XP system operation was adopted to perform docking analysis during the whole prediction process.

#### **2.1.2 Molecular file preparations**

##### **2.1.2.1 Molecular 3D structure information**

Chemdraw Ultra 8.0 was applied to build the structure of monomers. Hyperchem 8.0 software package (Hypercube, Inc.) was applied to optimize the monomer geometrically. Semi-empirical method was adopted to perform geometry optimization with the combination of Steepest Descent and Conjugate Gradient Algorithm. The resultant molecules were saved as PDB format for further application. The 3D structure information of SMO was extracted from PDB structure of SMO that bound to protein



complex (PDB ID: 3TZF). 3D structure of SDZ was obtained by the modification of SMO followed by geometrical optimization using semi-empirical method.

#### **2.1.2.2 AutoDock input file preparation and docking experiment**

The AutoDock input file of the ligand (SMO or SDZ) and receptors (monomers) were prepared using AutoDockTools software and saved in PDBQT format. Each molecule was added with polar hydrogen atoms and its non-polar hydrogen atoms were merged. As for ligands, non-polar hydrogen atoms were merged with assigned Gasteiger charges. All rotatable bonds of ligands were set to be rotatable. Docking was performed using genetic algorithm and local search methods (termed as Lamarckian Genetic Algorithm). The population size of 10 million energy evaluations was used for 100 times searches. The grid definition, adjusting to the monomer active site, was set up manually, following the recommendations of the program manual (Trott and Olson, 2010; Sanner, 1999). Thus, a 40\*40\*40 dimension of grid box size and 0.375 Å grid was spacing around the monomer. Clustering histogram analyses were performed after the docking searches. Before running each docking calculations, a configuration file was generated with grid size and coordinates information, as well as indicating ligand and receptor files. The reports (log files) for each calculation were analyzed, in order to obtain free-energy ( $\text{kcal mol}^{-1}$ ) values of each ligand conformations with its respective complex. The best conformations were chosen from the lowest docked energy that populated in the highest number of molecules in a particular cluster with not more than 1.5 Å root-mean-square deviation (rmsd). The hydrogen bond was also analyzed using AutoDockTools.

### 2.1.3 Computational study of MIP and template interaction

Geometrical optimizations in the search of possible interaction between the monomers, with the templates (SDZ) and SMR, were carried out using Semiempirical (PM3), ab initio (HF/6-31G(d)) and Density Functional Theory (DFT) using Becke's three-parameter Lee-Yang-Par (B3LYP) functional and 6-31G(d) basis set. Then, single point energy calculation was performed on the optimized structure to estimate the interaction energy ( $\Delta E_{int}$ ) between the template and monomer from the equation;  $\Delta E_{int} = E_{complex} - E_{template} - E_{monomer}$ . The optimized structures from B3LYP/6-31G(d) method have been adopted in scanning the interaction energy between the SDZ and SMR with monomer against the distance from -1.000 to +4.000 angstrom of the distance with the step size of 0.200 Å. All the quantum calculations were performed using Gaussian 09 software.

## 2.2 Synthesis of amino acid based monomer

### 2.2.1 Materials

Ethylene glycol dimethacrylate (EGDMA, 97.5%), iron(II) chloride tetrahydrate ( $\text{FeCl}_2 \cdot 4\text{H}_2\text{O}$ , 99.0%), iron(III) chloride ( $\text{FeCl}_3$ , 98%), ammonium hydroxide (25.0%), 1-ethyl-3-(3-dimethylaminopropyl)carbodiimide hydrochloride (EDCI HCl, 99.0%), *N,N*-diisopropylethylamine (DIEA, 98.0%), dichloromethane (DCM, 99.8%), sodium bicarbonate ( $\text{NaHCO}_3$ , 99.7%) were purchased from Merck. 3-(methacryloyloxy)-propyltrimethoxysilane (MPS, 97.0%) was obtained from Alfa Aesar. Sulfadiazine (SDZ, 98.0%), acetic acid (HAc, 99.7%), triethylamine (TEA,

99.5%), allylamine hydrochloride (98.0%), benzoyl peroxide (BPO, 75%), dimethylformamide (DMF, 99.8%) were from Sigma-Aldrich. Acetonitrile (ACN, 99.9%), ethyl acetate (EA, 99.8%), methanol (99.9%) were from RCI Labscan. Acrylamide (AA, 98.0%), 4-dimethylaminopyridine (DMAP, 98.0%) were purchased from Fluka. Toluene (99.5%), magnesium sulfate ( $\text{MgSO}_4$ , 98.0%) were from Friendemann Schmidt. Ethanol (99.9%) was obtained from Kollin Chemicals. Hydroxybenzotriazole (HOBT) and Fmoc-O-trityl-L-serine were obtained from Novabiochem.

### 2.2.2 Procedure of monomer-2 synthesis

Figure 2.1 shows the process of synthesis for Monomer-2. Coupling reagents HOBT (0.196 g), EDCI HCl (0.243 g), DMAP (0.013g) and Fmoc-O-trityl-L-serine (0.6 g) were mixed and sealed in 100 mL round bottom flask. The mixture was dried using vacuum pump. Anhydrous DIEA (0.805 mL) was added thereafter following by dried DCM (30 mL) as solvent. The mixture was stirred for 1h before adding dried allylamine hydrochloride (0.098 g), which was pre-dissolved in DCM in advance. The reaction was conducted at room temperature for 24 h, under nitrogen atmosphere. After reaction, the excess solvent was removed by rotary-evaporator and EA (25 mL) was added to dissolve the solid residue. The resultant suspension was filtered and the filtrate was washed with water (2 x 20 mL), saturated sodium bicarbonate solution (10 mL), and brine (10 mL). The filtrate was then dried with  $\text{MgSO}_4$  and the solvent was removed using rotary-evaporator to give the faint yellow product (0.69 g, 85.0%).

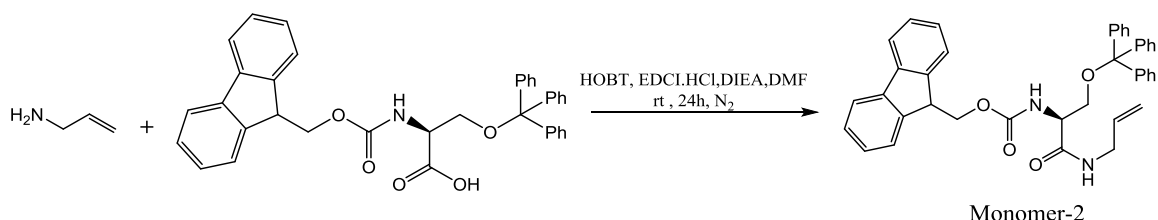


**Figure 2.1** Synthesis pathway of Monomer-2.

### Spectral Data of Monomer:

<sup>1</sup>H NMR (CDCl<sub>3</sub>, 400 MHz, ppm): 7.69-7.15(m, 23H, Fmoc and TRT), 6.37(m, 1H, Ally-CH<sub>2</sub>-NH), 5.75-5.71 (m, 1H, CH<sub>2</sub>-CH-CH<sub>2</sub>), 5.542 (d, 1H, NH-COO), 5.06-5.02 (m, 2H, Ally), 4.31-4.29 (m, 3H, CO-CH-NH, CH<sub>2</sub>-Fmoc), 4.12-4.03 (m, 1H, TRT), 3.85-3.82 (d, 2H, Ally-CH<sub>2</sub>), 3.62-3.60 (d, 1H, CH<sub>2</sub>-O-TRT), 3.14-3.10 (m, 1H, CH<sub>2</sub>-O-TRT). <sup>13</sup>C NMR: 42.22, 47.19, 63.77, 67.24, 87.40, 116.94, 120.11, 125.15, 127.19, 127.44, 127.87, 128.15, 128.62, 133.75, 141.39, 143.41, 143.82, 156.14, 169.80.

### 2.3 Preparation of MMIP

Before proceeding through the synthesized monomers, model study regarding preparation of MMIP was conducted by commercially available monomer. This commercially available monomer is acrylamide (AA). The synthesis of MMIP via a multistep procedure is illustrated in Figure 2.2. In this protocol, MION was synthesized by a co-precipitation method. Then the hydroxyl groups on the surface of the MION were reacted with MPS to introduce vinyl groups. The polymer shells were coated on the surface of MION by the copolymerization of functional monomer, cross-linking agent (EGDMA), initiator (BPO), and template molecule (SDZ). Finally, the templates were removed and the imprinted polymer was obtained. The magnetic non imprinted

polymer (MNIP) were also prepared using the similar procedure, but without the addition of template SDZ. SMIP and SNIP were also synthesized using the same procedure.

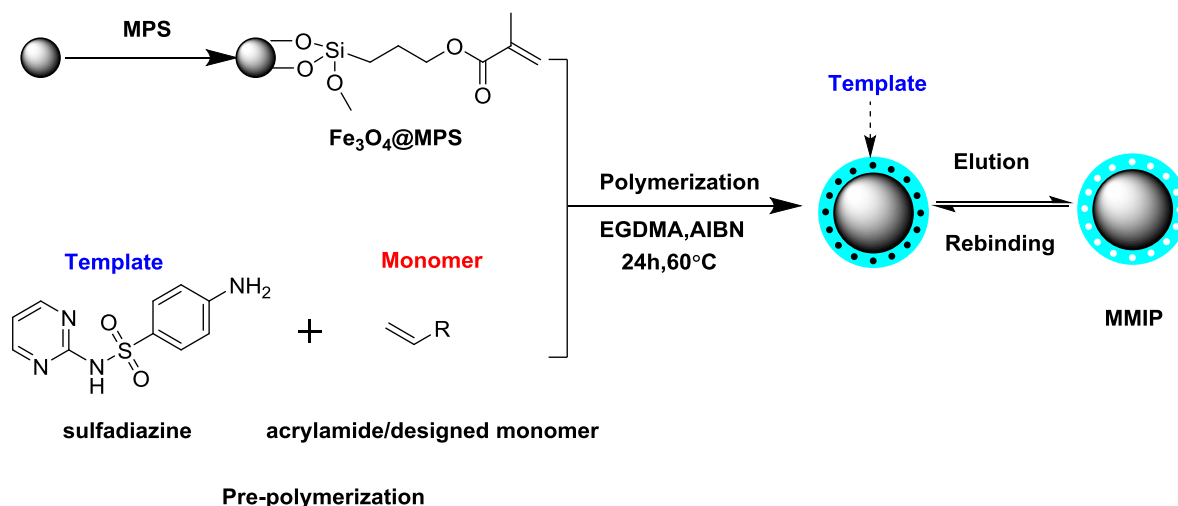


**Figure 2.2** Overview of the synthesis of MMIPs.

### 2.3.1 Synthesis of MION

MION was synthesized by using co-precipitation method as reported by Karaagac et al (Karaagac et al. 2010). Briefly, FeCl<sub>2</sub> 4H<sub>2</sub>O (15.90 g) and FeCl<sub>3</sub> (19.46 g) were dissolved in 100 mL of deionized water containing in a 250 mL round bottom flask and the mixture was vigorously stirred. As the temperature elevated to 80 °C, 50 mL of ammonium hydroxide was added through 20 min, and the reaction mixture was stirred for 60 min. After the reaction, the black precipitate was separated by external magnetic field and the supernatant was decanted. The black precipitate was washed for six times with distilled water, then the MION was freeze dried.

### **2.3.2 Synthesis of MION@MPS**

Surface modification of MION with MPS was performed as follows: 200 mg MION was vacuumed for 30 minutes before adding 100 mL anhydrous toluene and 0.1 mL triethylamine. Then the mixture was dispersed by sonication in 20 minutes and stirred vigorously (500 rpm). 0.4 mL of MPS was added. The reactant was refluxed for 36 h under nitrogen atmosphere and vigorous stirring. The resultant product was collected by an external magnetic field, and rinsed thoroughly with ethanol by six times and dried under vacuum at room temperature.

### **2.3.3 Preparation of MMIP and MNIP**

#### **2.3.3.1 Preparation of AMIP and ANIP**

AMIP were prepared by non-covalent imprinting approach. SDZ (95 mg) and AA (135 mg) was mixed in 60 mL ACN-toluene with the ratio of 3:1 (v/v), and the mixture was refrigerated 12 h to form a pre-assembly solution. Then, MION (100 mg), EGDMA (1 mL) and BPO (138 mg) were added to a 250 mL flat bottom flask containing ACN-Toluene mixture. The mixture was sonicated for 20min and simultaneously purged with nitrogen gas. Then, the pre-assembly solution was added through a cannula under nitrogen atmosphere. This combined mixture solution was first prepolymerized at 50 °C for 6 h, polymerized at 60 °C by 24 h, and further aged at 85 °C in 6 h. After polymerization, the MION-MIP was precipitated by external magnetic field and rinsed with ACN. The SDZ (template) in AMIP were extracted with methanol-HAc (9:1, v/v).

Then, the AMIP was repeatedly washed with methanol and dried under vacuum. ANIP was prepared following the same procedure in the absence of template.

### **2.3.3.2 Preparation of SMIP and SNIP**

The SMIP were prepared by using similar method as AMIP. SDZ (25 mg) and monomer-2 (243 mg) was mixed in 20 mL ACN and the mixture was put in refrigerator for 12 h to form template-monomer complex. Then, MION@MPS (200 mg), EGDMA (3.77 mL) and BPO (20 mg) were added to a 250 mL flat bottom flask containing ACN-Toluene mixture. The mixture was sonicated for 20 min and simultaneously purged with nitrogen gas. Then, the pre-assembly mixture solution was added, the mixture was prepolymerized at 50 °C for 6 h, polymerized at 60 °C for 24 h, and further aged at 85 °C for 6h. After the reaction, the SMIP was separated by external magnetic beads and rinsed with ACN 3 times. The template was extracted with methanol-HAc (9:1, v/v). Finally, the product was repeatedly washed with methanol to remove the acetic acid and dried under vacuum. SNIP was prepared following the same procedure without involving template SDZ.

## **2.4 Binding experiments**

### **2.4.1 Binding experiment of AMIP and ANIP**

All binding experiments were carried out at room temperature as described by Kong et al (2012). In kinetic adsorption experiment, 10 mg of AMIP or ANIP was added to 3 mL of 10  $\mu\text{g mL}^{-1}$  SDZ solution with ACN as solvent. The mixture was vortexed at

regular time intervals ranging from 10s to 1800s. The AMIP or ANIP was separated by an external magnetic field and the concentration of the remaining SDZ in the solution was measured by using HPLC. In the isothermal binding experiment, 10 mg of AMIP or ANIP were added to 3 mL of SDZ solution with the concentration ranging from 0.50 to 30  $\mu\text{g mL}^{-1}$ . The mixture was vortexed by 20 minutes at room temperature. The AMIP or ANIP were separated from SDZ solution by an external magnetic field and the concentration of SDZ in the supernatant was measured by HPLC.

#### **2.4.2 Binding experiment of SMIP and SNIP**

In kinetic adsorption experiment, 10mg of SMIP or SNIP were added to 3 mL of 10  $\mu\text{g mL}^{-1}$  of SDZ solution, and shaken at fixed time intervals vary from 10 to 1200 s. After the supernatants and polymers were separated by an external magnetic field, the amount of SDZ bound to the SMIP or SNIP was determined by a HPLC method. In the isothermal adsorption study, 10 mg of SMIP or SNIP were added to 3mL SDZ solution of various concentrations from 0.50 to 30  $\mu\text{g mL}^{-1}$ . The mixture were shaken in 20 minutes at room temperature. The supernatant and polymer were separated by an external magnetic field, and the concentration of SDZ in the supernatant was examined by HPLC.

#### **2.4.3 Specific recognition of AMIP and ANIP**

10 mg of AMIP or ANIP were added to the 3 mL of ACN solution consist of SDZ, SMR, SAA, SMZ, and SMO with a concentration of 10  $\mu\text{g mL}^{-1}$  for each compound. After being shaken 20 min at room temperature, the supernatants and polymers were



separated by an external magnetic field, the amount of SDZ and its analogues in the supernatants was measured by HPLC.

#### **2.4.4 Specific recognition of SMIP and SNIP**

10 mg of SMIP or SNIP were added to the 3 mL of ACN solution containing the mixture of SDZ, STZ, SPY, SMR, DEET and benzylparaben with a concentration of  $10 \mu\text{g mL}^{-1}$  respectively. After being shaken for 20 min at room temperature, the supernatant and polymers were separated by an external magnetic field, the amount of SDZ and its analogues in the supernatant were tested by HPLC.

#### **2.5 Instrumental analysis**

Infrared spectra were recorded with a Perkin Elmer 400 ATR-FTIR spectrophotometer. IR spectra of MMIP and MNIP were collected in transmission mode by pressing the particle sample with potassium bromide powder to form pellets. A resolution of  $2 \text{ cm}^{-1}$  and a total of 8 scans were applied to collect the IR spectra.

Thermal gravimetric analysis (TGA) measurements were employed in order to investigate the difference of decomposition stages of particles stability of the polymer at high temperature condition. The study was performed on a TGA 4000 Perkin-Elmer instrument. Each sample was heated between  $40 \text{ }^{\circ}\text{C} - 900 \text{ }^{\circ}\text{C}$  ( $10 \text{ }^{\circ}\text{C min}^{-1}$ ) under air flow ( $30 \text{ mL min}^{-1}$ ).

The morphology of the MMIP and MNIP were obtained by scanning electron microscopy (SEM) (Hitachi SU8220). Samples were mounted on carbon tape onto aluminum sample holders for analysis.

All HPLC analyses were performed using Shimadzu HPLC system consisted of a LC-20AT pump, a SPD-M20A diode array detector, a SIL-20AHT auto sampler, a CTO-20AC column oven and a CBM-20A communication bus module (Shimadzu, Japan). A reversed-phase Supelco Ascentis C18 column (150 mm  $\times$  4.6 mm; Sigma-Aldrich, USA) was used in analyte separation. The mobile phase was a mixture of ACN and 0.1% formic acid in deionized water. The flow rate was maintained at 1.0 mL min<sup>-1</sup> for all runs. Isocratic elution was performed with 70% of ACN. The injection volume was 10  $\mu$ L, and the column effluent was monitored at 258 nm.

## CHAPTER 3 RESULTS AND DISCUSSION

### 3.1. Design of monomer through the molecular docking

Based on the literature search, only one crystal structure that related to SAs was reported by Protein Data Bank (PDB). This crystal structure was formed through the interaction between dihydropteroate-synthase and SMO (Figure 3.1). The crystal structure showed that the SMO binds to the dihydropteroate-synthase through one of the amino acid called serine. In this crystal structure, SMO interacts with serine through hydrogen bonds that formed at its sulfonyl group (Figure 3.2). Presumably, serine is a good candidate in order to prepare multi-functional MIP since the binding site is not at the substituted group of SA. To enable the serine to be used as monomer, the molecular structure of serine need to be modified for the addition of unsaturated double bond. As a result, the first designed monomer was (L)-N-allyl-2-amino-3-hydroxypropanamide (Figure 3.3). This monomer was labeled as Monomer-1.

A series of binding energies were then calculated by using molecular docking method in order to compare the strength of the interaction between SMO with Monomer-1 and various commercially available monomers. As compared with other commercially available monomers, Monomer-1 produced the lowest binding energy of  $-2.87 \text{ kcal mol}^{-1}$  (Table 3.1). This result indicated that SMO can form more stable complex with Monomer-1 as compared to other commercially available monomers.

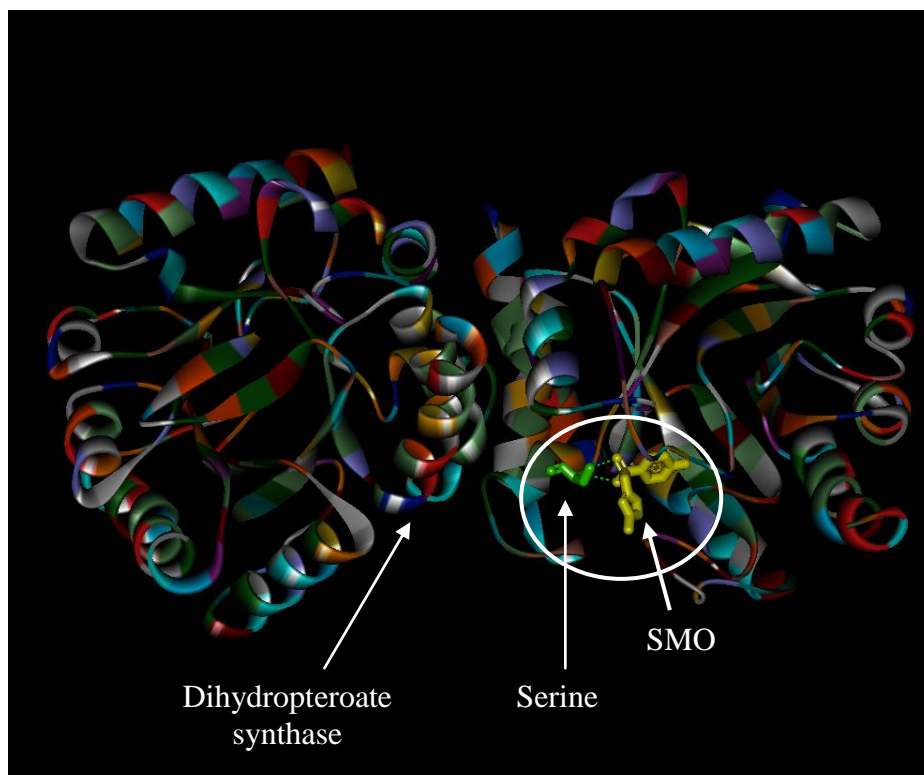


**Figure 3.1** The crystal structure of SMO-dihydropteroate synthase.

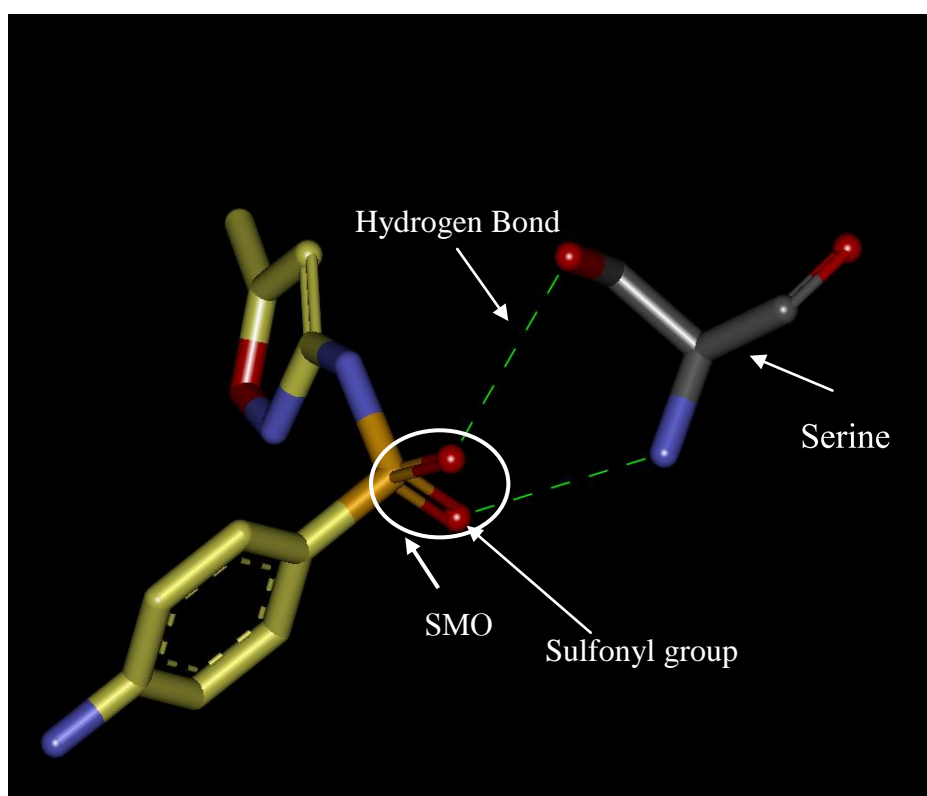


**Figure 3.2** Interaction between SMO and serine in dihydropteroate synthase.

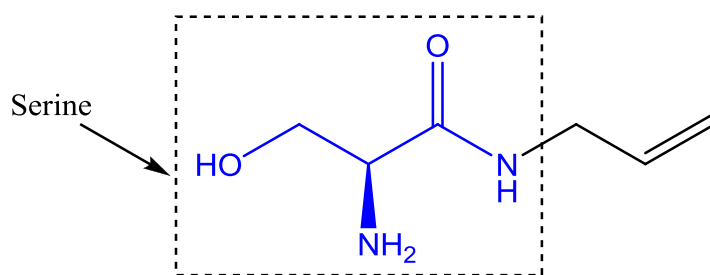


**Figure 3.3** The structure of Monomer-1.

**Table 3.1** Binding energies of SMO with Monomer-1 and commercially available monomers estimated using the Autodock Tools 1.5.6.

Monomer	Lowest Binding Energy (kcal mol <sup>-1</sup> )
Monomer-1	-2.87
Commercially Available monomers	
Allylamine	1.47
N-(3-aminopropyl)methacrylamide hydrochloride	-2.29
Aminoethyl methacrylate.HCl	-0.12
Ethyleneglycol methacrylate phosphate (EGMP)	-0.37
N,N'-Methylenebis(acrylamide)	-1.94
Acrylamido-2-methyl-1-propanesulfonic acid	-1.65
Aminoethyl methacrylate	-1.32
Itaconic acid	-2.58
1,3,5-Trihydroxystyrene	-1.78
AA	-1.94
N,N-Diethylamino ethylmethacrylate (DEAEM)	-1.40
EGDMA	-1.58
MAA	-1.87
N-(3-aminopropyl)methacrylamide (APMA)	11.94
Allylamide	-1.94

According to the interaction between Monomer-1 with SMO (Figure 3.4), the result indicated that hydrogen bonds were formed at 3 locations: oxygen atom at 5-methylisoxazole moiety (1), oxygen atom at sulfonyl group (2) and the hydrogen atom at the amine group (3) of SMO. In order to produce a multi-functional MMIP that enables the extraction of sulfa drugs homologue series, the binding site should be located at 4-aminobenzenesulfonamide moiety of the sulfa drugs. Although Monomer-1 can interact with SMO with the lowest binding energy, but it is not a suitable candidate in the preparation of multifunctional MMIP of this study.

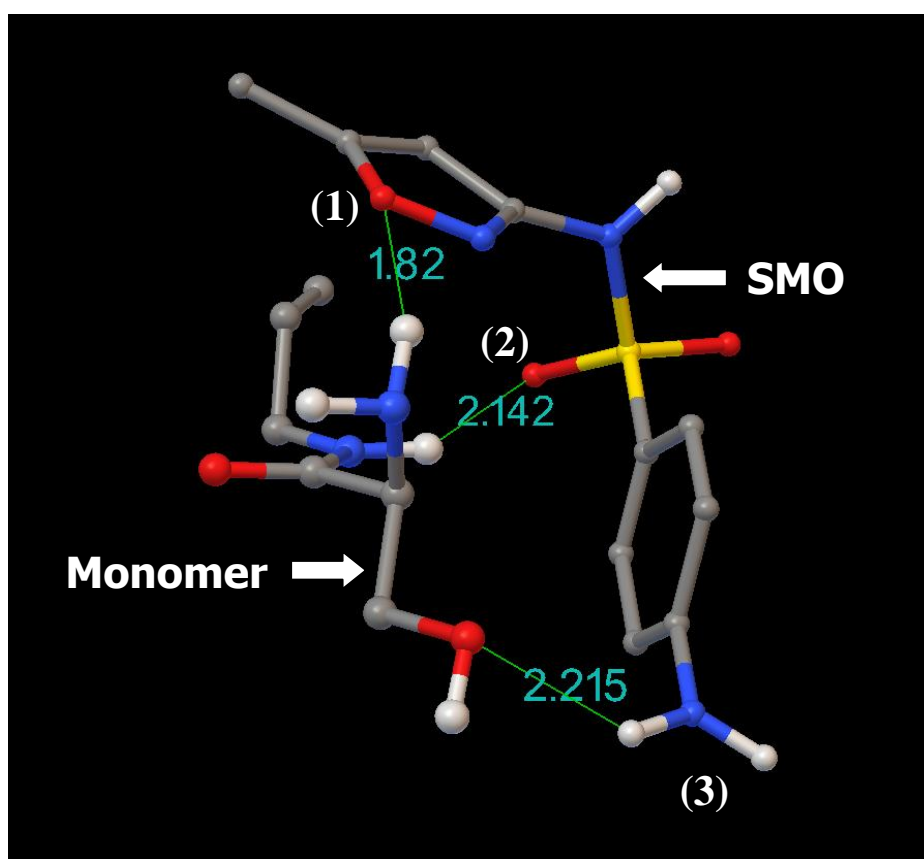


**Figure 3.4** Interaction between SMO and Monomer-1. (Green line representing the hydrogen bonding).

The following step of this experiment was to replace the template molecule and Monomer-1, in order to obtain the best monomer and template that interacts at 4-aminobenzenesulfonamide moiety of the sulfa drugs. Based on the literature search, serine with different protecting groups are commercially available. These serine derivatives include Boc-Ser-OH, Boc-D-Ser-OH, Boc-Ser-Bzl-OH, Boc-Ser-Me-OH, Boc-Ser-tBu-OH-DCHA and Fmoc-O-Trityl-L-Serine (Figure 3.5). According to Kareuhanon et al., (2009), hydrophobic interaction can enhance the interaction between MIP and template. Therefore, the binding energy of the interaction between serine with various non-polar protecting groups was calculated. Fmoc-O-Trityl-L-Serine has two protecting groups, Fmoc that bonded to the amine group of serine and trityl group that attached to the hydroxyl group of serine. The computational study was started by calculating the binding energy of the interaction between Fmoc-O-Trityl-L-Serine with new template molecule, SDZ, by using molecular docking method. Then, the obtained binding energy was compared with the binding energy in the interaction between SDZ with all serine derivatives and common commercially available monomers. The binding energies are presented in Table 3.2 The result indicated that the interaction between Fmoc-O-Trityl-L-Serine with SDZ showed the lowest binding energy ( $-4.43 \text{ kcal mol}^{-1}$ ) as compared with other monomers and serine derivatives.

Similar to serine, Fmoc-O-Trityl-L-Serine is not suitable to be applied directly as the monomer in the preparation of MIP. Therefore, modification is required to introduce unsaturated double-bond onto the Fmoc-O-Trityl-L-Serine. The structure of Fmoc-O-Trityl-L-Serine with unsaturated double-bonds ((L)-(9H-fluoren-9-yl)methyl-1-(allylaminoxy)-1-oxo-3-(trityloxy)propan-2-ylcarbama te) is presented in Figure 3.6. This newly designed monomer was labeled as Monomer-2.

The result obtained indicated that Monomer-2 and SDZ were bind at the 4-aminobenzenesulfonamide moiety of the sulfa drugs (Figure 3.7). The binding location is the desired binding site in the preparation of multi-functional magnetic MIP. In term of binding energy, Monomer-2 showed the binding energy of  $-3.79 \text{ kcal mol}^{-1}$ , which is the lowest as compared with other commercially available monomers. Therefore, Monomer-2 was selected as the monomer for the preparation of multi-functional magnetic MIP.

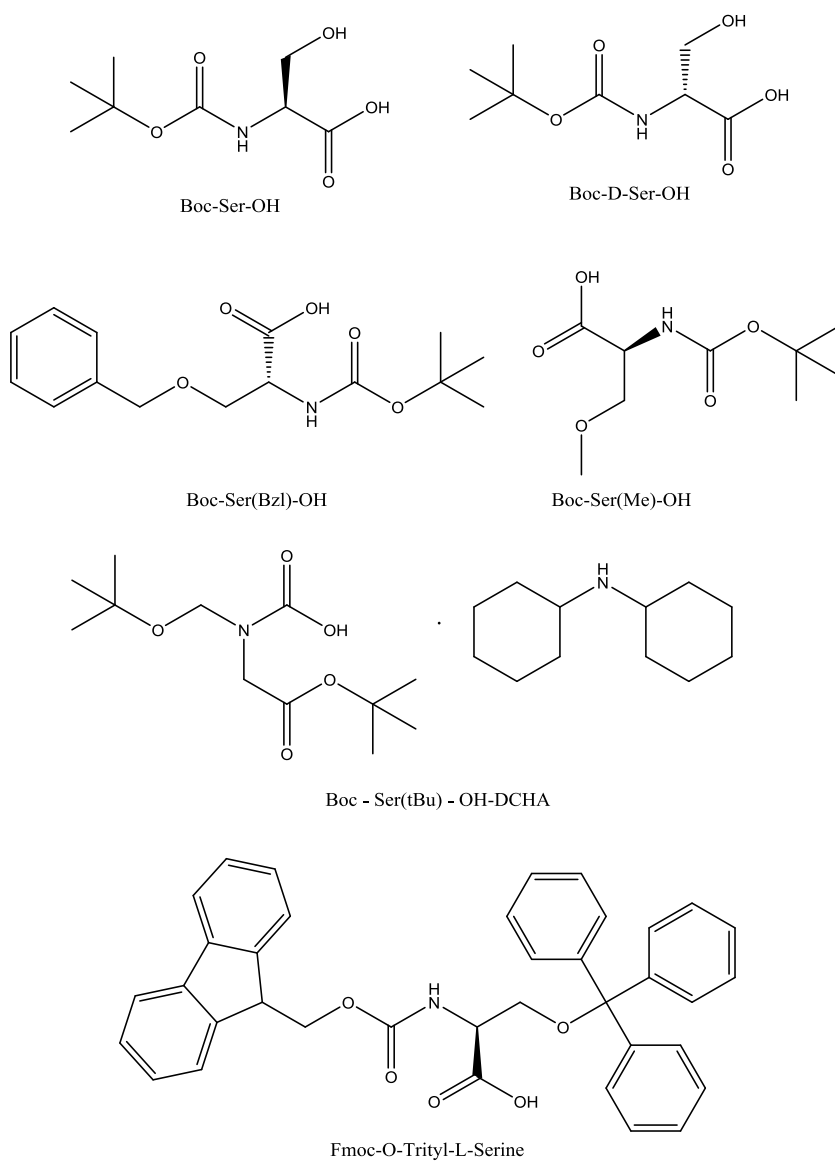


**Figure 3.5** Structure of serine with different protecting groups.



**Table 3.2** Binding energy between selected monomers and new template molecule (SDZ) estimated using the AutoDock Tools 1.5.6.

Sources	Candidates	Binding Energy (kcal mol <sup>-1</sup> )
Commercially Available	AA	-1.81
	Allyl alcohol	-1.68
	EGDMA	-2.13
	EGMP	-2.52
	MAA	-2.81
Serine with Different Protecting Group	Boc-Ser-OH	-2.77
	Boc-D-Ser-OH	-2.94
	Boc-Ser-Bzl-OH	-3.05
	Boc-D-Ser-Bzl-OH	-3.23
	Boc-Ser-Me-OH	-2.78
	Boc-Ser-tBu-OH-DCHA	-2.91
	Fmoc-O-Trityl-L-Serine	-4.43
	Monomer-2	-3.79

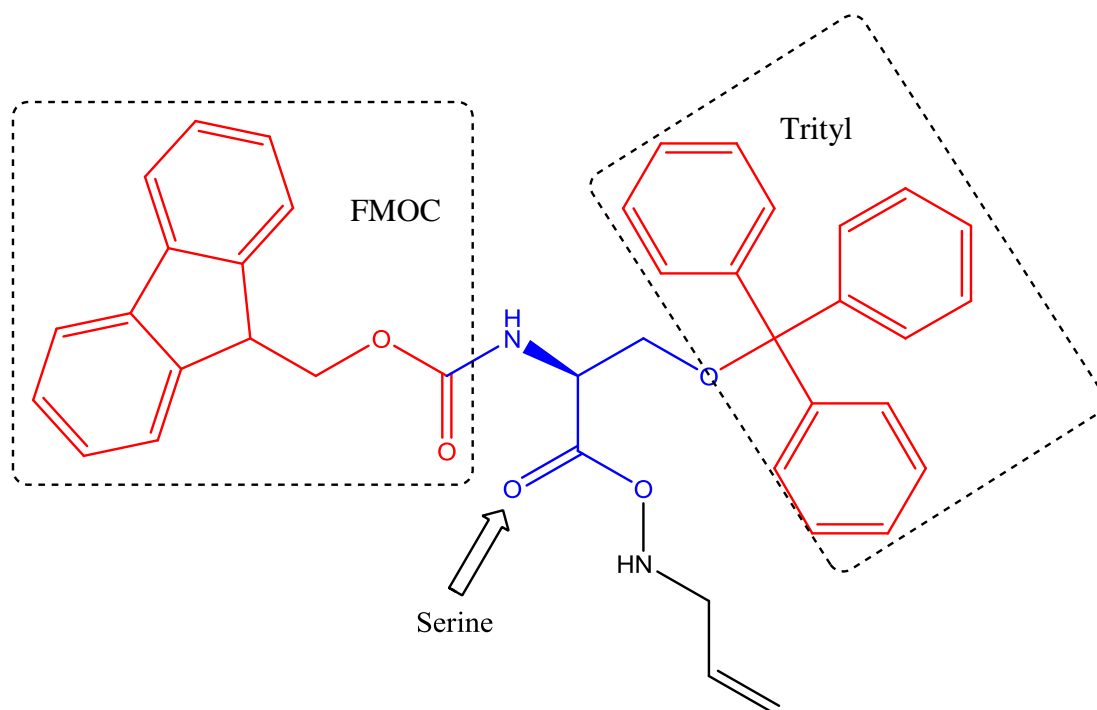


**Figure 3.6** The structure of Monomer-2.

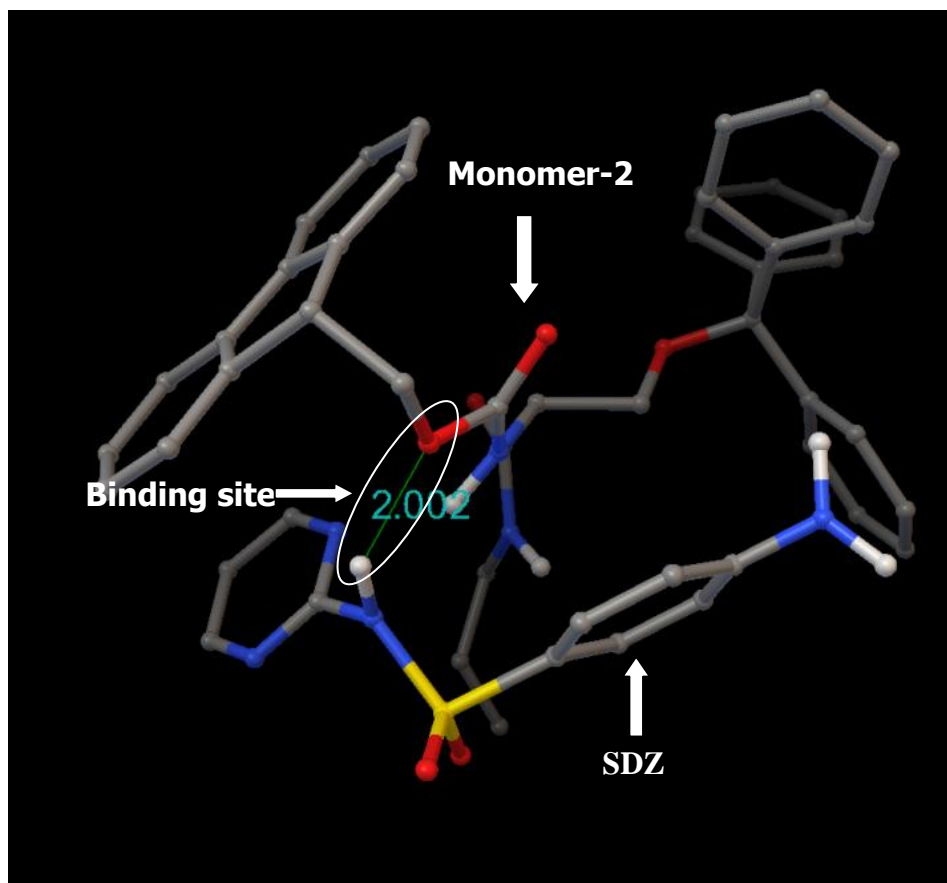


**Figure 3.7** The interaction between Monomer-2 and SDZ.

### 3.2 Synthesis of Monomer-2

The synthesis of Monomer-2 was performed according to the coupling method which has been widely used to the peptide synthesis (Montalbetti and Falque, 2005). Monomer-2 was synthesized by coupling the allylamine that containing unsaturated double-bond to the Fmoc-O-trityl-L-serine. Through this reaction, allylamine was bonded to carboxylic group of Fmoc-O-trityl-L-serine through an amide bond. The reagents involved in this coupling method were HOBt, EDCI HCl and DIEA. DMAP was used as the catalyst for the reaction and DCM was selected as solvent (Figure 2.1).

The mechanism in the formation of Monomer-2 is presented in Figure 3.8. This amide coupling involved the reaction between the carboxylic acid group of Fmoc-O-trityl-L-serine with EDCI for the formation of O-acylsourea intermediate *I*. *I* was then reacted with HOBt for the formation of intermediate *II*. OBt group was then replaced by the allylamine to form Monomer-2. The NMR spectrum of Monomer-2 are presented in Appendix 1.

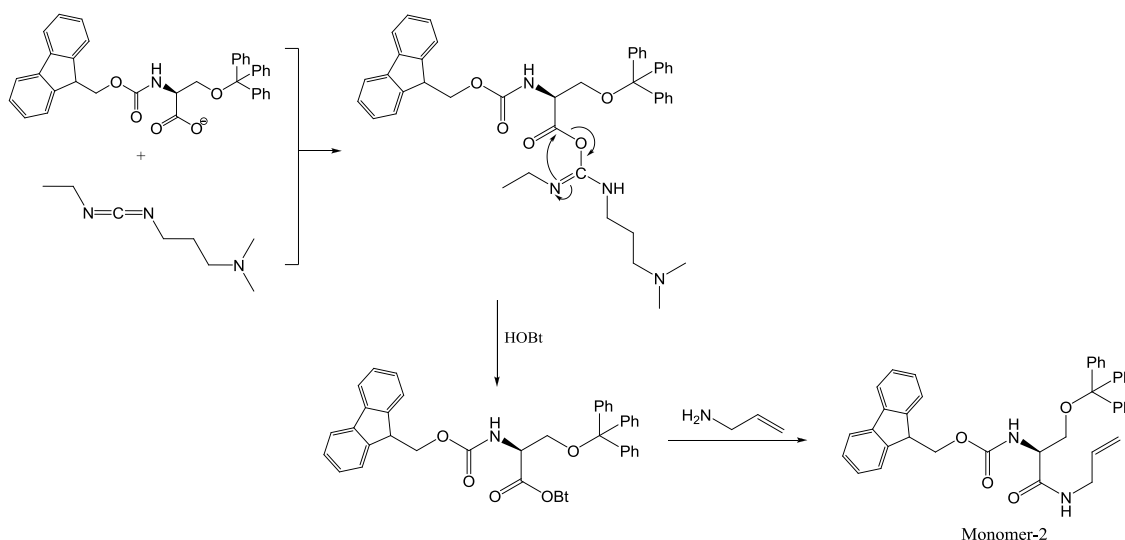


**Figure 3.8** Mechanism for the formation of Monomer-2.

### 3.3 Characterization of synthesized MMIP

In this study, MION@MPS was first synthesized via surface modification of MION using MPS in order to introduce the vinyl group onto the surface of MION. During surface modification, the hydroxy groups on the surface of the MION reacted with the methoxy group of MPS leading to the addition of 3-methacryloyloxypropyl group onto the surface of MION through Si-O bonding (Figure 2.2). Then, MIP was fabricated through copolymerization of selected monomers (AA and Monomer-2) and EGDMA

(cross-linker) with SDZ as template. The synthesized AMIP and SMIP were characterized using IR spectroscopy, TGA, SEM and EDX.

### 3.3.1 AMIP

The IR spectrum for MION, MION@MPS and AMIP is presented in Figure 3.9. As for MION, an intensive peak at  $583\text{ cm}^{-1}$  was attributed to Fe-O. The curve of MION@MPS, a few new absorption peaks appeared in the range of  $800\text{-}1700\text{ cm}^{-1}$ . The characteristic peaks of Si-O-Si group appeared at about  $1018\text{ cm}^{-1}$  and the carbonyl group at  $1717\text{ cm}^{-1}$ . These peaks indicated that the 3-methacryloyloxypropyl group was successfully grafted onto the surface of MION. In addition, the peak at around  $2934\text{ cm}^{-1}$  was attributed to the C-H stretching. This peak further showed the presence of 3-methacryloyloxypropyl group on the MION. For AMIP, the peaks around  $2980$  and  $1725\text{ cm}^{-1}$  were more intense. This result indicated the presence of MIP shell on MION@MIP. Also, the peak at  $1717\text{ cm}^{-1}$  was shifted to  $1725\text{ cm}^{-1}$  indicating the formation polymer through the reaction between the double bond of AA and vinyl groups of 3-methacryloyloxypropyl.

Result from the TGA showed that the weight loss for MION@MPS was greater than MION (Figure 3.10). This result indicated that MPS was successfully added onto the surface of MION. AMIP showed the greatest weight loss as compared to MION and MION@MPS. This result showed that MIP was successfully imprinted onto the surface of MION-MPS.

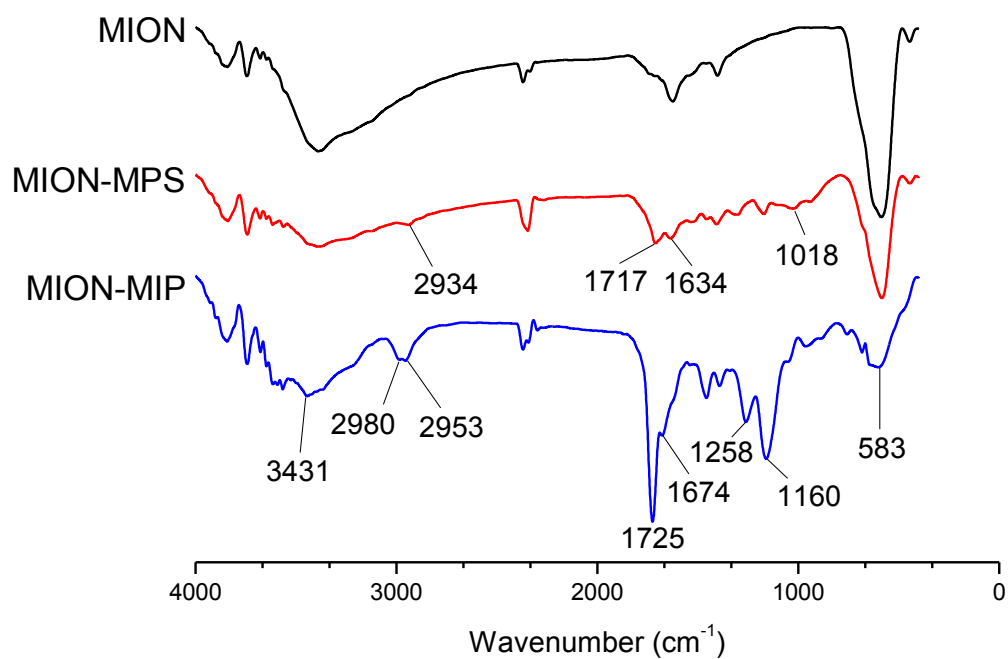


**Figure 3.9** FTIR spectra recorded between 4000 and 400  $\text{cm}^{-1}$  of MION, MION@MPS and AMIP.

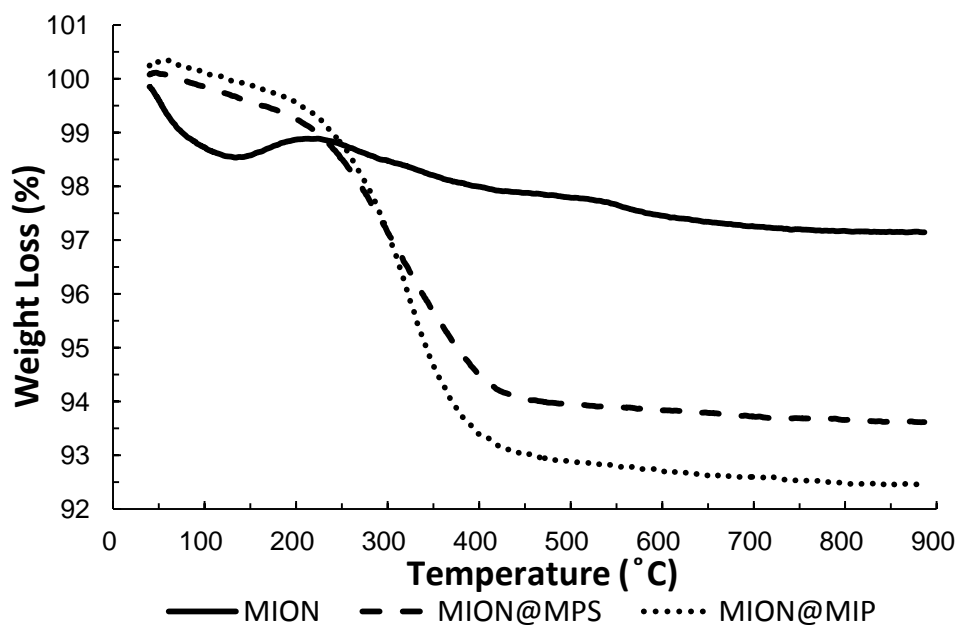


**Figure 3.10** TGA curves of MION, MION@MPS and AMIP.

The size and shape of MION@MPS and AMIP were examined by SEM technique. Figure 3.11a shows the SEM image of MION. It was observed that the diameter of MION@MPS was about 10 nm (Figure 3.11b). As reported by Tay et al (2013), the morphology of MION does not influence by the surface modification by using silane derivatives. After the formation of MIP, the diameter of AMIP was increased to about 100 nm (Figure 3.11c).

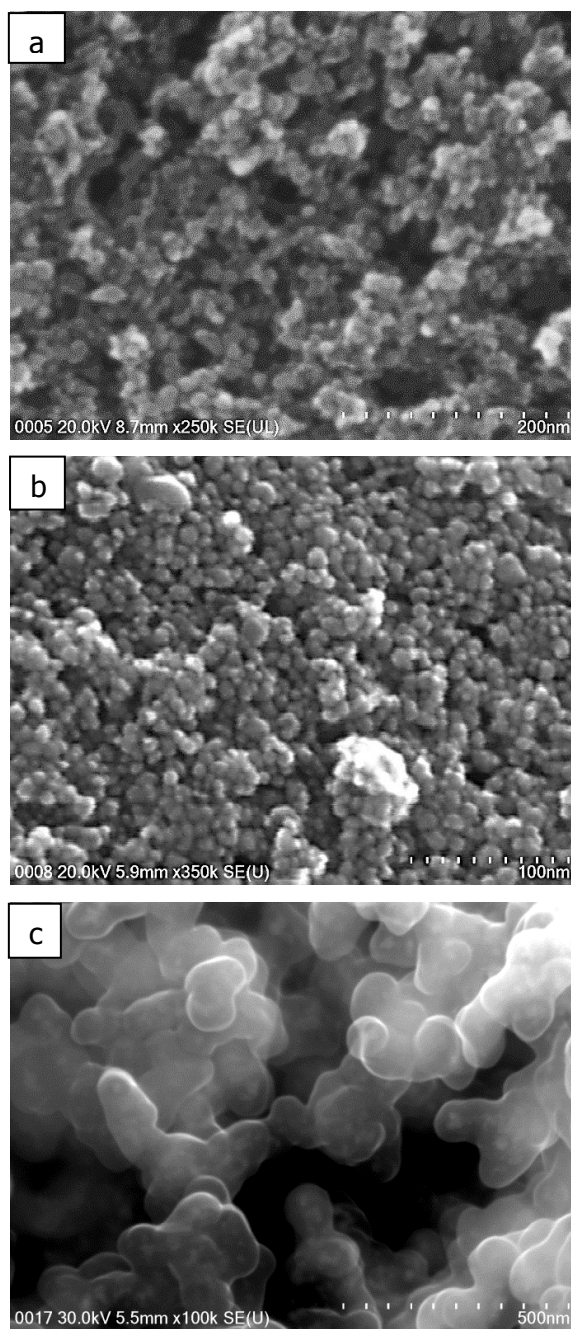


**Figure 3.11** SEM images of (a) MION, (b) MION@MPS and (c) AMIP.

### 3.3.2 SMIP

The IR spectrum of MION@MPS and SMIP are presented in Figure 3.12. The IR spectrum of MION@MPS and SMIP does not show any significant difference. However, it can be observed that some peaks such as 2936 and 1716  $\text{cm}^{-1}$  were shifted after polymerization. The peaks at 2936 and 1716  $\text{cm}^{-1}$  were attributed to alkyl and carbonyl groups. These shifted peaks indicated the presence of MIP on the surface of MION@MPS. The presence of new peak at 1540  $\text{cm}^{-1}$  was attributed to the secondary amine group (Nikolic, 2011) of Monomer-2.

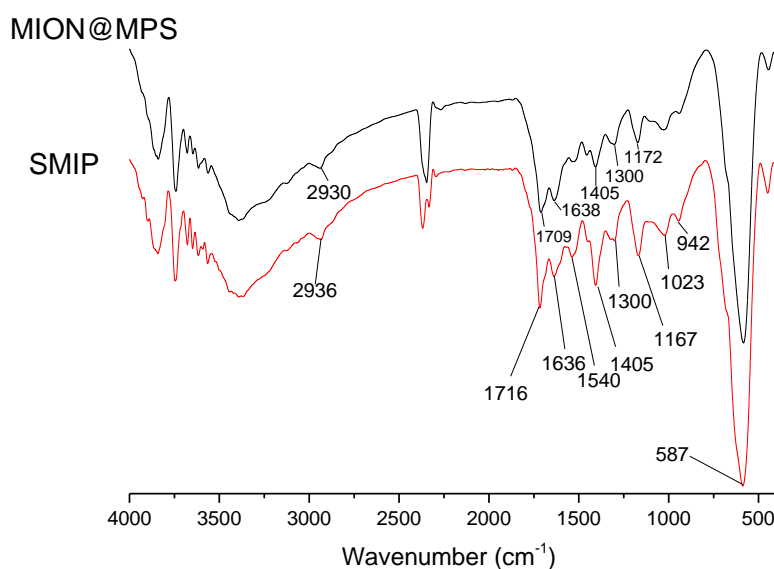


**Figure 3.12** FTIR spectra recorded between 4000 and 400  $\text{cm}^{-1}$  of MION@MPS and SMIP.

To further verify the presence of Monomer-2-based MIP on MION@MPS, TGA, SEM and Energy-dispersive X-ray spectroscopy (EDX) analysis were performed. Figure 3.13 illustrated the TGA plot for MION, MION@MPS and SMIP. SMIP showed the greatest weight loss as compared to MION and MION@MPS. Based on the weight

loss obtained, it is confirmed that the imprinted polymer has been successfully coated onto MION@MPS.

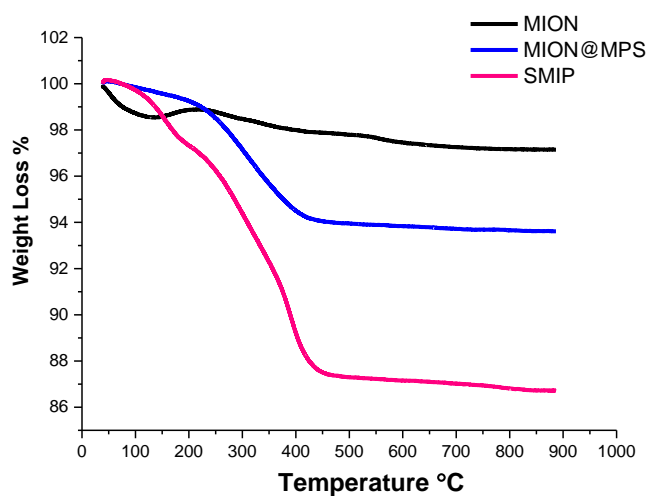


**Figure 3.13** TGA curves of MION@MPS and SMIP.

The size and shape of SMIP was examined by using SEM. Figure 3.14 showed the SEM image of SMIP. As compared to MION@MPS (Figure 3.11b), the diameter of SMIP was slightly increased to around 20 nm due to the presence of MIP. Result from EDX analysis (Figure 3.15) showed the presence of nitrogen atoms that originated from the Monomer-2. MION and MION@MPS does not contain any nitrogen atom. Based on these results, the presence of Monomer-2-based MIP was confirmed.



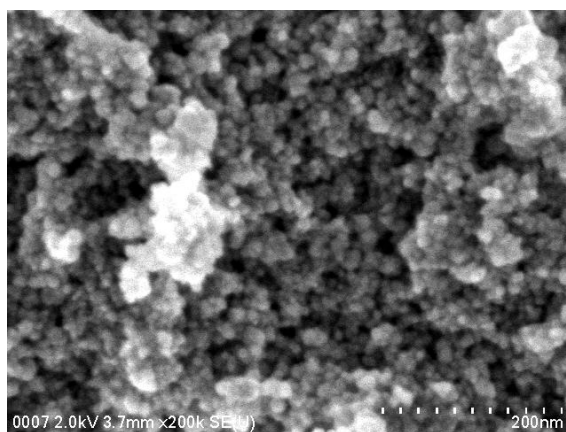


**Figure 3.14** SEM images of SMIP.

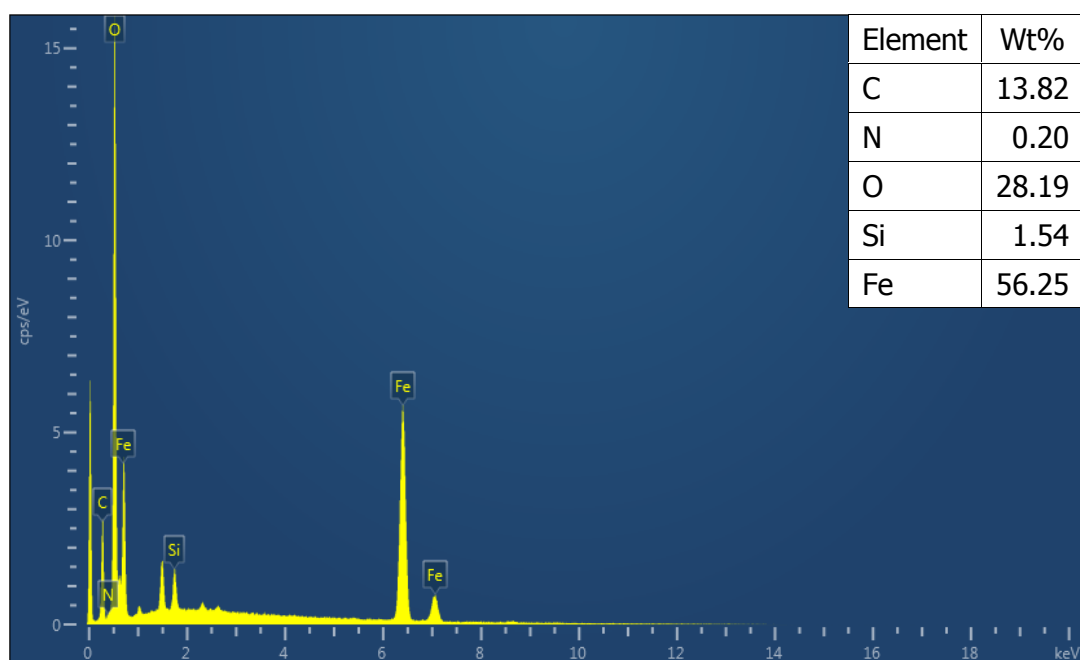


**Figure 3.15** EDX pattern for SMIP and the result of elemental analysis.

### **3.4 Binding properties of MMIP**

#### **3.4.1 Adsorption kinetic studies**

According to Kong et al. (2012), adsorption of SAs in ACN by MIP produced the highest adsorption capacity for the selected SAs such as SMZ, SDM, SMO, SMR and SDZ. However, the presence of water and methanol can disturb the binding effect of the magnetic MIPs by destroying the hydrogen bond. Therefore, in this study, all adsorption experiment was carried out in ACN in order to evaluate the performance of the synthesized MMIP. Adsorption kinetics experiment was carried out to study the adsorption capacity of AMIP and ANIP with adsorption time (Figure 3.16a). ANIP is non-imprinted polymer that prepared using the similar method as AMIP but without the presence of template. AMIP showed a fast adsorption rate on SDZ in the first 150 s and then increasing slightly to reach equilibrium after 400 s. This was probably due to the SDZ that were captured in the cavities located on the surface of the MIP at the first stage and after most of the cavities were occupied, the SDZ had to be penetrated into deeper part of the polymer, which would be more time-consuming (Kong et al., 2012). Moreover, the maximum adsorption capacity of AMIP towards SDZ was found to be almost 3 times higher than that of ANIP. This result showed the contribution of the cavities of AMIP on the adsorption of SDZ.

The amino acid-based MIP (Figure 3.16b), both SMIP and SNIP showed a faster adsorption rate as compared to AMIP and ANIP. SMIP and SNIP reached the equilibrium level with only 200 s. This phenomenon demonstrated that the SMIP have more effective recognition sites and faster adsorption kinetic properties. This result was

in agreement with the computational study that showed the binding energy between SDZ and Monomer-2 was lower than the interaction between SDZ and AA. The maximum adsorption capacity of SMIP towards SDZ was almost 10 times higher than that of SNIP.

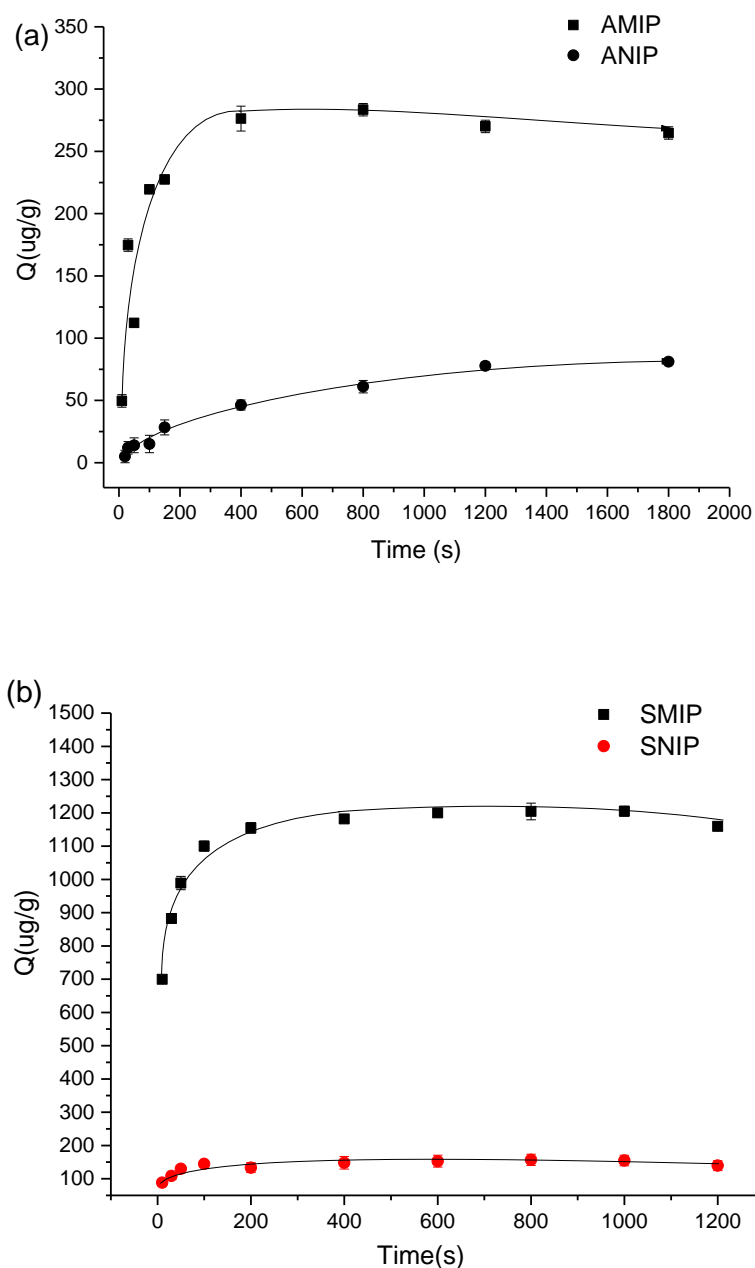


**Figure 3.16** Adsorption kinetics of (a) AMIP and ANIP, and (b) SMIP and SNIP.

### 3.4.2 Binding isotherm

The binding isotherm of AMIP and ANIP was determined using SDZ solution with the concentration ranging from 0.5 to 30  $\mu\text{g mL}^{-1}$ . The amount of SDZ bound to AMIP increased sharply with increasing SDZ concentration from 0.5 to 20  $\mu\text{g mL}^{-1}$  (Figure 3.17a). But the curve reached it equilibrium when SDZ concentration was greater than 20  $\mu\text{g mL}^{-1}$ . The amount of SDZ bound to ANIP also increased with SDZ concentration but the adsorption ability was significantly lower than AMIP. Apparently, AMIP possessed higher loading ability towards template as compared to the ANIP. This result suggested that the existence of imprinting cavities on AMIP that differentiated the binding ability of ANIP. In order to further study the binding mechanism of SDZ onto the AMIP, Langmuir analysis was performed by using the data from binding isotherm. The equation of Langmuir adsorption isotherm model is as follows (Kong et al, 2012):

$$\frac{[\text{SDZ}]}{Q} = \frac{1}{Q_{\text{MAX}} K_D} + \frac{[\text{SDZ}]}{Q_{\text{MAX}}} \quad (\text{Equation 3.1})$$

where  $Q$  represents the amount of SDZ bound to AMIP,  $K_D$  is the dissociation constant,  $Q_{\text{MAX}}$  represents the apparent maximum adsorption capacity, and  $[\text{SDZ}]$  is the free SDZ concentration at equilibrium. The value of  $K_D$  and  $Q_{\text{MAX}}$  can be obtained from the slope and intercept of Figure 3.17b. The result showed that the experimental data was fitted to Langmuir adsorption isotherm model with the correlation coefficient ( $R^2$ ) of 0.998. Therefore, based on Langmuir adsorption isotherm model, adsorption of SDZ occurred uniformly on the active site of the AMIP. As suggested by Langmuir model, once the SDZ occupied the active binding site at the monolayer, no further adsorption could take place at this site (Foo and Hameed, 2010). According to the slope and intercept of Figure 3.17b, the  $Q_{\text{MAX}}$  and  $K_D$  of the high affinity sites were 775  $\mu\text{g g}^{-1}$  and 0.047  $\mu\text{g}$

$\text{mL}^{-1}$ . The  $Q_{MAX}$  obtained from this study was almost two times larger than the  $Q_{MAX}$  value obtained by Kong et al (2012) in the adsorption of SMR by using core-shell MIP. This result might due to the smaller size of AMIP which provided larger surface area for the adsorption of template molecule.

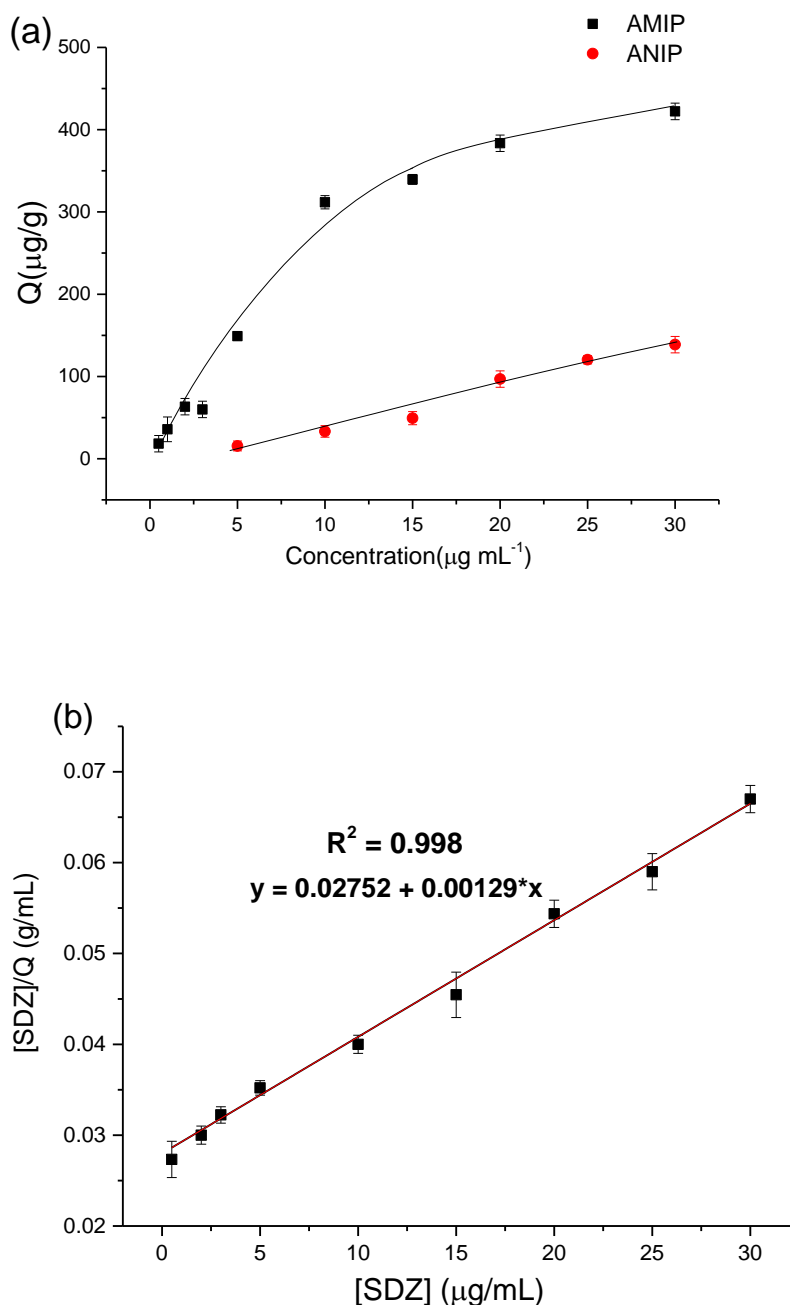


**Figure 3.17** (a) Adsorption isotherm of SDZ onto AMIP and ANIP; (b) Langmuir plot to estimate the binding mechanism of AMIP towards SDZ.

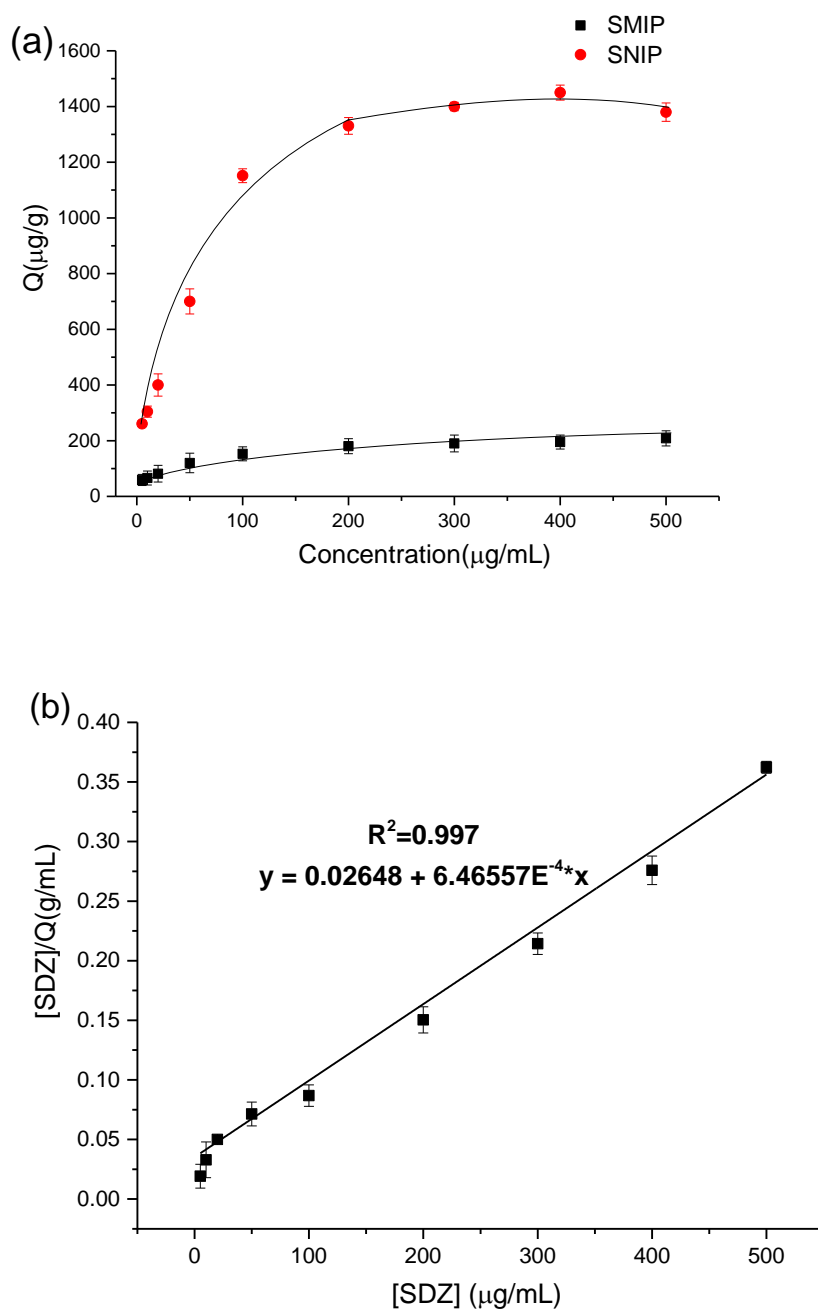


**Figure 3.18** (a) Adsorption isotherm of SDZ onto SMIP and SNIP; (b) Langmuir plot to estimate the binding mechanism of SMIP towards SDZ.

The binding isotherm of SMIP and SNIP was determined using SDZ solutions with the concentration ranging from 5 to 500  $\mu\text{g mL}^{-1}$ . Higher concentration of SDZ solution was selected for this study because SMIP show higher adsorption capacity as

compared with AMIP. The amount of SDZ bound to SMIP increased sharply with increasing SDZ concentration from 5 to 200  $\mu\text{g mL}^{-1}$  (Figure 3.18a). The curve reached its equilibrium when SDZ concentration was greater than 200  $\mu\text{g mL}^{-1}$ . The amount of SDZ bound to SNIP also increased with SDZ concentration but the adsorption ability was significantly lower than SMIP. Overall, this result indicated that the designed amino acid-based MIP was able to absorb higher amount of SDZ as compared to AMIP. Langmuir plot for the adsorption of SDZ by SMIP is presented in Figure 3.18b. It can be observed that the sorption data fitted well to Langmuir Isotherm model with the correlation coefficient ( $R^2$ ) of 0.997. Based on the slope and intercept, the obtained  $Q_{MAX}$  and  $K_D$  values were 1547  $\mu\text{g g}^{-1}$  and 0.026  $\mu\text{g mL}^{-1}$ , respectively. The  $Q_{MAX}$  value of SMIP was almost two times higher than AMIP. This result indicated that the presence of Monomer-2 can enhance the adsorption of SDZ as compared with AA. This result was also in agreement with the results obtained from the computational study that showed the interaction between Monomer-2 and SDZ were more favorable than AA-SDZ interaction.

Instead of Langmuir adsorption isotherm model, Freundlich adsorption isotherm is another adsorption model which has been frequently used to characterize the adsorption behavior of MIP and other materials (Dada et al., 2012; Desta, 2013; Yusof et al., 2013). The Freundlich isotherm has been used to study the relationship of equilibrium between liquid and solid phase based on the multilayer adsorption. The data obtained from the equilibrium between liquid and solid phase based on the multilayer adsorption often fit the empirical equation proposed by Freundlich (Dada et al., 2012):

$$Q = K_f [SDZ]^{\frac{1}{n}} \quad (\text{Equation 3.2})$$

where  $K_f$  is Freundlich isotherm constant;  $Q$  is the amount of SDZ adsorbed per gram of the adsorbent at equilibrium,  $[SDZ]$  represents the equilibrium concentration of SDZ and  $n$  is the adsorption capacity. By linearizing the above Freundlich equation, the following equation can be obtained:

$$\log_{10} Q = \log_{10} K_f + \frac{1}{n} \log_{10} [SDZ] \quad (\text{Equation 3.3})$$

Freundlich plots for the sorption of SDZ by AMIP and SMIP are shown in Figure 3.19. Either AMIP or SMIP, the Freundlich model has lower  $R^2$  (0.970 and 0.958) as compared to Langmuir model (0.995 and 0.997). Therefore, it can be concluded that the adsorption of SDZ by both AMIP and SMIP was due to the interaction at the monolayer of MIP coated on the MION and there is high possibility for AMIP and SMIP to appear as monolayer adsorbates.

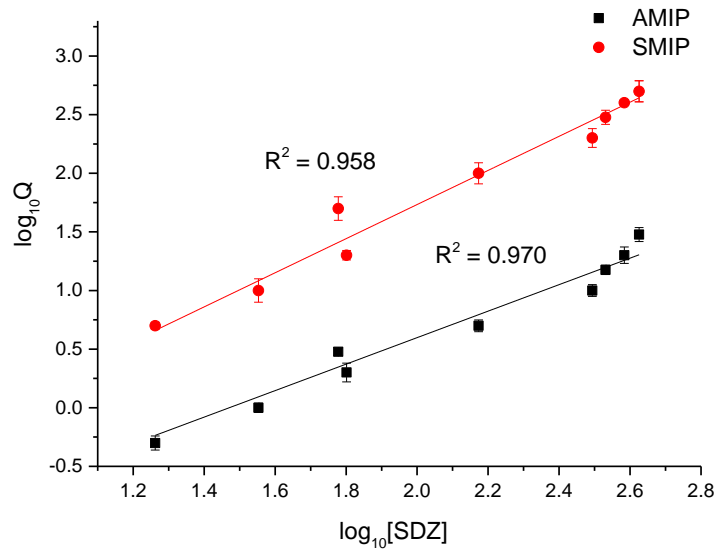


**Figure 3.19** Freundlich plot for the adsorption of SDZ by AMIP and SMIP.



### 3.5 Binding specificity of AMIP, ANIP, SMIP and SNIP

The competitive binding test was applied to determine the selectivity of AMIP towards the adsorption of SDZ. Five SAs (SDZ, SMR, SAA, SMZ, and SMO) were selected in this study. As shown in Figure 3.20, the adsorption of SAs on ANIP is non-specific, so every SA has the equal opportunity to occupy the non-specific binding site. The adsorption of SDZ and SMR on AMIP was dramatically higher than SAA, SMZ, and SMO. However, the adsorption of SMR by AMIP was found to be slightly higher than the template (SDZ). In order to further investigate the root reason for such result, computational modeling was carried out to imitate the molecular interactions between AA with SDZ and SMR.

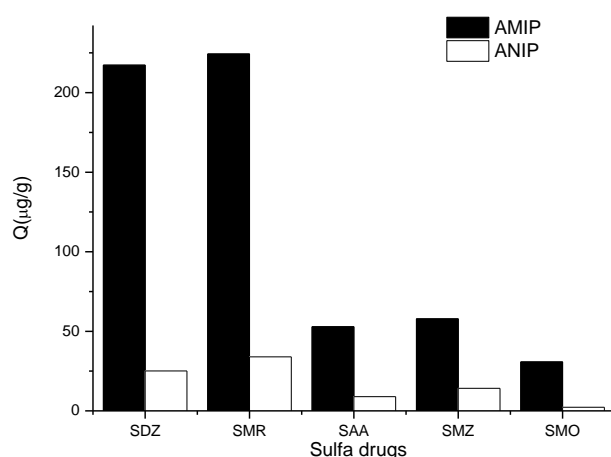


**Figure 3.20** Adsorption capacity of MION-MIP and MION-NIP towards SDZ, SMR, SAA, SMZ and SMO.

It has been reported that the adsorption of template molecule by MIP was mimicked to the natural recognition pathways by natural recognition elements such as enzyme (Kryscio and Peppas, 2012). Therefore, the optimized structures between the

selected SAs and AA are expected to mimic the interaction of SMO with dihydropteroate synthase found in the protein databank (Figure 3.21). The X-ray crystal structure of dihydropteroate synthase-SMO complex (PDB ID: 3TZF) shows the SMO was bound to serine (SER) and Threonine (THR) through hydrogen bonding at sulfonyl and amine group of SAs (Figure 3.21a). Presumably, SDZ and SMR also have relatively similar interactions pattern as THR and SER with SMO in dihydropteroate synthase-SMO complex. The calculation was focused at AA1 and AA2 positions as indicated in Figure 3.21b and 3.21c. The interaction energy between SDZ and SMR with AA was compared with three different levels of calculation (Table 3.3). SMR has slightly stronger interaction with AA than SDZ (template) by about  $3.50 \text{ kcal mol}^{-1}$  with PM3 and almost the same interaction with HF and DFT method. With B3LYP, the binding energies between SDZ and SMR with monomers are slightly different by  $0.29 \text{ kcal mol}^{-1}$ . The interaction energies between AA1 and the SDZ are also very similar to SMR which were  $-133.30$  and  $-132.07 \text{ kcal mol}^{-1}$ , respectively. However, the interaction energies between AA2 and the SDZ and SMR are slightly higher by about  $3.04$  and  $3.37 \text{ kcal mol}^{-1}$  with HF and B3LYP, respectively. From this result, AA at AA2 position bound stronger than AA1 and contributed to SDZ and SMR recognition. Based on the optimized structures, interaction energy between the template and each monomer was investigated by scanning the distance of AA1 and AA2 along the  $\text{O} \cdots \text{H}$  distance for SDZ and SMR (Figure 3.22). The lowest point in the graph represents the lowest interaction energy structure and the interaction between the SDZ and SMR with monomer is similar to each other. Thus, SDZ and SMR can bind to AMIP through similar interaction during the extraction process.

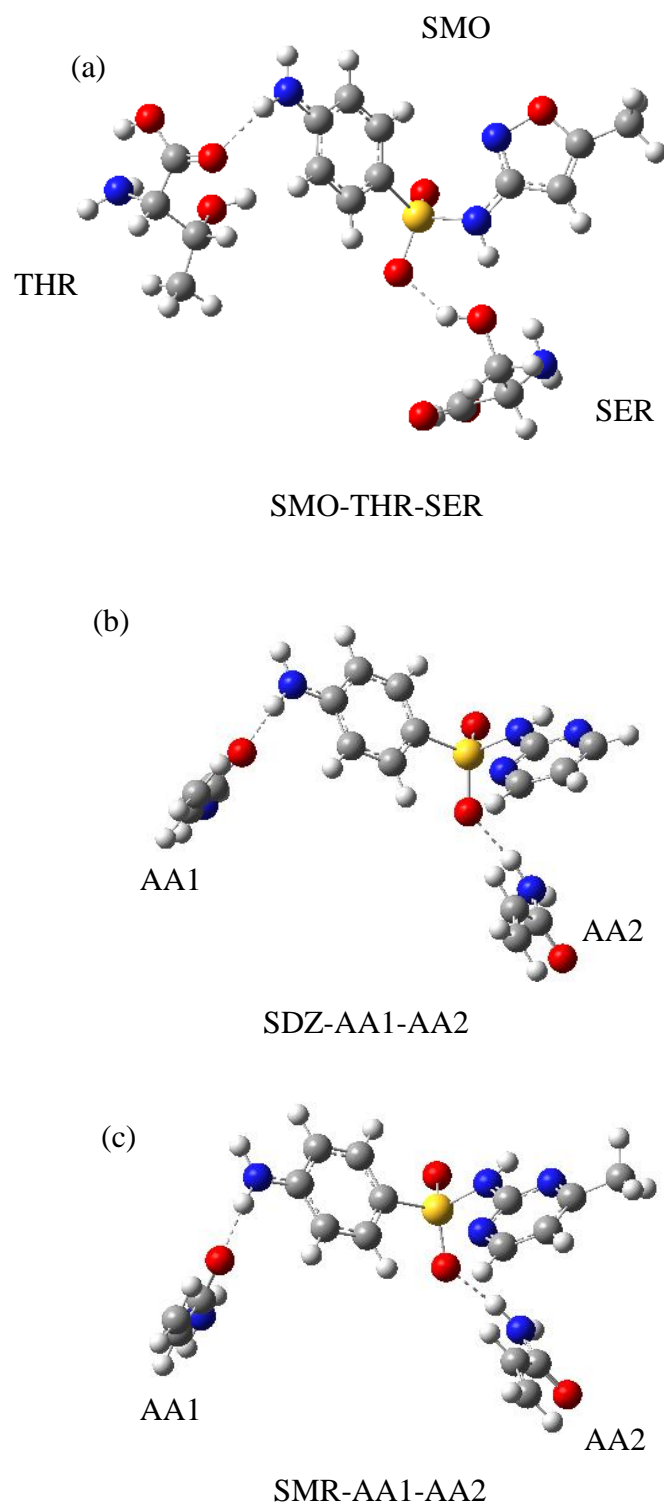


**Figure 3.21** The interaction between the template and the monomer in comparison of the crystal structure of SA drug (SMO) from the protein database (PDB ID: 3TZF): (a) SMO with THR and SER. (b) SDZ and Acrylamide. (c) SMR and Acrylamides. (The dashed line shows the hydrogen bonding interaction).

**Table 3.3** The interaction energy between the templates and monomers with three different basis sets calculations.

Complex		Interaction Energy (kcal mol <sup>-1</sup> )		
		PM3	HF/6-31G(d)	DFT/B3LY P/6-31G(d)
SDZ-AA1-AA2	ESDZ/AA1-AA2	-92.19	-150.95	-137.20
	ESDZ-AA2/AA1	-86.77	-147.02	-133.30
	ESDZ-AA1/AA2	-92.75	-159.34	-143.96
SMR-AA1-AA2	ESMR/AA1-AA2	-95.69	-150.72	-137.49
	ESMR-AA2/AA1	-89.28	-144.92	-132.07
	ESMR-AA1/AA2	-97.53	-162.38	-147.23
SMO-THR-SER	ESMO/THR-SER	-211.87	-661.36	-641.99
Relative interaction energy between SDZ and SMR with monomers	ESDZ/AA1-AA2 - ESMR/AA1-AA2	3.50	-0.23	0.29
Relative interaction energy between SDZ and SMR with AA1	ESDZ-AA2/AA1 - ESMR-AA2/AA1	2.51	-2.10	-1.23
Relative interaction energy between SDZ and SMR with AA2	ESDZ-AA1/AA2- ESMR-AA1/AA2	4.78	3.04	3.27

Another possible reason for poor recognition towards SDZ and SMR might due to the smaller size effect of AMIP which creates the larger absorption surface area for template. Besides the interaction energy, surface effect, the swelling behavior which depends on the solvents as reported by (Koohpaei et al., 2008) and (Faizal et al., 2009) would also cause in the difference of the three dimensional configuration of the functional groups which resulting in poorer capacity for sites recognition between SDZ and SMR.

One of the main purposes of this study was to design and synthesis the multi-functional MMIP that can be used to adsorb the homologue series of SAs antibiotics. In order to study the adsorption of SAs on SMIP, a mixture of four SAs (SDZ, SMR, SPY, and STZ) and two non-SA compounds (DEET and benzylparaben) were selected in this study. The structure of DEET and benzyl paraben are presented in Figure 3.23.

As shown in Figure 3.24, the adsorption of SAs on SNIP is non-specific. So every selected SA including DEET and benzylparaben has the equal opportunity to occupy the non-specific binding site. As compared to SMIP, the amount of selected compounds that adsorbed on the SNIP was significantly lower. This result indicated that the adsorption of SAs on SMIP was contributed by specific binding site and the contribution of non-specific binding sites was not significant. The adsorption of SAs by SMIP was dramatically higher than DEET and benzylparaben.

The specificity of SMIP was estimated by the partition coefficients of the selected sulfonamides between polymers and solution. The partition coefficient  $K$  was determined according to the following formula:

$$K = \frac{C_p}{C_s} \quad (\text{Equation 3.4})$$

where  $C_p$  is the amount of selected sulfonamide bound by SMIPs or SNIPs and  $C_s$  is the concentration of test analyte remaining in solution. Additionally, the imprinting factor ( $IF$ ) and selectivity coefficient ( $SC$ ) were generally used to evaluate the selectivity properties of SMIPs and SNIPs towards SDZ and structurally related sulfonamides SMR, SPY, STZ, DEET and benzylparaben. The  $IF$  and  $SC$  were calculated by the following formulas:

$$\text{Imprinting factor (IF)} = \frac{K_i}{K_c} \quad (\text{Equation 3.5})$$

$$\text{Selectivity coefficient (SC)} = \frac{IF_{SDZ}}{IF_i} \quad (\text{Equation 3.6})$$

where  $K_i$  and  $K_c$  represent the partition coefficients of analyte for the SMIPs and SNIPs,  $IF_{SDZ}$  and  $IF_i$  are the imprinting factor for SDZ and five other compounds respectively. Table 3.4 illustrates the partition coefficients, imprinting factors and selectivity coefficients of SDZ and its analogues STZ, SPY, SMR, DEET and Benzylparaben for SMIPs and SNIPs. The result from Table 3.4 showed that the synthesized SMIP possesses the high recognition property on SAs than others structural unrelated compounds (DEET and benzylparaben). The adsorption of SMR, SPY, STZ were slightly higher than template, it might be due to the non-specific hydrophobic adsorption (Kareuhanon et al., 2009). In conclusion, this experimental result was in agreement with computational study, presented at table 3.3.

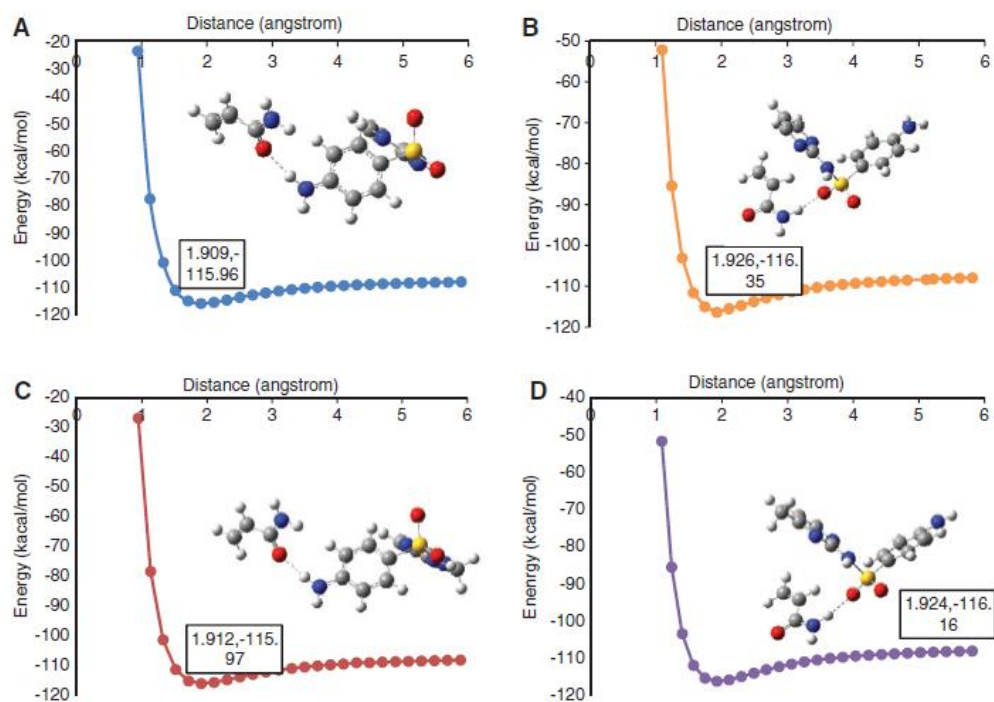


**Figure 3.22** Interaction energy plotted against the O–H-distance (A) SDZ and AA1, (B) SDZ and AA2, (C) SMR and AA1, (D) SMR and AA.

**Table 3.4** The partition coefficients, imprinting factors and selectivity coefficients of SDZ and its analogues STZ, SPY, SMR, DEET and Benzylparaben for SMIPs and SNIPs.

Compound	$K_{SMIP}$	$K_{SNIP}$	$IF$	$SC$
SDZ	0.171	0.025	6.789	
STZ	0.259	0.059	4.376	1.551
SPY	0.427	0.045	9.401	0.722
SMR	0.205	0.026	7.931	0.856
DEET	0.011	0.016	0.692	9.806
Benzylparaben	0.071	0.026	2.764	2.456

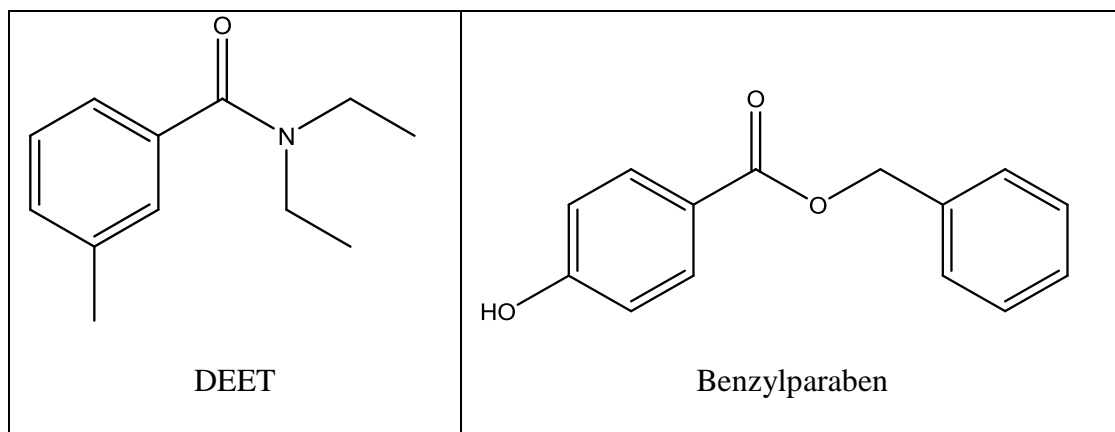


**Figure 3.23** Structure of DEET and benzylparaben.

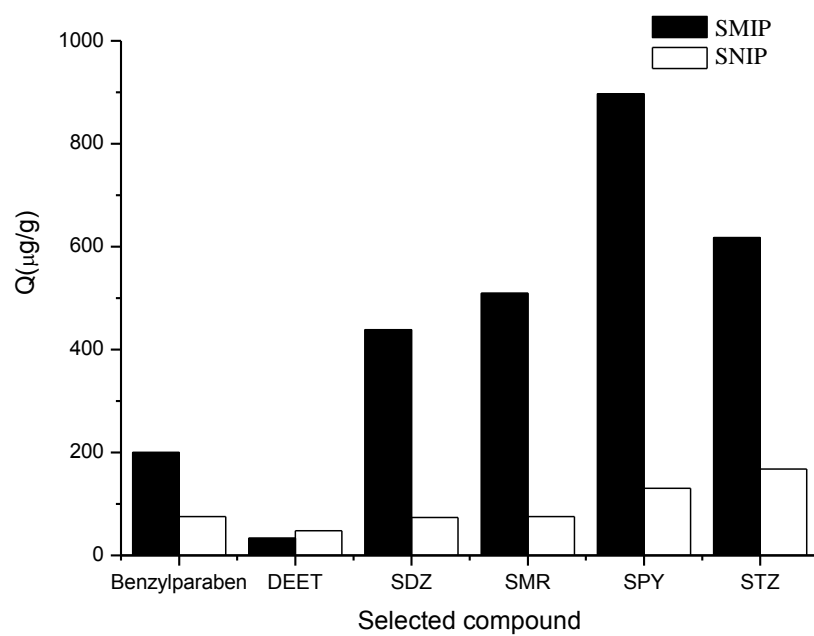


**Figure 3.24** Adsorption capacity of SMIP and SNIP towards sulphonamides, DEET and benzylparaben.



## CHAPTER 4. CONCLUSION

### 4.1 Conclusions

The first area of this research involved the design of monomer in the preparation of multi-functional MMIP. Based on the crystal structure of SMO and dihydropteroate synthase, it was observed that SMO was bound to the protein through serine. Since it has been reported that the recognition of template by MIP is mimic to the enzyme-ligand interaction, therefore, serine-based Monomer-1 and Monomer-2 were proposed. The result from computational study showed that Monomer-1 is not a suitable monomer for the preparation multi-functional MMIP due to its interaction with SMO at undesired position. Then, Monomer-2 was designed and the calculation was performed using new template molecule, SDZ. The computational result indicated that the interaction between Monomer-2 and SDZ possessed the lowest binding energy as compared to other commercially available monomers. The interaction between Monomer-2 and SDZ was also at the desired site in the preparation of multi-functional MMIP. Then, Monomer-2 was synthesized. By using the synthesized Monomer-2, Monomer-2-based MIP was prepared by using SDZ as template. Then, experimental study was carried out in order to verify the results from the computational study. The performance of Monomer-2-based MIP (SMIP) was then compared with the AA-based MIP (AMIP).

The experimental study was started from the preparation of AMIP and followed by the evaluation of the performance of the synthesized AMIP. This AA based MIP was imprinted directly onto the surface of MPS-modified MION. The result showed that the

obtained AMIP possessed adsorption kinetics with 400 s to reach equilibrium. The results also indicated that maximum adsorption capacity of  $775 \mu\text{g g}^{-1}$  was achieved. Langmuir adsorption isotherm model was found to describe well for the equilibrium adsorption data. The results from the competitive binding experiment showed that AMIP was not only selective towards SDZ but the adsorption of SMR was dramatically high. In this case, SDZ and SMR have almost similar sub-structure where these two compounds were only differentiated by one methyl group. In order to explain this result, computational study was carried out. From different level of calculation with PM3, HF, and DFT calculation, both SDZ and SMR showed similar interactions energy and interaction mechanism with AA monomer. Therefore, both SDZ and SMR could have the same binding property in the AMIP.

SMIP as Monomer-2 based MMIP showed a faster adsorption rate with only 200 s to reach equilibrium level and the maximum adsorption capacity of SMIP was around  $1547 \mu\text{g g}^{-1}$ . This result is in agreement with the computational study. As shown by computational study, Monomer-2 showed more favourable interaction with template as compared with AA. Importantly, in the selectivity experiment, SMIP showed overwhelming advantage in the recognition of different SAs with the presence of 2 structural unrelated compounds. Therefore, it can be concluded that the multifunctional MMIP was designed by using molecular docking method and amino acid based monomer can be used for the preparation of MMIP that mimic to the ligand-enzyme interaction.

## 4.2 Future studies

While this thesis has demonstrated the potential of the developed method in the preparation of multi-functional MMIP. There are still many opportunities of extending the scope of this research such as:

(1) development of water compatible MMIP is a urgent need since a lot of studies need to be done in the aqueous,

(2) application of MMIP can be further utilized into the field of chiral separation, this area is important in the organic synthesis laboratory.

(3) MIPs could be applied as sensing devices, artificial antibodies and catalysts. Their selective recognition properties should be also evaluated using real samples in future research.

## Reference

- Akhtar, M. H., Wong, M., Crooks, S. R. H., & Sauve, A. (1998). Extraction of incurred sulphamethazine in swine tissue by microwave assisted extraction and quantification without clean up by high performance liquid chromatography following derivatization with dimethylaminobenzaldehyde\*. *Food Additives & Contaminants*, 15(5), 542-549.
- Albretsen, C., Kalland, K. H., Haukanes, B. I., Håvarstein, L. S., & Kleppe, K. (1990). Applications of magnetic beads with covalently attached oligonucleotides in hybridization: isolation and detection of specific measles virus mRNA from a crude cell lysate. *Analytical biochemistry*, 189(1), 40-50.
- Alizadeh, T. (2014). Preparation of magnetic TNT-imprinted polymer nanoparticles and their accumulation onto magnetic carbon paste electrode for TNT determination. *Biosensors and Bioelectronics*, 61(15), 532-540.
- Andersson, H. S., Karlsson, J. G., Piletsky, S. A., Koch-Schmidt, A. C., Mosbach, K., & Nicholls, I. A. (1999). Study of the nature of recognition in molecularly imprinted polymers, II: influence of monomer–template ratio and sample load on retention and selectivity. *Journal of Chromatography A*, 848(1), 39-49.
- Andersson, L. I. (2000). Molecular imprinting: developments and applications in the analytical chemistry field. *Journal of Chromatography B: Biomedical Sciences and Applications*, 745(1), 3-13.
- Andersson, L. I., & Mosbach, K. (1990). Enantiomeric resolution on molecularly imprinted polymers prepared with only non-covalent and non-ionic interactions. *Journal of Chromatography A*, 516(2), 313-322.
- Andersson, L. I., Paprica, A., & Arvidsson, T. (1997). A highly selective solid phase extraction sorbent for pre-concentration of sameridine made by molecular imprinting. *Chromatographia*, 46(1-2), 57-62.
- Ansell, R. J., & Mosbach, K. (1997). Molecularly imprinted polymers by suspension polymerisation in perfluorocarbon liquids, with emphasis on the influence of the porogenic solvent. *Journal of Chromatography A*, 787(1), 55-66.
- Arnold, B. R., Euler, A. C., Jenkins, A. L., Uy, O. M., & Murray, G. M. (1999). Progress in the development of molecularly imprinted polymer sensors. *Johns Hopkins APL Technical Digest*, 20(2), 190-199.
- Arshady, R., & Mosbach, K. (1981). Synthesis of substrate-selective polymers by host-guest polymerization. *Die Makromolekulare Chemie*, 182(2), 687-692.
- Baran, W., Adamek, E., Ziemiańska, J., & Sobczak, A. (2011). Effects of the presence of sulfonamides in the environment and their influence on human health. *Journal of hazardous materials*, 196, 1-15.

- Baselt, D. R., Lee, G. U., Hansen, K. M., Chrisey, L. A., & Colton, R. J. (1997). A high-sensitivity micromachined biosensor. *Proceedings of the IEEE*, 85(4), 672-680.
- Batt, A. L., Bruce, I. B., & Aga, D. S. (2006). Evaluating the vulnerability of surface waters to antibiotic contamination from varying wastewater treatment plant discharges. *Environmental pollution*, 142(2), 295-302.
- Becheker, I., Berredjem, H., Boutefnouchet, N., Berredjem, M., & Ladjama, A. (2014). Antibacterial activity of four sulfonamide derivatives against multidrug-resistant *Staphylococcus aureus*. *Journal of Chemical and Pharmaceutical Research*, 6(11), 893-899.
- Bedendo, G. C., Jardim, I. C. S. F., & Carasek, E. (2010). A simple hollow fiber renewal liquid membrane extraction method for analysis of sulfonamides in honey samples with determination by liquid chromatography–tandem mass spectrometry. *Journal of Chromatography A*, 1217(42), 6449-6454.
- Bergmann, N. M., & Peppas, N. A. (2008). Molecularly imprinted polymers with specific recognition for macromolecules and proteins. *Progress in Polymer Science*, 33(3), 271-288.
- Beveridge, J. S., Stephens, J. R., & Williams, M. E. (2011). Differential magnetic catch and release: experimental parameters for controlled separation of magnetic nanoparticles. *Analyst*, 136(12), 2564-2571.
- Boonpangrak, S., Whitcombe, M. J., Prachayasittikul, V., Mosbach, K., & Ye, L. (2006). Preparation of molecularly imprinted polymers using nitroxide-mediated living radical polymerization. *Biosensors and Bioelectronics*, 22(3), 349-354.
- Bucak, S., Yavuztürk, B., & Sezer, A. D. (2012). *Magnetic nanoparticles: synthesis, surface modifications and application in drug delivery*. INTECH Open Access Publisher.
- Burkhart, C. G., & Burkhart, C. N. (2009). Overview of Sulfonamides and Related Medications: Query if Mesalamine should be Preferred Over Dapsone and Sulfasalazine. *The Open Dermatology Journal*, 3(1), 65-67.
- Burns, M. A., & Graves, D. J. (1987). Application of magnetically stabilized fluidized beds to bioseparations. *Reactive Polymers, Ion Exchangers, Sorbents*, 6(1), 45-50.
- Businova, P., Chomoucka, J., Prasek, J., Hrdy, R., Drbohlavova, J., Sedlacek, P., & Hubalek, J. (2011). *Polymer-coated iron oxide magnetic nanoparticles—preparation and characterization*. In Proc. Conf. Nanocon.
- Cai, W., & Gupta, R. B. (2004). Molecularly-imprinted polymers selective for tetracycline binding. *Separation and purification technology*, 35(3), 215-221.

- Cai, Y., Chen, Y., Hong, X., Liu, Z., & Yuan, W. (2013). Porous microsphere and its applications. *International journal of Nanomedicine*, 8, 1111-1120.
- Caro, E., Masqu   N., Marc   R. M., Borrull, F., Cormack, P. A., & Sherrington, D. C. (2002). Non-covalent and semi-covalent molecularly imprinted polymers for selective on-line solid-phase extraction of 4-nitrophenol from water samples. *Journal of Chromatography A*, 963(1), 169-178.
- Chaitidou, S., Kotrotsiou, O., Kotti, K., Kammona, O., Bukhari, M., & Kiparissides, C. (2008). Precipitation polymerization for the synthesis of nanostructured particles. *Materials Science and Engineering: B*, 152(1), 55-59.
- Chen, F. F., Xie, X. Y., & Shi, Y. P. (2012). Magnetic molecularly imprinted polymer for the detection of rhaponticin in Chinese patent medicines. *Journal of Chromatography A*, 1252, 8-14.
- Chen, H., Zhang, Y., Gao, B., Xu, Y., Zhao, Q., Hou, J., ... & Zhao, C. (2013). Fast determination of sulfonamides and their acetylated metabolites from environmental water based on magnetic molecularly imprinted polymers. *Environmental Science and Pollution Research*, 20(12), 8567-8578.
- Chen, L., & Li, B. (2012). Application of magnetic molecularly imprinted polymers in analytical chemistry. *Analytical Methods*, 4(9), 2613-2621.
- Chen, L., Zeng, Q., Wang, H., Su, R., Xu, Y., Zhang, X., ... & Ding, L. (2009a). On-line coupling of dynamic microwave-assisted extraction to solid-phase extraction for the determination of sulfonamide antibiotics in soil. *Analytica Chimica Acta*, 648(2), 200-206.
- Chen, L., Zhang, X., Sun, L., Xu, Y., Zeng, Q., Wang, H., ... & Ding, L. (2009b). Fast and selective extraction of sulfonamides from honey based on magnetic molecularly imprinted polymer. *Journal of agricultural and food chemistry*, 57(21), 10073-10080.
- Chen, L., Zhang, X., Xu, Y., Du, X., Sun, X., Sun, L., ... & Ding, L. (2010). Determination of fluoroquinolone antibiotics in environmental water samples based on magnetic molecularly imprinted polymer extraction followed by liquid chromatography–tandem mass spectrometry. *Analytica Chimica Acta*, 662(1), 31-38.
- Chen, M., Yi, Q., Hong, J., Zhang, L., Lin, K., & Yuan, D. (2015). Simultaneous determination of 32 antibiotics and 12 pesticides in sediment using ultrasonic-assisted extraction and high performance liquid chromatography-tandem mass spectrometry. *Analytical Methods*, 7, 1896-1905.
- Cheng, W., Ma, H., Zhang, L., & Wang, Y. (2014). Hierarchically imprinted mesoporous silica polymer: an efficient solid-phase extractant for bisphenol A. *Talanta*, 120, 255-261.

- Cheong, C. K., Hajeb, P., Jinap, S., & Ismail-Fitry, M. R. (2010). Sulfonamides determination in chicken meat products from Malaysia. *International Food Research Journal*, 17, 885-892.
- Cheong, W. J., Yang, S. H., & Ali, F. (2013). Molecular imprinted polymers for separation science: A review of reviews. *Journal of separation science*, 36(3), 609-628.
- Chern, C. S. (2006). Emulsion polymerization mechanisms and kinetics. *Progress in polymer science*, 31(5), 443-486.
- Chianella, I., Lotierzo, M., Piletsky, S. A., Tothill, I. E., Chen, B., Karim, K., & Turner, A. P. (2002). Rational design of a polymer specific for microcystin-LR using a computational approach. *Analytical chemistry*, 74(6), 1288-1293.
- Cormack, P. A., & Elorza, A. Z. (2004). Molecularly imprinted polymers: synthesis and characterisation. *Journal of Chromatography B*, 804(1), 173-182.
- Combs, M. T., Ashraf-Khorassani, M., & Taylor, L. T. (1997a). Method development for the separation of sulfonamides by supercritical fluid chromatography. *Journal of chromatographic science*, 35(4), 176-180.
- Combs, M. T., Gandee, M., Ashraf-Khorassani, M., & Taylor, L. T. (1997b). Temperature and pressure effects on the supercritical fluid extraction profiles of sulfonamides from a spiked matrix using CHF<sub>3</sub> and CO<sub>2</sub>. *Analytica Chimica Acta*, 341(2), 285-295.
- Courtois, J. (2006). Monolithic separation media synthesized in capillaries and their applications for molecularly imprinted networks. (Doctoral dissertation). Umeå University, Umeå Sweden. Retrieved from <http://www.diva-portal.org/smash/get/diva2:145067/FULLTEXT01.pdf>
- Dada, A. O., Olalekan, A. P., Olatunya, A. M., & Dada, O. (2012). Langmuir, Freundlich, Temkin and Dubinin–Radushkevich Isotherms Studies of Equilibrium Sorption of Zn<sup>2+</sup> Unto Phosphoric Acid Modified Rice Husk. *Journal of Applied Chemistry*, 3(1), 38-45.
- Desta, M. B. (2013). Batch sorption experiments: Langmuir and Freundlich isotherm studies for the adsorption of textile metal ions onto Teff Straw (Eragrostis tef) agricultural waste. *Journal of Thermodynamics*, 2013, 1-6.
- De Prada, A. G. V., Martínez-Ruiz, P., Reviejo, A. J., & Pingarrón, J. M. (2005). Solid-phase molecularly imprinted on-line preconcentration and voltammetric determination of sulfamethazine in milk. *Analytica Chimica Acta*, 539(1), 125-132.
- Díaz-Álvarez, M., Barahona, F., Turiel, E., & Martínez-Esteban, A. (2014). Supported liquid membrane-protected molecularly imprinted beads for micro-solid phase extraction of sulfonamides in environmental waters. *Journal of Chromatography A*, 1357, 158-164.

- D áz-D áz, G., Di ñeiro, Y., Men ández, M. I., Blanco-L ópez, M. C., Lobo-Casta ñón, M. J., Miranda-Ordieres, A. J., & Tu ñón-Blanco, P. (2011). Molecularly imprinted catalytic polymers with biomimetic chloroperoxidase activity. *Polymer*, 52(12), 2468-2473.
- Doungsoongnuen, S., Pingaew, R., Prachayasittikul, S., Prachayasittikul, V., Ruchirawat, S., Suksrichavalit, T., & Worachartcheewan, A. (2011). Investigation on biological activities of anthranilic acid sulfonamide analogs. *EXCLI Journal*, 10, 155-161.
- EU Commission. (2010). Commission regulation (EU) No 37/2010 of 22 December 2009 on pharmacologically active substances and their classification regarding maximum residue limits in foodstuffs of animal origin. *Official Journal of the European Union*. L15/1-L15/72.
- Faizal, C. K. M., Kikuchi, Y., & Kobayashi, T. (2009). Molecular imprinting targeted for  $\alpha$ -tocopherol by calix [4] resorcarenes derivative in membrane scaffold prepared by phase inversion. *Journal of Membrane Science*, 334(1), 110-116.
- Fitzhenry, L., (2011). Development of Molecularly Imprinted Polymers for Corticosteroids (Doctoral dissertation, Waterford Institute of Technology). Retrieved from <http://repository.wit.ie/1697/1/Thesis%20-%20Laurence%20Fitzhenry.pdf>
- Fontanals, N., Marc é R. M., & Borrull, F. (2011). Overview of the novel sorbents available in solid-phase extraction to improve the capacity and selectivity of analytical determinations. *Contributions to science*, 6(2), 199-213.
- Foo & Hameed, B. H. (2010). Insights into the modeling of adsorption isotherm systems. *Chemical Engineering Journal*, 156(1), 2-10.
- Galarini, R., Diana, F., Moretti, S., Puppini, B., Saluti, G., & Persic, L. (2014). Development and validation of a new qualitative ELISA screening for multiresidue detection of sulfonamides in food and feed. *Food Control*, 35(1), 300-310.
- Gao, P., Mao, D., Luo, Y., Wang, L., Xu, B., & Xu, L. (2012). Occurrence of sulfonamide and tetracycline-resistant bacteria and resistance genes in aquaculture environment. *Water research*, 46(7), 2355-2364.
- Garc á-Gal án, M. J., D áz-Cruz, M. S., & Barcel ó, D. (2008). Identification and determination of metabolites and degradation products of sulfonamide antibiotics. *TrAC Trends in Analytical Chemistry*, 27(11), 1008-1022.
- Göbel, A., Thomsen, A., McArdell, C. S., Alder, A. C., Giger, W., Theiß, N., ... & Ternes, T. A. (2005). Extraction and determination of sulfonamides, macrolides, and trimethoprim in sewage sludge. *Journal of Chromatography A*, 1085(2), 179-189.



- Guesdon, J. L., & Avrameas, S. (1977). Magnetic solid phase enzyme-immunoassay. *Immunochemistry*, 14(6), 443-447.
- Haginaka, J., Takehira, H., Hosoya, K., & Tanaka, N. (1998). Molecularly imprinted uniform-sized polymer-based stationary phase for naproxen: comparison of molecular recognition ability of the molecularly imprinted polymers prepared by thermal and redox polymerization techniques. *Journal of Chromatography A*, 816(2), 113-121.
- Haiba, E., Lillenberg, M., Kipper, K., Astover, A., Herodes, K., Ivask, M., ... & Nei, L. (2013). Fluoroquinolones and sulfonamides in sewage sludge compost and their uptake from soil into food plants. *African Journal of Agricultural Research*, 8(23), 3000-3006.
- Halling-Sørensen, B., Nielsen, S. N., Lanzky, P. F., Ingerslev, F., Lützhøft, H. H., & Jørgensen, S. E. (1998). Occurrence, fate and effects of pharmaceutical substances in the environment-A review. *Chemosphere*, 36(2), 357-393.
- Hanaee, J., Jouyban, A., Dastmalchi, S., Adibkia, K., Mirzazadeh, A., & Barzegarjalali, M. (2005). Solubility prediction of sulfonamides at various temperatures using a single determination. *DARU Journal of Pharmaceutical Sciences*, 13(2), 37-45.
- Haupt, K., & Mosbach, K. (2000). Molecularly imprinted polymers and their use in biomimetic sensors. *Chemical Reviews*, 100(7), 2495-2504.
- He, J. F., Zhu, Q. H., & Deng, Q. Y. (2007). Investigation of imprinting parameters and their recognition nature for quinine-molecularly imprinted polymers. *Spectrochimica Acta Part A: Molecular and Biomolecular Spectroscopy*, 67(5), 1297-1305.
- Health Canada.(2014). List of Maximum Residue Limits (MRLs) for Veterinary Drugs in Foods, Canada.  
[http://www.hc-sc.gc.ca/dhp-mps/vet/mrl-lmr/mrl-lmr\\_versus\\_new-nouveau-eng.php](http://www.hc-sc.gc.ca/dhp-mps/vet/mrl-lmr/mrl-lmr_versus_new-nouveau-eng.php) (Accessed on 01 Apr 2015)
- Heberer, T. (2002). Occurrence, fate, and removal of pharmaceutical residues in the aquatic environment: a review of recent research data. *Toxicology letters*, 131(1), 5-17.
- Hirayama, K., Sakai, Y., & Kameoka, K. (2001). Synthesis of polymer particles with specific lysozyme recognition sites by a molecular imprinting technique. *Journal of applied polymer science*, 81(14), 3378-3387.
- Hoa, P. T. P., Managaki, S., Nakada, N., Takada, H., Anh, D. H., VIET, P. H., ... & Suzuki, S. (2010). Abundance of sulfonamide-resistant bacteria and their resistance genes in integrated aquaculture-agriculture ponds, North Vietnam. Interdisciplinary studies on environmental chemistry-biological responses to contaminants. *Tokyo: TERRAPUB*, 15-22.

- Hood, M. A., Mari, M., & Muñoz-Espí R. (2014). Synthetic Strategies in the Preparation of Polymer/Inorganic Hybrid Nanoparticles. *Materials*, 7(5), 4057-4087.
- Hruska, K., & Franek, M. (2012). Sulfonamides in the environment: a review and a case report. *Veterinarni Medicina*, 57(1), 1-35.
- Hu, X., Pan, J., Hu, Y., Huo, Y., & Li, G. (2008). Preparation and evaluation of solid-phase microextraction fiber based on molecularly imprinted polymers for trace analysis of tetracyclines in complicated samples. *Journal of Chromatography A*, 1188(2), 97-107.
- Hu, Y., Li, Y., Zhang, Y., Li, G., & Chen, Y. (2011). Development of sample preparation method for auxin analysis in plants by vacuum microwave-assisted extraction combined with molecularly imprinted clean-up procedure. *Analytical and Bioanalytical Chemistry*, 399(10), 3367-3374.
- Huang, Y. P., Liu, Z. S., Zheng, C., & Gao, R. Y. (2009). Recent developments of molecularly imprinted polymer in CEC. *Electrophoresis*, 30(1), 155-162.
- Huber, M. M., Göbel, A., Joss, A., Hermann, N., Löffler, D., McArdell, C. S., ... Gunten, U. V. (2005). Oxidation of pharmaceuticals during ozonation of municipal wastewater effluents: a pilot study. *Environmental Science & Technology*, 39(11), 4290-4299.
- Ji, J., Sun, X., Tian, X., Li, Z., & Zhang, Y. (2013). Synthesis of acrylamide molecularly imprinted polymers immobilized on graphite oxide through surface-initiated atom transfer radical polymerization. *Analytical Letters*, 46(6), 969-981.
- Ji, W., Chen, L., Ma, X., Wang, X., Gao, Q., Geng, Y., & Huang, L. (2014). Molecularly imprinted polymers with novel functional monomer for selective solid-phase extraction of gastradin from the aqueous extract of *Gastrodia elata*. *Journal of Chromatography A*, 1342, 1-7.
- Jiang, D., Sun, X., & Zhang, Y. (2012). Preparation and application of acrylamide molecularly imprinted composite solid-phase extraction materials. *Analytical Methods*, 4(11), 3760-3766.
- Jiang, L., Hu, X., Yin, D., Zhang, H., & Yu, Z. (2011). Occurrence, distribution and seasonal variation of antibiotics in the Huangpu River, Shanghai, China. *Chemosphere*, 82(6), 822-828.
- Jones, O. A. H., Voulvoulis, N., & Lester, J. N. (2005). Human pharmaceuticals in wastewater treatment processes. *Critical Reviews in Environmental Science and Technology*, 35(4), 401-427.
- Kan, C. A., & Petz, M. (2000). Residues of veterinary drugs in eggs and their distribution between yolk and white. *Journal of Agricultural and Food Chemistry*, 48(12), 6397-6403.

- Karaagac, O., Kockar, H., Beyaz, S., & Tanrisever, T. (2010). A simple way to synthesize superparamagnetic iron oxide nanoparticles in air atmosphere: iron ion concentration effect. *Magnetics, IEEE Transactions on*, 46(12), 3978-3983.
- Kareuhanon, W., Lee, V. S., Nimmanpipug, P., Tayapiwatana, C., & Pattarawarapan, M. (2009). Synthesis of Molecularly Imprinted Polymers for Nevirapine by Dummy Template Imprinting Approach. *Chromatographia*, 70(11-12), 1531-1537.
- Karim, K., Breton, F., Rouillon, R., Piletska, E. V., Guerreiro, A., Chianella, I., & Piletsky, S. A. (2005). How to find effective functional monomers for effective molecularly imprinted polymers?. *Advanced Drug Delivery Reviews*, 57(12), 1795-1808.
- Karimi, M., Aboufazeli, F., Zhad, H. R. L. Z., Sadeghi, O., & Najafi, E. (2014). Determination of Sulfonamides in Chicken Meat by Magnetic Molecularly Imprinted Polymer Coupled to HPLC-UV. *Food Analytical Methods*, 7(1), 73-80.
- Kartasasmita, R. E., Hasanah, A. N., & Ibrahim, S. (2013). Synthesis of selective molecularly imprinted polymer for solid-phase extraction of glipizide by using a pseudo-template. *Journal of Chemical & Pharmaceutical Research*, 5(10), 351-355.
- Kemper, N. (2008). Veterinary antibiotics in the aquatic and terrestrial environment. *Ecological indicators*, 8(1), 1-13.
- Kong, X., Gao, R., He, X., Chen, L., & Zhang, Y. (2012). Synthesis and characterization of the core-shell magnetic molecularly imprinted polymers (Fe<sub>3</sub>O<sub>4</sub>@MIPs) adsorbents for effective extraction and determination of sulfonamides in the poultry feed. *Journal of Chromatography A*, 1245, 8-16.
- Koohpaei, A. R., Shahtaheri, S. J., Ganjali, M. R., Forushani, A. R., & Golbabaei, F. (2008). Application of multivariate analysis to the screening of molecularly imprinted polymers (MIPs) for ametryn. *Talanta*, 75(4), 978-986.
- Kryscio, D. R., & Peppas, N. A. (2012). Critical review and perspective of macromolecularly imprinted polymers. *Acta Biomaterialia*, 8(2), 461-473.
- Kuo, C. C., Wang, S. P., & Grayston, J. T. (1977). Antimicrobial activity of several antibiotics and a sulfonamide against Chlamydia trachomatis organisms in cell culture. *Antimicrobial agents and chemotherapy*, 12(1), 80-83.
- Lai, J. P., Lu, X. Y., Lu, C. Y., Ju, H. F., & He, X. W. (2001). Preparation and evaluation of molecularly imprinted polymeric microspheres by aqueous suspension polymerization for use as a high-performance liquid chromatography stationary phase. *Analytica Chimica Acta*, 442(1), 105-111.

- Lan, H., Gan, N., Pan, D., Hu, F., Li, T., Long, N., & Qiao, L. (2014). An automated solid-phase microextraction method based on magnetic molecularly imprinted polymer as fiber coating for detection of trace estrogens in milk powder. *Journal of Chromatography A*, 1331, 10-18.
- Lee, W. C., Huang, C. Y., & Hwang, C. C. (2008). Separation of Cholesterol from Other Steroids Using Molecularly Imprinted Polymer Prepared by Seeded Suspension Polymerization. *Chemical and Biochemical Engineering Quarterly*, 22(2), 151-156.
- Li, Y. W., Wu, X. L., Mo, C. H., Tai, Y. P., Huang, X. P., & Xiang, L. (2011). Investigation of sulfonamide, tetracycline, and quinolone antibiotics in vegetable farmland soil in the Pearl River Delta area, Southern China. *Journal of Agricultural and Food Chemistry*, 59(13), 7268-7276.
- Li, X., Wang, X., Li, L., Duan, H., & Luo, C. (2015). Electrochemical sensor based on magnetic graphene oxide@ gold nanoparticles-molecular imprinted polymers for determination of dibutyl phthalate. *Talanta*, 131, 354-360.
- Lindsey, M. E., Meyer, M., & Thurman, E. M. (2001). Analysis of trace levels of sulfonamide and tetracycline antimicrobials in groundwater and surface water using solid-phase extraction and liquid chromatography/mass spectrometry. *Analytical Chemistry*, 73(19), 4640-4646.
- Lipmann, F. (1945). Acetylation of sulfanilamide by liver homogenates and extracts. *Journal of Biological Chemistry*, 160(1), 173-190.
- Liu, J., Jiang, M., Li, G., Xu, L., & Xie, M. (2010). Miniaturized salting-out liquid-liquid extraction of sulfonamides from different matrices. *Analytica Chimica Acta*, 679(1), 74-80.
- Liu, L., Xia, N., Xing, Y., & Deng, D. H. (2013). Boronic acid-based electrochemical sensors for detection of biomolecules. *International Journal of Electrochemical Science*, 8(9), 11161-11174.
- Lu, Y., Li, C., Wang, X., Sun, P., & Xing, X. (2004). Influence of polymerization temperature on the molecular recognition of imprinted polymers. *Journal of Chromatography B*, 804(1), 53-59.
- Lopes, R. P., de Freitas Passos, É. E., de Alkimim Filho, J. F., Vargas, E. A., Augusti, D. V., & Augusti, R. (2012). Development and validation of a method for the determination of sulfonamides in animal feed by modified QuEChERS and LC-MS/MS analysis. *Food Control*, 28(1), 192-198.
- Lorenzo, R. A., Carro, A. M., Alvarez-Lorenzo, C., & Concheiro, A. (2011). To remove or not to remove? The challenge of extracting the template to make the cavities available in molecularly imprinted polymers (MIPs). *International Journal of Molecular Sciences*, 12(7), 4327-4347.

- Ma, R. T., & Shi, Y. P. (2015). Magnetic molecularly imprinted polymer for the selective extraction of quercetagenin from *Calendula officinalis* extract. *Talanta*, 134, 650-656.
- Mayes, A. G., & Mosbach, K. (1996). Molecularly imprinted polymer beads: suspension polymerization using a liquid perfluorocarbon as the dispersing phase. *Analytical Chemistry*, 68(21), 3769-3774.
- Masque, N., Marce, R. M., & Borrull, F. (2001). Molecularly imprinted polymers: new tailor-made materials for selective solid-phase extraction. *TrAc Trends in Analytical Chemistry*, 20(9), 477-486.
- Mitra, S. (Ed.). (2004). *Sample preparation techniques in analytical chemistry*(Vol. 237). United States: John Wiley & Sons.
- Miyabayashi, A., & Mattiasson, B. (1988). An enzyme electrode based on electromagnetic entrapment of the biocatalyst bound to magnetic beads. *Analytica Chimica Acta*, 213, 121-130.
- Montalbetti, C. A., & Falque, V. (2005). *Amide bond formation and peptide coupling*. *Tetrahedron*, 61(46), 10827-10852.
- Msagati, T. A., & Nindi, M. M. (2004). Multiresidue determination of sulfonamides in a variety of biological matrices by supported liquid membrane with high pressure liquid chromatography-electrospray mass spectrometry detection. *Talanta*, 64(1), 87-100.
- National Registration Authority for Agricultural and Veterinary Chemicals. (2000), The NRA Review of SULPHONAMIDES, Canberra: Australia.  
<http://www.apvma.gov.au/products/review/docs/sulphonamides.pdf>
- Nikaido, H. (2009). Multidrug resistance in bacteria. *Annual Review of Biochemistry*, 78, 119-146.
- Nikolic, G. (2011). *Fourier Transforms-New Analytical Approaches and FTIR Strategies*. InTech, Rijeka.
- Olariu, R. I., Vione, D., Grinberg, N., & Arsene, C. (2010). Sample preparation for trace analysis by chromatographic methods. *Journal of Liquid Chromatography & Related Technologies*, 33(9-12), 1174-1207.
- Payán, M. R., López, M. Á. B., Fernández-Torres, R., Navarro, M. V., & Mochón, M. C. (2011). Hollow fiber-based liquid phase microextraction (HF-LPME) for a highly sensitive HPLC determination of sulfonamides and their main metabolites. *Journal of Chromatography B*, 879(2), 197-204.
- Pavlović, D. M., Babić, S., Horvat, A. J., & Kaštelan-Macan, M. (2007). Sample preparation in analysis of pharmaceuticals. *TrAC Trends in Analytical Chemistry*, 26(11), 1062-1075.

- Peng, X., Wang, Z., Kuang, W., Tan, J., & Li, K. (2006). A preliminary study on the occurrence and behavior of sulfonamides, ofloxacin and chloramphenicol antimicrobials in wastewaters of two sewage treatment plants in Guangzhou, China. *Science of the Total Environment*, 371(1), 314-322.
- Pérez-Moral, N., & Mayes, A. G. (2004). Comparative study of imprinted polymer particles prepared by different polymerisation methods. *Analytica Chimica Acta*, 504(1), 15-21.
- Pauling, L. (1940). A Theory of the Structure and Process of Formation of Antibodies\*. *Journal of the American Chemical Society*, 62(10), 2643-2657.
- Pichon, V. (2007). Selective sample treatment using molecularly imprinted polymers. *Journal of Chromatography A*, 1152(1), 41-53.
- Piletsky, S. A., Karim, K., Piletska, E. V., Day, C. J., Freebairn, K. W., Legge, C., & Turner, A. P. F. (2001). Recognition of ephedrine enantiomers by molecularly imprinted polymers designed using a computational approach. *Analyst*, 126(10), 1826-1830.
- Puoci, F.; Cirillo, G.; Curcio, M.; Iemma, F.; Parisi, O.I.; Spizzirri, U.G. & Picci, N. (2010). *Molecularly Imprinted Polymers (MIPs) in Biomedical Applications*. In: *Biopolymers*, 547-574, Rijeka, Croatia: Sciyo.
- Rahiminezhad, M., Shahtaheri, S. J., Ganjali, M. R., Koohpaei, A. R., Forushani, A. R., & Golbabaie, F. (2010). An experimental investigation of the molecularly imprinted polymers as tailor-made sorbents of diazinon. *Journal of Analytical Chemistry*, 65(7), 694-698.
- Renew, J. E., & Huang, C. H. (2004). Simultaneous determination of fluoroquinolone, sulfonamide, and trimethoprim antibiotics in wastewater using tandem solid phase extraction and liquid chromatography–electrospray mass spectrometry. *Journal of Chromatography A*, 1042(1), 113-121.
- Safarik, I., Safarikova, M., & Forsythe, S. J. (1995). The application of magnetic separations in applied microbiology. *Journal of Applied Bacteriology*, 78(6), 575-585.
- Sambe, H., Hoshina, K., & Haginaka, J. (2007). Molecularly imprinted polymers for triazine herbicides prepared by multi-step swelling and polymerization method: Their application to the determination of methylthiotriazine herbicides in river water. *Journal of Chromatography A*, 1152(1), 130-137.
- Sanagi, M. M., Salleh, S., Ibrahim, W. A. W., Ibrahim, W. A., & Naim, A. A. (2011). Determination of organophosphorus pesticides using molecularly imprinted polymer solid phase extraction. *The Malaysian Journal of Analytical Science*, 15(2), 175-183.
- Sanner, M. F. (1999). Python: a programming language for software integration and development. *Journal of Molecular Graphics and Modelling*, 17(1), 57-61.

- Schumacher, S., Grüneberger, F., Katterle, M., Hettrich, C., Hall, D. G., Scheller, F. W., & Gajovic-Eichmann, N. (2011). Molecular imprinting of fructose using a polymerizable benzoboroxole: Effective complexation at pH 7.4. *Polymer*, 52(12), 2485-2491.
- Shen, F., & Ren, X. (2014). Covalent molecular imprinting made easy: a case study of mannose imprinted polymer. *RSC Advances*, 4(25), 13123-13125.
- Shi, X., Meng, Y., Liu, J., Sun, A., Li, D., Yao, C., ... & Chen, J. (2011). Group-selective molecularly imprinted polymer solid-phase extraction for the simultaneous determination of six sulfonamides in aquaculture products. *Journal of Chromatography B*, 879(15), 1071-1076.
- Sicherer, S. H., & Leung, D. Y. (2013). Advances in allergic skin disease, anaphylaxis, and hypersensitivity reactions to foods, drugs, and insects in 2012. *Journal of Allergy and Clinical Immunology*, 131(1), 55-66.
- Singh, S., Chawla, P., Chawla, V., & Saraf, S. K. (2013). Syntheses and characterization of some novel substituted pyridosulfonamide derivatives as antimicrobial agents. *Rasayan journal of chemistry*, 6(3), 196-200.
- Spielmeyer, A., Ahlborn, J., & Hamscher, G. (2014). Simultaneous determination of 14 sulfonamides and tetracyclines in biogas plants by liquid-liquid-extraction and liquid chromatography tandem mass spectrometry. *Analytical and Bioanalytical Chemistry*, 406(11), 2513-2524.
- Spivak, D. A. (2005). Optimization, evaluation, and characterization of molecularly imprinted polymers. *Advanced Drug Delivery Reviews*, 57(12), 1779-1794.
- Spivak, D. A., & Shea, K. J. (1998). Binding of nucleotide bases by imprinted polymers. *Macromolecules*, 31(7), 2160-2165.
- Stohs, S. J., & Miller, M. J. (2014). A case study involving allergic reactions to sulfur-containing compounds including, sulfite, taurine, acesulfame potassium and sulfonamides. *Food and Chemical Toxicology*, 63, 240-243.
- Sun, H., Zuo, Y., Qi, H., & Lv, Y. (2012). Accelerated solvent extraction combined with capillary electrophoresis as an improved methodology for simultaneous determination of residual fluoroquinolones and sulfonamides in aquatic products. *Analytical Methods*, 4(3), 670-675.
- Sun, X., Wang, J., Li, Y., Yang, J., Jin, J., Shah, S. M., & Chen, J. (2014). Novel dummy molecularly imprinted polymers for matrix solid-phase dispersion extraction of eight fluoroquinolones from fish samples. *Journal of Chromatography A*, 1359, 1-7.
- Tadeo, J. L., Sánchez-Brunete, C., Albero, B., & García-Valcárcel, A. I. (2010). Application of ultrasound-assisted extraction to the determination of contaminants in food and soil samples. *Journal of Chromatography A*, 1217(16), 2415-2440.

- Tan, C. J., & Tong, Y. W. (2007). Preparation of superparamagnetic ribonuclease a surface-imprinted submicrometer particles for protein recognition in aqueous media. *Analytical Chemistry*, 79(1), 299-306.
- Tan, G. H., & Chai, M. K. (2011). *Sample Preparation in the Analysis of Pesticides Residue in Food by Chromatographic Techniques*. In: *Pesticides - Strategies For Pesticides Analysis*, Kuala Lumpur, Malaysia: InTech..
- Tewari, S., Jindal, R., Kho, Y. L., Eo, S., & Choi, K. (2013). Major pharmaceutical residues in wastewater treatment plants and receiving waters in Bangkok, Thailand, and associated ecological risks. *Chemosphere*, 91(5), 697-704.
- Tay, K. S., Rahman, N. A., & Abas, M. R. B. (2013). Magnetic nanoparticle assisted dispersive liquid-liquid microextraction for the determination of 4-n-nonylphenol in water. *Analytical Methods*, 5(12), 2933-2938.
- Trehan, N., Kaur, S., Kaur, B., & Kaur, G. Effect of monomer on the synthesis of molecularly imprinted polymers for quercetin. *International Research Journal of Pharmaceutical and Applied Sciences*, 3(5):19-25.
- Trott, O., & Olson, A. J., (2010). Software news and update AutoDock Vina: improving the speed and accuracy of docking with a new scoring function, efficient optimization, and multithreading. *Journal of Computational Chemistry*, 31(2), 455-461.
- Vasapollo, G., Sole, R. D., Mergola, L., Lazzoi, M. R., Scardino, A., Scorrano, S., & Mele, G. (2011). Molecularly imprinted polymers: present and future prospective. *International Journal of Molecular Sciences*, 12(9), 5908-5945.
- Vlatakis, G., Andersson, L. I., Müller, R., & Mosbach, K. (1993). Drug assay using antibody mimics made by molecular imprinting. *Nature*, 361, 645-647.
- Wang, J., Cormack, P. A., Sherrington, D. C., & Khoshdel, E. (2003). Monodisperse, molecularly imprinted polymer microspheres prepared by precipitation polymerization for affinity separation applications. *Angewandte Chemie International Edition*, 42(43), 5336-5338.
- Wei, R., Ge, F., Huang, S., Chen, M., & Wang, R. (2011). Occurrence of veterinary antibiotics in animal wastewater and surface water around farms in Jiangsu Province, China. *Chemosphere*, 82(10), 1408-1414.
- Wei, X., & Husson, S. M. (2007). Surface-grafted, molecularly imprinted polymers grown from silica gel for chromatographic separations. *Industrial & Engineering Chemistry Research*, 46(7), 2117-2124.
- Wulandari, M., Urraca, J. L., Descalzo, A. B., Amran, M. B., & Moreno-Bondi, M. C. (2014). Molecularly imprinted polymers for cleanup and selective extraction of curcuminoids in medicinal herbal extracts. *Analytical and Bioanalytical Chemistry*, 407(3), 803-812

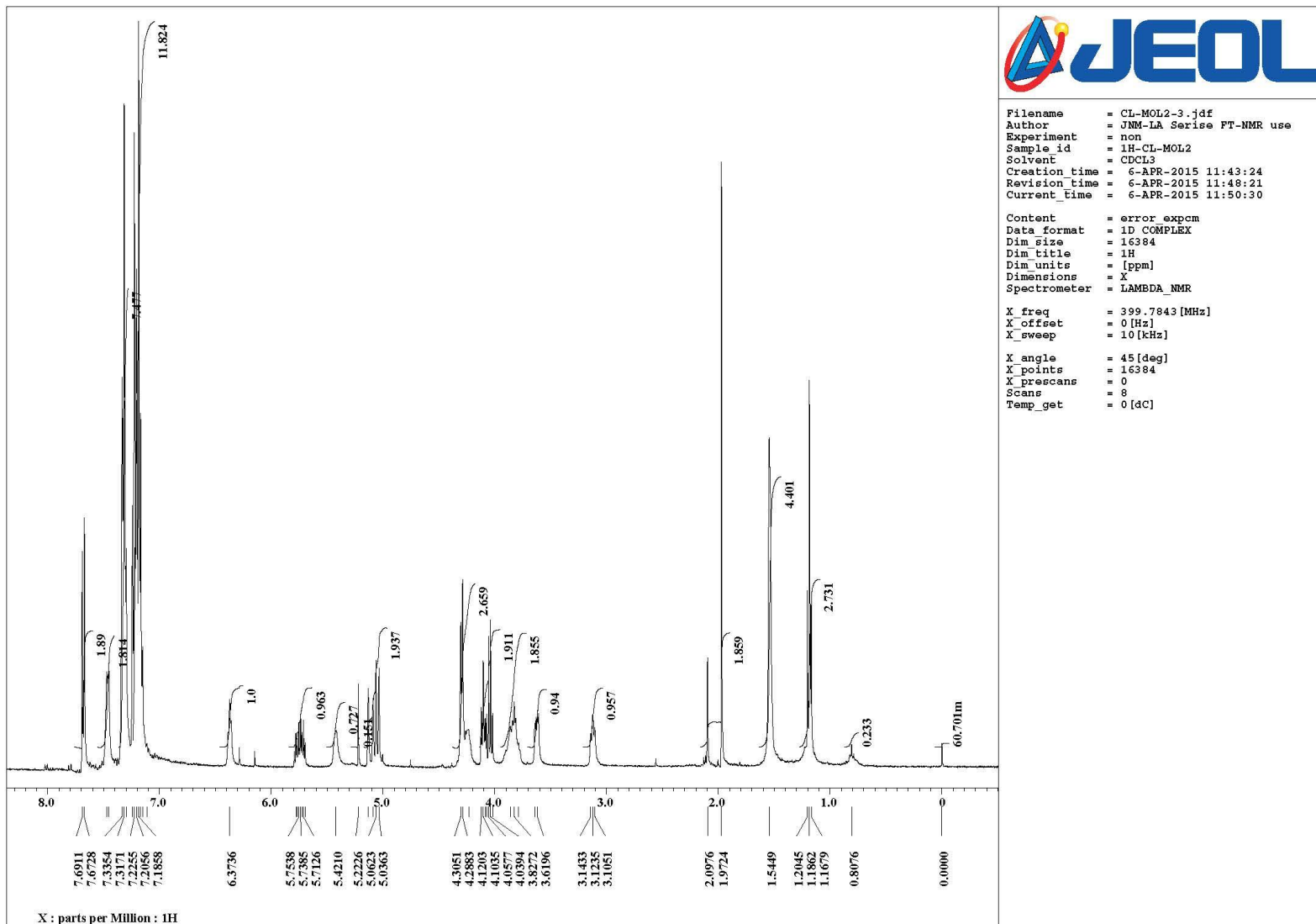


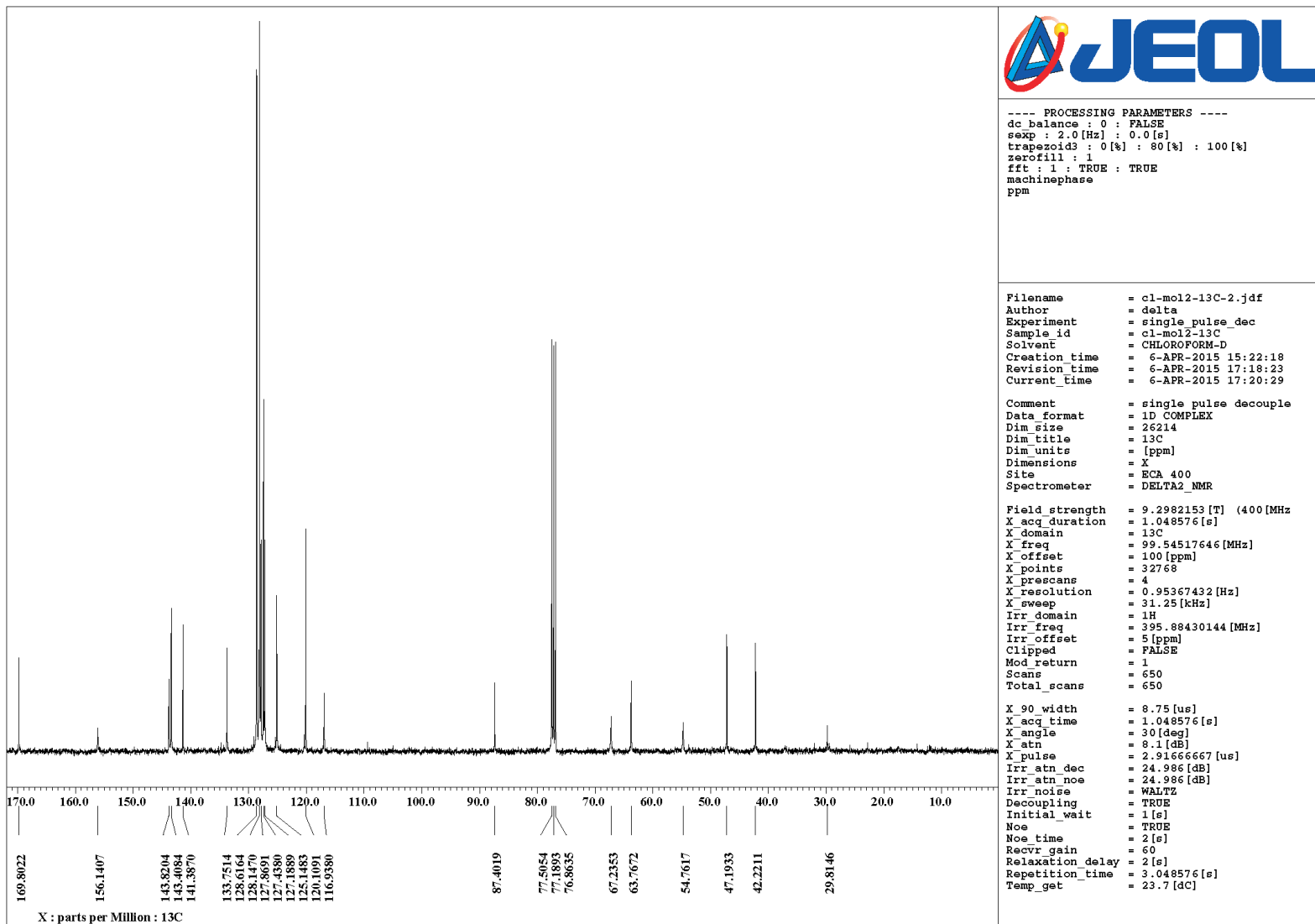
- Wulff, G., & Sarhan, A. (1972). The use of polymers with enzyme-analogous structures for the resolution of racemate. *Journal of the Angewandte Chemie International Edition*, 11(3), 341-345.
- Wulff, G., Sarhan, A., & Zabrocki, K. (1973). Enzyme-analogue built polymers and their use for the resolution of racemates. *Tetrahedron Letters*, 14(44), 4329-4332.
- Wulff, G., Vietmeier, J., & Poll, H. G. (1987). Enzyme-analog built polymers. 22. Influence of the nature of the cross-linking agent on the performance of imprinted polymers in racemic-resolution. *Die Makromolekulare Chemie*, 188(4), 731-740.
- Wulff, G., Vesper, W., Grobe - Einsler, R., & Sarhan, A. (1977). Enzyme - analogue built polymers, 4. On the synthesis of polymers containing chiral cavities and their use for the resolution of racemates. *Die Makromolekulare Chemie*, 178(10), 2799-2816.
- Xie, L., Guo, J., Zhang, Y., & Shi, S. (2014). Efficient Determination of Protocatechuic Acid in Fruit Juices by Selective and Rapid Magnetic Molecular Imprinted Solid Phase Extraction Coupled with HPLC. *Journal of Agricultural and Food Chemistry*, 62(32), 8221-8228.
- Yamak, H. B. (2013). *Emulsion Polymerization: Effects of Polymerization Variables on the Properties of Vinyl Acetate Based Emulsion Polymers*. Turkey: INTECH Open Access Publisher.
- Yan, H., & Row, K. H. (2006). Characteristic and synthetic approach of molecularly imprinted polymer. *International Journal of Molecular Sciences*, 7(5), 155-178.
- You, Q., Zhang, Y., Zhang, Q., Guo, J., Huang, W., Shi, S., & Chen, X. (2014). High-capacity thermo-responsive magnetic molecularly imprinted polymers for selective extraction of curcuminoids. *Journal of Chromatography A*, 1354, 1-8.
- Yu, C., & Mosbach, K. (2000). Influence of mobile phase composition and cross-linking density on the enantiomeric recognition properties of molecularly imprinted polymers. *Journal of Chromatography A*, 888(1), 63-72.
- Yusof, N. A., Rahman, S. K. A., Hussein, M. Z., & Ibrahim, N. A. (2013). Preparation and Characterization of Molecularly Imprinted Polymer as SPE Sorbent for Melamine Isolation. *Polymers*, 5(4), 1215-1228.
- Zakaria, N. D., Yusof, N. A., Haron, J., & Abdullah, A. H. (2009). Synthesis and evaluation of a molecularly imprinted polymer for 2,4-dinitrophenol. *International Journal of Molecular Sciences*, 10(1), 354-365.
- Zhang, W., Qin, L., He, X. W., Li, W. Y., & Zhang, Y. K. (2009). Novel surface modified molecularly imprinted polymer using acryloyl- $\beta$ -cyclodextrin and acrylamide as monomers for selective recognition of lysozyme in aqueous solution. *Journal of Chromatography A*, 1216(21), 4560-4567.

- Zhang, X., Chen, L., Xu, Y., Wang, H., Zeng, Q., Zhao, Q., ... Ding, L. (2010). Determination of  $\beta$ -lactam antibiotics in milk based on magnetic molecularly imprinted polymer extraction coupled with liquid chromatography–tandem mass spectrometry. *Journal of Chromatography B*, 878(32), 3421-3426.
- Zhao, Y. G., Zhou, L. X., Pan, S. D., Zhan, P. P., Chen, X. H., & Jin, M. C. (2014). Fast determination of 22 sulfonamides from chicken breast muscle using core–shell nanoring amino-functionalized superparamagnetic molecularly imprinted polymer followed by liquid chromatography-tandem mass spectrometry. *Journal of Chromatography A*, 1345, 17-28.
- Zheng, H. B., Mo, J. Z., Zhang, Y., Gao, Q., Ding, J., Yu, Q. W., & Feng, Y. Q. (2014). Facile synthesis of magnetic molecularly imprinted polymers and its application in magnetic solid phase extraction for fluoroquinolones in milk samples. *Journal of Chromatography A*, 1329, 17-23.
- Zheng, H. L., Sun, Y. J., Zhu, C. J., Guo, J. S., Zhao, C., Liao, Y., & Guan, Q. Q. (2013). UV-initiated polymerization of hydrophobically associating cationic flocculants: Synthesis, characterization, and dewatering properties. *Chemical Engineering Journal*, 234, 318-326.
- Zhou, J., Gan, N., Li, T., Hu, F., Li, X., Wang, L., & Zheng, L. (2014). A cost-effective sandwich electrochemiluminescence immunosensor for ultrasensitive detection of HIV-1 antibody using magnetic molecularly imprinted polymers as capture probes. *Biosensors and Bioelectronics*, 54, 199-206.
- Zhou, J., Ma, C., Zhou, S., Ma, P., Chen, F., Qi, Y., & Chen, H. (2010). Preparation, evaluation and application of molecularly imprinted solid-phase microextraction monolith for selective extraction of pirimicarb in tomato and pear. *Journal of Chromatography A*, 1217(48), 7478-7483.
- Zhou, Y., Zhou, T., Jin, H., Jing, T., Song, B., Zhou, Y., ... & Lee, Y. I. (2015). Rapid and selective extraction of multiple macrolide antibiotics in foodstuff samples based on magnetic molecularly imprinted polymers. *Talanta*, 137, 1-10.
- Zhu, L., Cao, Y., & Cao, G. (2014). Electrochemical sensor based on magnetic molecularly imprinted nanoparticles at surfactant modified magnetic electrode for determination of bisphenol A. *Biosensors and Bioelectronics*, 54, 258-261.
- Zwiener, C., & Frimmel, F. H. (2000). Oxidative treatment of pharmaceuticals in water. *Water Research*, 34(6), 1881-1885.

## **Appendix 1**

### **$^1\text{H}$ and $^{13}\text{C}$ NMR SPECTRUM OF SYNTHESIZED MONOMER-2**





**APPENDIX 2**  
**DATA FROM ISOTHERM STUDIES**

Data of adsorption kinetics of AMIP and ANIP.		
Time (s)	AMIP	ANIP
10	49.6	
20		5.0
30	174.7	12.0
50	112.2	14.0
100	219.4	15.0
150	227.4	28.4
400	276.3	46.3
800	283.5	61.1
1200	270.0	77.7
1800	264.7	81.1

Data of adsorption kinetics of SMIP and SNIP.		
Time (s)	SMIP	SNIP
10	699.6	88.3
30	882.2	108.6
50	989.0	129.8
100	1100.0	144.9
200	1154.7	133.5
400	1181.8	148.0
600	1200.0	152.9
800	1204.4	156.9
1000	1205.0	155.0
1200	1159.6	139.6

Data of adsorption isotherm of SDZ onto AMIP and ANIP		
Concentration ( $\mu\text{g mL}^{-1}$ )	AMIP	ANIP
0.5	18.3	15.5
1.0	35.7	33.2
2.0	63.3	49.3
3.0	59.9	96.8
4.0		120.4
5.0	149.0	138.7
10.0	311.8	
15.0	339.5	
20.0	383.5	
30.0	422.2	

Adsorption isotherm of SDZ onto SMIP and SNIP		
Concentration ( $\mu\text{g mL}^{-1}$ )	SMIP	SNIP
5.0	59.0	260.7
10.0	66.0	304.1
20.0	81.5	400.0
50.0	120.0	700.0
100.0	152.9	1151.5
200.0	180.2	1330.4
300.0	190.0	1400.0
400.0	195.0	1450.0
500.0	208.4	1380.0



### **APPENDIX 3**

#### **PUBLICATIONS**

Chen, L., Lee, Y. K., Manmana, Y., Tay, K. S., Lee, V. S., & Rahman, N. A. (2015). Synthesis, characterization, and theoretical study of an acrylamide-based magnetic molecularly imprinted polymer for the recognition of sulfonamide drugs. *e-Polymers*, 15(3), 141-150.

Lei Chen, Yean Kee Lee, Yanawut Manmana, Kheng Soo Tay\*, Vannajan Sanghiran Lee and Noorsaadah Abd Rahman

# Synthesis, characterization, and theoretical study of an acrylamide-based magnetic molecularly imprinted polymer for the recognition of sulfonamide drugs

**Abstract:** In this work, a magnetic molecularly imprinted polymer (MION-MIP) was prepared for the recognition and extraction of sulfadiazine (SDZ). The acrylamide-based MIP was imprinted directly onto the surface of 3-(trimethoxysilyl)propyl methacrylate-modified magnetic iron oxide nanoparticles. The synthesized MION-MIP with a diameter about 100 nm possesses fast adsorption kinetics and high adsorption capacity. The results also indicated that a higher maximum adsorption capacity ( $775 \mu\text{g g}^{-1}$ ) was achieved by the synthesized MION-MIP. The Langmuir adsorption isotherm model was found to describe well the equilibrium adsorption data. The results from the competitive binding experiment showed that MION-MIP was not only selective toward SDZ but the adsorption of sulfamerazine was also dramatically high. SDZ and sulfamerazine have an almost similar substructure where these two compounds were only differentiated by one methyl group. To explain this result, a computational study was carried out. From a different level of calculation with semiempirical (PM3), Hartree-Fock (HF), and density functional theory (DFT) calculation, SDZ and sulfamerazine showed similar interaction energy and interaction mechanism with the acrylamide monomer. Therefore, both SDZ and sulfamerazine could have the same binding property with the MION-MIP.

**Keywords:** adsorption; computer modeling; interaction energy; Langmuir adsorption isotherm model; magnetic iron oxide nanoparticles.

\*Corresponding author: **Kheng Soo Tay**, Faculty of Science, Department of Chemistry, University of Malaya, 50603 Kuala Lumpur, Malaysia, Tel.: +603-79677022 ext 2145, Fax: +603-79674193, e-mail: khengsoo@um.edu.my  
**Lei Chen**, **Yean Kee Lee**, **Vannajan Sanghiran Lee** and **Noorsaadah Abd Rahman**: Faculty of Science, Department of Chemistry, University of Malaya, 50603 Kuala Lumpur, Malaysia  
**Yanawut Manmana**: Faculty of Science, Department of Chemistry, Prince of Songkla University, Songkhla 90112, Thailand

DOI 10.1515/epoly-2015-0017

Received January 20, 2015; accepted March 12, 2015; previously published online April 14, 2015

## 1 Introduction

Antibacterial sulfonamides (sulfonamides) are a family of broad-spectrum synthetic bacteriostatic agents used in both human (1) and veterinary medicine (2) for therapeutic purposes. In animal feed, sulfonamides are used to promote livestock growth (3). Among various classes of pharmaceuticals, the presence of antibiotics in the environments has been one of the major concerns due to its ability to develop antibiotic-resistant bacteria (4, 5). Because of their extensive use, sulfonamides have been detected in various environments such as wastewaters, soils, and surface waters. Therefore, the development of a solid phase for the specific extraction of sulfonamides is an important consideration.

Molecular imprinted polymers (MIPs) are polymers containing designed artificial receptors with a predetermined selectivity and specificity for a given analyte (6). Owing to its molecular recognition ability, MIPs have appeared as very promising materials for the separation of target chemicals from different complex matrices such as environmental samples and biological fluids. Recently, various types of MIPs have been used as the adsorbent for solid phase extraction (SPE). These adsorbents have been widely used for the selective separation of various environmental pollutants (7–9), drugs and metabolites (10, 11), as well as bioactive compounds (12–14). Thus far, conventional MIPs are prepared by bulk polymerization or precipitation polymerization (8). These MIPs showed poor binding capacities and low binding kinetics of the target compounds because of the embedded binding sites (15). The application of these conventional MIPs as adsorbents for SPE also involved additional preparation steps, such as crushing and grinding of these polymers into fine

powder followed by SPE cartridge packing (14, 16). The major disadvantage of this conventional SPE is its extraction efficiency that is influenced by the uploading rate of sample and the eluent.

Recently, various approaches have been developed for imprinting MIPs onto the surface of different solid supports (15). This method can enhance the binding capacity of MIPs through the provided high surface area. In this study, acrylamide-based MIP was imprinted onto the surface of magnetic iron oxide nanoparticles (MIONs). MIONs with small particle size have been considered as an ideal solid support that provides a large surface area for adsorption (15). As compared to other solid supports, MIONs offer an added advantage of being magnetically separable, thereby eliminating the requirement of filtration and SPE cartridge packing.

The main objectives of this study were to synthesize acrylamide-based magnetic MIP (MION-MIP) with SDZ as template, and to investigate the adsorption property of MION-MIP toward SDZ. The binding conformation and the interaction between SDZ and acrylamide (monomer) were studied in detail by using computational methods to explain the sulfonamide adsorption. Recently, computational methods have been frequently used in various studies related to MIP (17). However, many studies only applied the computational methods for the selection of the most suitable monomer for MIP preparation based on the interaction between the monomer with the selected template (18–20). In this study, a computational method was used to explain the binding behavior of the synthesized MION-MIP. Based on a literature review, the application of core-shell methacrylic acid-based magnetic MIP for the adsorption of sulfamethazine has been reported by Kong et al. (3). However, in this study, the acrylamide-based MIP was imprinted directly onto the surface of MION; this study has not been reported elsewhere. With this method, MION-MIP with a higher apparent maximum adsorption capacity ( $Q_{MAX}$ ) was produced.

## 2 Experimental

### 2.1 Chemicals

Iron (II) chloride tetrahydrate ( $\text{FeCl}_2 \cdot 4\text{H}_2\text{O}$ , 99%), iron (III) chloride ( $\text{FeCl}_3$ , 98%), ethylene glycol dimethacrylate (EGDMA, 97.5%), ammonium hydroxide (25%), and all solvents used were purchased from Merck (Germany). 3-(Trimethoxysilyl)propyl methacrylate (MPS, 98%), acetic acid (HAc), and benzoyl peroxide were provided by

Sigma (Missouri, USA). Sulfadiazine (SDZ), sulfamerazine (SMR), sulfacetamide (SAA), sulfamethazine (SMZ), and sulfamethoxazole (SMO) were obtained from Alfa Aesar (UK). Acrylamide (98.0%) was supplied by Fluka (Missouri, USA). All chemicals and solvents were used without further purification.

### 2.2 Preparation of magnetic acrylamide-based nanoparticles

#### 2.2.1 Synthesis of MION-MPS

MION was synthesized by using a coprecipitation method as reported by Karaagac et al. (21). Briefly,  $\text{FeCl}_2$  and  $\text{FeCl}_3$  with a molar ratio of 2:3 were first dissolved in 100 ml deionized water. Fifty milliliters of 25% ammonium hydroxide was then added to the mixture of  $\text{FeCl}_2$  and  $\text{FeCl}_3$  under vigorous stirring for 30 min, and MION was precipitated by applying an external magnetic field. The collected MION was washed with deionized water and freeze dried.

Surface modification of MION with MPS was performed as follows: 0.2 g dried MION, 0.4 ml MPS, 0.1 ml triethylamine, and 100 ml anhydrous toluene were swirled for 10 min under nitrogen atmosphere. The mixture was refluxed for 36 h under nitrogen atmosphere and vigorous stirring. The MION-MPS was then collected by an external magnetic field, rinsed thoroughly with ethanol six times, and dried under vacuum at room temperature.

#### 2.2.2 Preparation of MION-MIP

SDZ (95 mg) and acrylamide (135 mg) was mixed in 60 ml acetonitrile-toluene with a ratio of 3:1 (v/v), and the mixture was refrigerated for 12 h to form a preassembly solution. Then, MION-MPS (100 mg), EGDMA (1 ml), and benzoyl peroxide (138 mg) were added to the acetonitrile-toluene with a ratio of 3:1 (v/v). The mixture was then degassed for 20 min by sonication and was simultaneously purged by nitrogen gas. Then, the preassembly solution was added through a cannula under nitrogen atmosphere. This combined mixture solution was heated at 50°C for 6 h, 60°C for 24 h, and 85°C for 6 h. After polymerization, the MION-MIP was separated using a magnet and rinsed with methanol. The SDZ (template) in MION-MIP were extracted with methanol-HAc (9:1, v/v). The presence of SDZ in methanol-HAc was determined using high-performance liquid chromatography (HPLC). Finally, the product was repeatedly washed with methanol and dried under vacuum.

The non-imprinted polymer (MION-NIP) was prepared by using the same procedure without SDZ.

## 2.3 Binding experiments

### 2.3.1 Binding experiments of MION-MIP and MION-NIP

All binding experiments were carried out at room temperature as described by Kong et al. (3). For the kinetic adsorption experiment, 10 mg of MION-MIP or MION-NIP was added to 3 ml of  $10 \mu\text{g ml}^{-1}$  SDZ solution with acetonitrile as solvent. The mixture was vortexed at regular time intervals ranging from 10 to 1800 s. The MION-MIP or MION-NIP was separated by an external magnetic field, and the concentration of the remaining SDZ in the solution was measured by using HPLC. For the isothermal binding experiment, 10 mg of MION-MIP or MION-NIP were added to 3 ml of SDZ solution with the concentration ranging from 0.50 to  $30 \mu\text{g ml}^{-1}$ . The mixtures were vortexed for 20 min at room temperature. The MION-MIP or MION-NIP was separated from the SDZ solution by an external magnetic field, and the concentration of SDZ in the supernatants was measured by HPLC.

### 2.3.2 Specific recognition of MION-MIP and MION-NIP

Ten milligrams of MION-MIP or MION-NIP was added to 3 ml acetonitrile containing SDZ, SMZ, SMO, and SMR with a concentration of  $10 \mu\text{g ml}^{-1}$  for each compound. After shaking for 10 min at room temperature, the MION-MIP or MION-NIP was separated from the solution by an external magnetic field, and the concentration of selected sulfonamide supernatants were measured by HPLC.

## 2.4 Characterization of MION-MIP

Infrared spectra were recorded using a Perkin-Elmer Fourier transform infrared (FTIR) spectrophotometer. The IR spectra of samples were collected in transmission mode by pressing the particle sample with potassium bromide powder to form pellets. A resolution of  $2 \text{ cm}^{-1}$  and a total of 96 scans were applied for the collection of IR spectra. Thermal gravimetric analysis (TGA) measurements were performed on a TGA4000 Perkin-Elmer instrument. Each sample was heated between  $50^\circ\text{C}$  and  $800^\circ\text{C}$  ( $10^\circ\text{C min}^{-1}$ ) under air flow ( $30 \text{ ml min}^{-1}$ ). The morphology of the MION and MION-MIP was obtained by scanning

electron microscopy (SEM) (Hitachi SU8220). Samples were mounted on carbon tape onto aluminum sample holders for analysis.

## 2.5 Instrumental analysis

All HPLC analyses were performed using a Shimadzu HPLC system consisting of an LC-20AT pump, an SPD-M20A diode array detector, an SIL-20AHT autosampler, a CTO-20AC column oven, and a CBM-20A communication bus module (Shimadzu, Japan). A reversed-phase Supelco Ascentis C18 column ( $150 \text{ mm} \times 4.6 \text{ mm}$ ; Sigma-Aldrich, USA) was used for separation. The mobile phase was a mixture of acetonitrile and 0.1% formic acid in deionized water. The flow rate was maintained at  $1.0 \text{ ml min}^{-1}$  for all runs. Isocratic elution was performed with 70% of acetonitrile. The detection wavelength was 258 nm.

## 2.6 Computational study

Geometrical optimizations for the search of possible interactions between the monomer, acylamide with the templates (SDZ), and SMR were carried out using semi-empirical (PM3), *ab initio* (HF/6-31G(d)), and density functional theory (DFT) using Becke's three-parameter Lee-Yang-Par (B3LYP) functional and 6-31G(d) basis set. Then, single point energy calculation was performed on the optimized structure to estimate the interaction energy ( $\Delta E_{\text{int}}$ ) between the template and monomer from the equation  $\Delta E_{\text{int}} = E_{\text{complex}} - E_{\text{template}} - E_{\text{monomer}}$ . The optimized structures from the B3LYP/6-31G(d) method have been used for scanning the interaction energy between the SDZ and SMR with the monomer against the distance from -1.000 to +4.000 Å of the distance with the step size of 0.200 Å. All the quantum calculations were performed using Gaussian 09 software.

# 3 Results and discussion

## 3.1 Characteristic of MION-MIP

In this study, MION-MPS was first synthesized via surface modification of MION using MPS in order to introduce the vinyl group onto the surface of MION. During surface modification, the hydroxyl groups on the surface of the MION reacted with the methoxy group of MPS, leading to



the addition of 3-methacryloyloxypropyl group onto the surface of MION through Si-O bonding (Figure 1). Then, MIP shell was fabricated through copolymerization of the acrylamide (monomer) and EGDMA (cross-linker) with BPO and SDZ as the radical initiator and template, respectively. The surface modification of MION and MIP shell fabrication were confirmed using IR spectroscopy (Figure 2A). For MION, an intense peak at  $583\text{ cm}^{-1}$  was attributed to Fe-O. For MION-MPS, a few new absorption peaks appeared in the range of  $800\text{--}1700\text{ cm}^{-1}$ . The characteristic peaks of the Si-O-Si group appeared at about  $1018\text{ cm}^{-1}$  and the carbonyl group at  $1717\text{ cm}^{-1}$ . These peaks indicated that MPS was successfully grafted onto the surface of MION. In addition, the peak at around  $2934\text{ cm}^{-1}$  was attributed to C-H stretching. This peak further showed the presence of MPS on the MION. For MION-MIP, the peaks around  $2980$  and  $1725\text{ cm}^{-1}$  were more intense. This result indicated the presence of the MIP shell on MION. Also, the peak at  $1717\text{ cm}^{-1}$  was shifted to  $1725\text{ cm}^{-1}$ , indicating the formation of a polymer through the reaction between the double bond of acrylamide and vinyl groups of MPS.

The result from the TGA showed that the weight loss for MION-MPS was greater than that for MION (Figure 2B). This result indicated that MPS was successfully added onto the surface of MION. MION-MIP showed the greatest weight loss as compared to MION and MION-MPS. This result showed that polymerization was successfully imprinted onto the surface of MION-MPS. The size and shape of MION-MPS and MION-MIP were examined by the SEM technique. It was observed that the diameter of MION and MION-MPS was about  $10\text{ nm}$  (Figure 2Ci and 2Cii). As reported by Tay et al. (22), the morphology of MION is not influenced by the surface modification of MION by using silane derivatives. After the formation of MIP, the diameter of MION-MIP was increased to about  $100\text{ nm}$  (Figure 2Ciii).

## 3.2 Binding properties

### 3.2.1 Adsorption kinetic studies of MION-MIP and MION-NIP

According to Kong et al. (3), the adsorption of sulfonamides in acetonitrile produced the highest adsorption capacity, whereas the presence of water and methanol can disturb the binding effect of the magnetic MIPs by destroying the hydrogen bond. Therefore, in this study, all adsorption experiments were carried out in acetonitrile in order to evaluate the performance of the synthesized MION-MIP. An adsorption kinetics test was carried out to study the adsorption capacity of MION-MIP and MION-NIP with adsorption time (Figure 3A). The result showed that the MION-MIP showed a fast adsorption rate in the first  $150\text{ s}$  and then increasing slightly to reach equilibrium after  $400\text{ s}$ . This was probably due to the template molecules that were captured in the cavities on the surface of the polymer at the first stage and after most of the cavities were occupied, the target molecules had to be penetrated into the deeper part of the polymer, which would be more time consuming (3). Moreover, the maximum adsorption capacity of MION-MIP toward SDZ was found to be three times higher than that of MION-NIP. This result showed the contribution of the cavities of MIP to the adsorption of template molecules.

### 3.2.2 Binding isotherm

The binding isotherm of MION-MIP and MION-NIP was determined using SDZ solutions with the concentration ranging from  $0.5$  to  $30\text{ }\mu\text{g ml}^{-1}$ . The amount of SDZ bound to MION-MIP increased sharply with increasing SDZ concentration from  $0.5$  to  $20\text{ }\mu\text{g ml}^{-1}$  (Figure 3B). However, the curve was

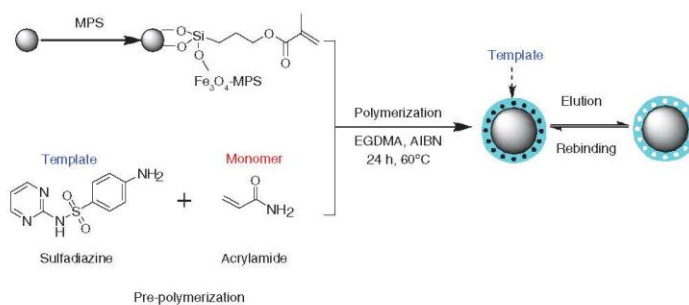
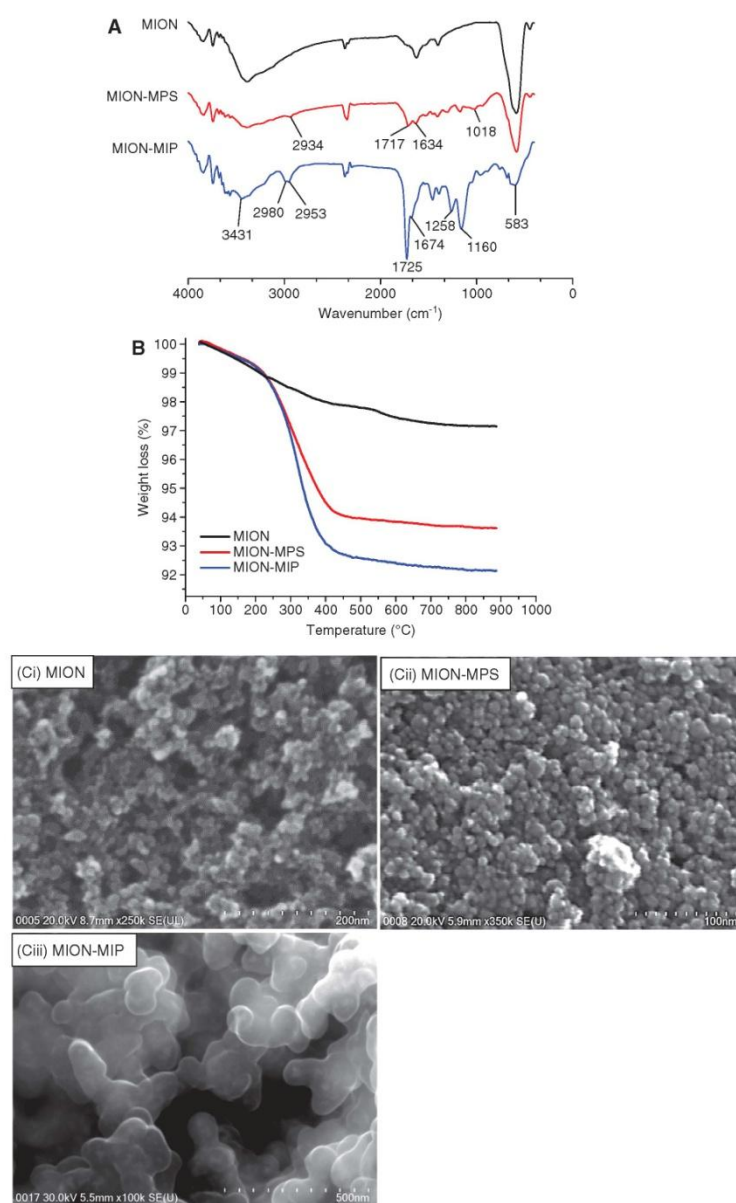
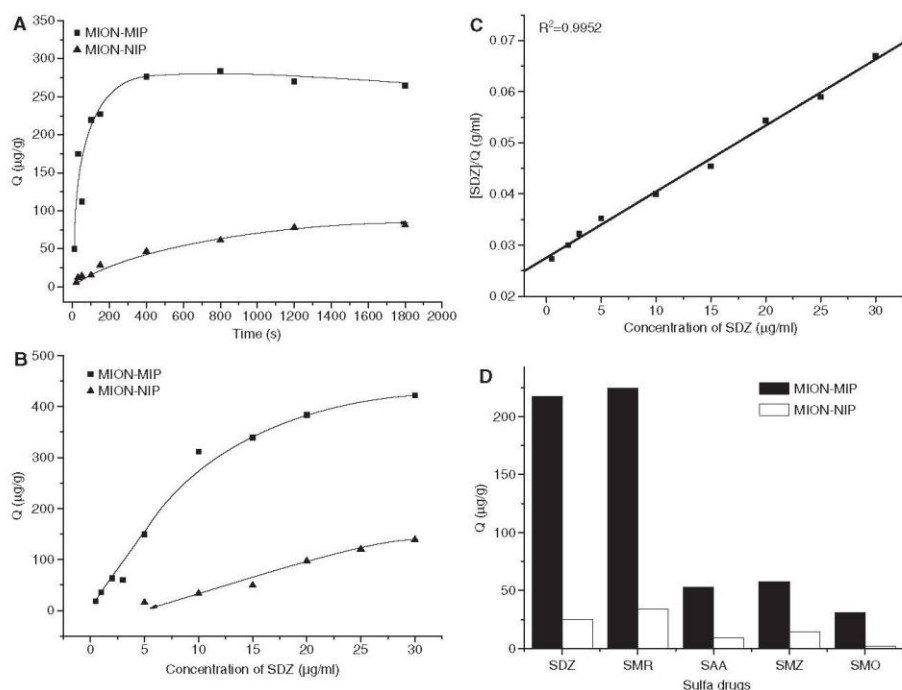


Figure 1: Schematic diagram for MION-MIP synthesis.



**Figure 2:** Characterization of MION, MION-MPS, and MION-MIP. (A) FTIR spectra recorded from 4000 to 400  $\text{cm}^{-1}$ ; (B) TGA curves; (C) SEM image of MION-MPS and MION-MIP.



**Figure 3:** (A) Adsorption dynamic curves of MION-MIPs and MION-NIPs. (B) Adsorption isotherm of SDZ onto MION-MIPs and MION-NIPs. (C) Langmuir plot to estimate the binding mechanism of MION-MIPs toward SDZ. (D) Adsorption capacity of MION-MIP and MION-NIP toward SDZ, SMR, SAA, SMZ, and SMO.

flattening after the concentration of SDZ was  $>20 \mu\text{g ml}^{-1}$ . The MION-NIP curve also showed an increasing tendency; however, the adsorption ability is not so obvious. Apparently, MION-MIP possessed a higher loading ability toward the template as compared to the MION-NIP. The result suggested that the existence of imprinting cavities differentiated the binding ability of MION-MIP as compared to MION-NIP. To further study the binding mechanism of SDZ onto the MION-MIP, Langmuir analysis was performed by using data of the binding isotherm. The equation for Langmuir adsorption isotherm model is as follows (3):

$$\frac{[\text{SDZ}]}{Q} = \frac{1}{Q_{\text{MAX}}K_D} + \frac{[\text{SDZ}]}{Q_{\text{MAX}}},$$

where  $Q$  represents the amount of SDZ bound to MION-MIP,  $K_D$  is the dissociation constant,  $Q_{\text{MAX}}$  represents the apparent maximum adsorption capacity, and  $[\text{SDZ}]$  is the

free SDZ concentration at equilibrium. The value of  $K_D$  and  $Q_{\text{MAX}}$  can be obtained from the slope and intercept of Figure 3C. The result showed that the experimental data were fitted to Langmuir adsorption isotherm model with the correlation coefficient ( $R^2$ ) of 0.9952. Therefore, based on the Langmuir adsorption isotherm model, the adsorption of SDZ occurred uniformly on the active site of the MION-MIP. Once the SDZ occupied the active site, no further adsorption could take place at this site. According to the slope and intercept of Figure 3C the  $Q_{\text{MAX}}$  and  $K_D$  of the high-affinity sites were  $775 \mu\text{g g}^{-1}$  and  $0.047 \mu\text{g ml}^{-1}$ , respectively. The  $Q_{\text{MAX}}$  obtained from this study was almost two times larger than the  $Q_{\text{MAX}}$  value obtained by Kong et al. (3) from the adsorption of SMR by using core-shell MIP. This result might be due to the smaller size of MION-MIP, which provided a larger surface area for the adsorption of template molecule.

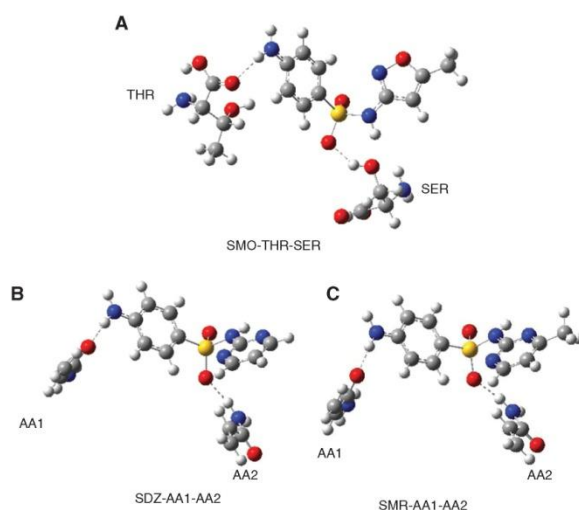
### 3.2.3 Selective adsorption of MION-MIP and binding mechanism

The competitive binding test was applied to determine selectivity of MION-MIP toward the adsorption of SDZ. Five sulfonamides (SDZ, SMR, SAA, SMZ, and SMO) were selected for this study. As shown in Figure 3D, the adsorption of MION-MIP toward SDZ and SMR was dramatically higher than that toward SAA, SMZ, and SMO. However, the adsorption of MION-MIP toward SMR was found to be slightly higher than that toward the template (SDZ). To further investigate the root reason for such a result, computational modeling was carried out to imitate the molecular interactions between the monomer and SDZ and SMR.

It has been reported that the adsorption of template molecule by MIP mimics the natural recognition pathways of natural recognition elements such as enzymes (23). Therefore, the optimized structures between the selected sulfonamides and acrylamide (AA) are expected to mimic the interaction of SMO with dihydropteroate synthase found in the protein databank (Figure 4A). The X-ray crystal structure of dihydropteroate synthase-SMO complex (PDB ID: 3TZF) shows that SMO was bound to two amino acids [serine (SER) and threonine (THR)] through hydrogen bonding at the sulfonyl and amine

group of SMO. Presumably, SDZ and SMR also have a relatively similar interaction pattern as THR and SER with SMO in the dihydropteroate synthase-SMO complex; the calculation was focused at the AA1 and AA2 positions, as indicated in Figure 4B and C.

The interaction energy between SDZ and SMR with acrylamide was compared with three different levels of calculations (Table 1). SMR had a slightly stronger interaction with acrylamide than SDZ (template) by about 3.50 kcal mol<sup>-1</sup> with PM3, and almost the same interaction with the HF and DFT method. With B3LYP, the binding energies between SDZ and SMR with monomers were slightly different by 0.29 kcal mol<sup>-1</sup>. The interaction energies between AA1 and SDZ were also very similar to SMR, which are -133.30 and -132.07 kcal mol<sup>-1</sup>, respectively. However, the interaction energies between AA2 and the selected sulfonamides were slightly higher by about 3.04 and 3.37 kcal mol<sup>-1</sup> with HF and B3LYP, respectively. From this result, acrylamide at AA2 position bound stronger than that at AA1, and contributed to SDZ and SMR recognition. Based on the optimized structures, the interaction energy between the template and each monomer was investigated by scanning the distance of AA1 and AA2 along the O...H distance for SDZ and SMR (Figure 5). The lowest point in the graph represents the lowest interaction

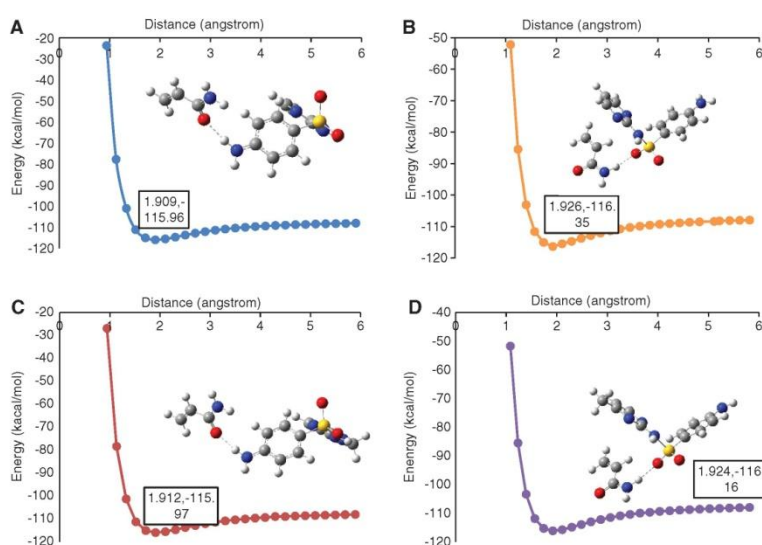


**Figure 4:** The interaction between the template and the monomer in comparison of the crystal structure of sulfonamide drug (SMO) from the protein databank (PDB ID=3TZF). The dashed line shows the hydrogen bonding interaction.



**Table 1:** The interaction energy between the templates and monomers with three different basis sets calculations.

Complex		Interaction energy (kcal mol <sup>-1</sup> )		
		PM3	HF/6-31G(d)	DFT/B3LYP/6-31G(d)
SDZ-AA1-AA2	ESDZ/AA1-AA2	-92.19	-150.95	-137.20
	ESDZ-AA2/AA1	-86.77	-147.02	-133.30
	ESDZ-AA1/AA2	-92.75	-159.34	-143.96
SMR-AA1-AA2	ESMR/AA1-AA2	-95.69	-150.72	-137.49
	ESMR-AA2/AA1	-89.28	-144.92	-132.07
	ESMR-AA1/AA2	-97.53	-162.38	-147.23
SMO-THR-SER	ESMO/THR-SER	-211.87	-661.36	-641.99
Relative interaction energy between SDZ and SMR with monomers		3.50	-0.23	0.29
Relative interaction energy between SDZ and SMR with AA1		2.51	-2.10	-1.23
Relative interaction energy between SDZ and SMR with AA2		4.78	3.04	3.27

**Figure 5:** Interaction energy plotted against the O-H distance for (A) SDZ and AA1, (B) SDZ and AA2, (C) SMR and AA1, and (D) SMR and AA2.

energy structure, and the interaction between the SDZ and SMR with the monomer was similar to each other. Thus, SDZ and SMR can bind to MION-MIP through a similar interaction during the extraction process.

Another possible reason for the poor recognition toward these two sulfonamides might be due to the smaller size effect of MION-MIP, which creates the

larger absorption surface area for the template. Besides the interaction energy and surface effect, the swelling behavior, which depends on the solvents, as reported by Koohpaei et al. (24) and Faizal et al. (25), would also cause the difference in the three-dimensional configuration of the functional groups that result in poorer capacity for site recognition between SDZ and SMR.

## 4 Conclusion

In this work, MION-MIP was prepared for the recognition and extraction of SDZ. By imprinting the acrylamide-based MIP onto the MPS-modified MION, the size of MION-MIP was around 100 nm. The result showed that the obtained MION-MIP possessed fast adsorption kinetics with only 400 s to reach equilibrium. The maximum adsorption capacity of MION-MIP was 775  $\mu\text{g g}^{-1}$ . The results from the competitive binding test indicated that the adsorption of MION-MIP toward SDZ and SMR was dramatically higher than that toward other selected sulfonamides. The result from the interaction energy calculation showed that the energies between SDZ and SMR are similar and could have the same binding property in the MION-MIP.

**Acknowledgments:** We thank the Ministry of Education Malaysia (ERGS-Project no. ER005-2013A) and the University of Malaya (UMRG- RP020C-14AFR and RP001C-13ICT) for financial support.

## References

- García-Galán MJ, Díaz-Cruz MS. Identification and determination of metabolites and degradation products of sulfonamide antibiotics. *TrAC-Trend Anal Chem.* 2008;27:1008–22.
- Msagati TAM, Nindi MM. Multiresidue determination of sulfonamides in a variety of biological matrices by supported liquid membrane with high pressure liquid chromatography-electrospray mass spectrometry detection. *Talanta.* 2004;64:87–100.
- Kong X, Gao R, He X, Chen L, Zhang Y. Synthesis and characterization of the core-shell magnetic molecularly imprinted polymers ( $\text{Fe}_3\text{O}_4$ @MIPs) adsorbents for effective extraction and determination of sulfonamides in the poultry feed. *J Chromatogr A.* 2014;1245:8–16.
- Mohanta T, Goel S. Prevalence of antibiotic-resistant bacteria in three different aquatic environments over three seasons. *Environ Monit Assess.* 2014;186:5089–100.
- Sidrach-Cardona R, Hijosa-Valseiro M, Marti E, Balcázar JL, Becares E. Prevalence of antibiotic-resistant fecal bacteria in a river impacted by both an antibiotic production plant and urban treated discharges. *Sci Total Environ.* 2014;488–489:220–7.
- Vasapollo G, Sole RD, Mergola L, Lazzoi MR, Scardino A, Scorrano S and Mele G. Molecularly imprinted polymers: present and future prospective. *Int J Mol Sci.* 2011;12:5908–45.
- Bakas I, Oujji NB, Istamboulié G, Piletsky S, Piletska E, Ait-Addi E, Ait Ichou I, Noguier T, Rouillon R. Molecularly imprinted polymer cartridges coupled to high performance liquid chromatography (HPLC-UV) for simple and rapid analysis of fenthion in olive oil. *Talanta.* 2014;125:313–8.
- Cheng W, Ma H, Zhang L, Wang Y. Hierarchically imprinted mesoporous silica polymer: an efficient solid-phase extractant for bisphenol A. *Talanta.* 2014;120:255–61.
- Xu S, Lu H, Chen L. Double water compatible molecularly imprinted polymers applied as solid-phase extraction sorbent for selective preconcentration and determination of triazines in complicated water samples. *J Chromatogr A.* 2014;1350:23–9.
- Du B, Qu T, Chen Z, Cao X, Han S, Shen G, Wang L. A novel restricted access material combined to molecularly imprinted polymers for selective solid-phase extraction and high performance liquid chromatography determination of 2-methoxyestradiol in plasma samples. *Talanta.* 2014;129:465–72.
- Urraca JL, Castellari M, Barrios CA, Moreno-Bondi MC. Multiresidue analysis of fluoroquinolone antimicrobials in chicken meat by molecularly imprinted solid-phase extraction and high performance liquid chromatography. *J Chromatogr A.* 2014;1343:1–9.
- Braga LR, Rosa AA, Dias ACB. Synthesis and characterization of molecularly imprinted silica mediated by Al for solid phase extraction of quercetin in *Ginkgo biloba* L. *Anal Method.* 2014;6:4029–37.
- Scorrano S, Mergola L, Sole RD, Lazzoi MR, Vasapollo G. A molecularly imprinted polymer as artificial receptor for the detection of indole-3-carbinol. *J Appl Polym Sci.* 2014;131:40819.
- Wulandari M, Urraca JL, Descalzo AB, Amran MB, Moreno-Bondi MC. Molecularly imprinted polymers for cleanup and selective extraction of curcuminoids in medicinal herbal extracts. *Anal Bioanal Chem.* 2015;407:803–12.
- Xie L, Guo J, Zhang Y, Shi S. Efficient determination of protocatechuic acid in fruit juices by selective and rapid magnetic molecular imprinted solid phase extraction coupled with HPLC. *J Agr Food Chem.* 2014;62:8221–8.
- Sun X, Wang J, Li Y, Yang J, Jin J, Shah SM, Chen J. Novel dummy molecularly imprinted polymers for matrix solid-phase dispersion extraction of eight fluoroquinolones from fish samples. *J Chromatogr A.* 2014;1359:1–7.
- Sobiech M, Zolek T, Lukiński P, Maciejewska D. A computational exploration of imprinted polymer affinity based on voriconazole metabolites. *Analyst* 2014;139:1779–88.
- Basozabal I, Gomez-Caballero A, Diaz-Diaz G, Guerreiro A, Gilby S, Goicolea MA, Barrio RJ. Rational design and chromatographic evaluation of histamine imprinted polymers optimized for solid-phase extraction of wine samples. *J Chromatogr A.* 2013;1308:45–51.
- Lakshmi D, Akbulut M, Ivanova-Mitseva PK, Whitcombe MJ, Piletska EV, Karim K, Güven O, Piletsky SA. Computational design and preparation of MIPs for atrazine recognition on a conjugated polymer-coated microtiter plate. *Ind Eng Chem.* 2013;52:13910–6.
- Abdin MJ, Altintas Z, Tothill IE. *In situ* designed nanoMIP based optical sensor for endotoxins monitoring. *Biosens Bioelectron.* 2015;67:177–83.
- Karaagac O, Kockar H, Beyaz S, Tanrısever T. A simple way to synthesize superparamagnetic iron oxide nanoparticles in air atmosphere: iron ion concentration effect. *IEEE T Magn.* 2010;46:3978–83.
- Tay KS, Rahman NA, Abas MRB. Magnetic nanoparticle assisted dispersive liquid-liquid microextraction for the determination of 4-nonylphenol in water. *Anal Methods.* 2013;5:2933–8.
- Kryscio DR, Peppas NA. Critical review and perspective of macromolecularly imprinted polymers. *Acta Biomater.* 2012;8:461–73.

24. Koohpaei AR, Shahtaheri SJ, Ganjali MR, Forushani AR, Golbabaie F. Application of multivariate analysis to the screening of molecularly imprinted polymers (MIPs) for ametryn. *Talanta*. 2008;75:978–86.
25. Faizal CKM, Kikuchi Y, Kobayashi T. Molecular imprinting targeted for  $\alpha$ -tocopherol by calix[4]resorcarenes derivative in membrane scaffold prepared by phase inversion. *J Membr Sci*. 2009;334:110–6.